Universidad Autónoma de Madrid
Faculty of Science
Department of Molecular Biology

The effects of p27Kip1 on the *in vivo* development and *in vitro* differentiation of mesencephalic dopaminergic neurons

DOCTORAL THESIS

Charlotte Marie Kvikne Palmer
Madrid 2019

Universidad Autónoma de Madrid
Faculty of Science
Department of Molecular Biology

The effects of p27Kip1 on the *in vivo* development and *in vitro* differentiation of mesencephalic dopaminergic neurons

Charlotte Marie Kvikne Palmer
MSc Molecular Biomedicine

Thesis Director: Isabel Liste Noya, PhD

GOBIERNO DE ESPAÑA MINISTERIO DE CIENCIA, INNOVACIÓN Y UNIVERSIDADES
Instituto de Salud Carlos III

ACKNOWLEDGEMENTS

Thinking back to my first day as a doctoral student, I am quickly reminded of all the things I am grateful for. I am especially grateful to the people who have accompanied me on this journey from beginning to end, and to those who have come and gone throughout the course of my degree.

The first person I would like to thank is my thesis supervisor, Isabel. Thank you for teaching me all the techniques and methods we use in the lab, as well as helping me develop as an independent thinker. I will forever be grateful for your support and guidance and thank you for taking a chance on a foreign student with practically no experience almost 4 years ago.

Second, I would like to thank my team in the lab, especially Adela, Raquel, and Andreea. Thank you for your daily support, endless encouragement, pep-talks, advice, and for all the laughs. I feel so lucky to have shared this journey with you. To the students who have come through over the last few years to do their end of year projects: thank you for the challenge!

To our fellow UFIEC members: thank you all for your professional and personal support throughout my stay at ISCIII. To our neighbors in NIF (Eva, Andrés, Patri and Alba) and to Alberto and Esme: thank you for always providing insightful discussion.

I would like to personally thank all the service departments that made it possible for me to complete my thesis. First of all, Sheila and the animal husbandry for doing an excellent job maintaining the mice and for helping me with crosses. To genomics for helping and providing all of the primers used for genotyping and RT-qPCR studies. To Fernando for teaching me how to use the confocal microscope, and to the confocal department for their expertise in helping me improve the quality of my images.

I would also like to thank our collaborators, starting with Manuel Serrano (IRB Barcelona) and Han Li (Pasteur Institute, France) for providing us with mice, cells and p27 plasmids; Carlos Villaescusa (Karolinska Institute, Sweden) for providing us with the CoMIP plasmid; Harold Cremer (IBDM, France) for the NeuroD1 plasmid and Marten Smidt

(University of Amsterdam, The Netherlands) for sharing antibodies with us. I am also grateful for the following sources of funding: MICINN-ISCIII (PI-10/00291 and MPY1412/09), MINECO (SAF2015-71440-R) and the Comunidad de Madrid (NEUROSTEMCM consortium S2010/BMD-2336).

Finally, I would like to thank everyone who has stood by me since day one. To my new family in Spain, thank you for making me feel like I have a second home. To Pablo, you have seen me through every step of the way and have provided a support that nobody else has (and lets not forget Iñaki and Oier). Last but certainly not least, I would like to say a special thank you to my family. Mom, Dad, Kingdon and Victoria, you are without a doubt the best team anyone could ask for. Thank you for your endless support and for always putting a smile on my face when I need one.

Thank you all for believing in me and for teaching me to believe in myself.

SUMMARY

Dopaminergic (DA) neuron development is a complex process, combining and coordinating the precise expression of numerous molecules. The importance of understanding this process is based on the growing interest in being able to reproduce their proper differentiation *in vitro*, in order to provide new treatment options for Parkinson's Disease (PD). However, obtaining DA neurons that are biologically, chemically and physiologically equivalent to those found in the brain is a complicated process, and for that reason it is important to investigate how these neurons develop in their normal physiological context.

We are investigating the role of the protein p27Kip1 (p27) in the differentiation process of these neurons. p27 is a cyclin/cyclin dependent kinase inhibitor (CKI) belonging to the Cip/Kip family of proteins. p27 is best known for its function in the cell cycle, where it specifically inhibits cyclin and cyclin dependent kinases (CDKs) of the G1 phase, and it is mainly regulated through controlling its degradation. However, in recent years, p27 has also been shown to have important implications outside of the cell cycle, including promoting primary neurogenesis in the cortex, inhibiting the transcription factor Sox2 and in promoting the differentiation of DA neurospheres.

In the context of the ventral mesencephalon (VM), we see that p27 deficiency appears to have a specific effect on DA neuron production, significantly decreasing the early differentiation of these neurons *in vivo* and *in vitro*. Interestingly, these differences are accompanied by an increased pool of neural precursors, increasing Sox2 and Ngn2 expression. However, despite these increases, downstream targets of Ngn2 (such as NeuroD1) necessary to promote progenitor progression towards mature DA neuronal phenotypes are diminished. We therefore suggest a novel role of p27 in regulating proper cell cycle exit to promote appropriate activation of genes involved in neurogenesis. This knowledge would allow us to better apply the use of this protein to improve current differentiation protocols of DA neurons for stem cell replacement therapies in PD.

RESUMEN

El desarrollo de las neuronas dopaminérgicas (ND) es un proceso muy complejo, que combina la expresión de varias moléculas en un contexto muy específico. La importancia de entender este proceso se basa en el interés de reproducir el proceso de diferenciación *in vitro,* con el fin de buscar posibles terapias para la enfermedad de Parkinson (EP). Sin embargo, la obtención de ND *in vitro,* equivalentes a las del cerebro en relación a su biología, química y fisiología, es un proceso muy complicado y, por lo tanto, la investigación de cómo esas neuronas se desarrollan en su entorno normal es muy importante.

Estamos investigando la función de la proteína p27Kip1 (p27) en la diferenciación de ND. p27 es un inhibidor de ciclinas/ciclinas dependiente de kinasas (CDKs) que pertenece a la familia de proteínas Cip/Kip. La función más conocida de p27 es el papel que juega en el ciclo celular, donde inhibe ciclinas y CDKs de la fase G1, y su regulación está mayormente controlada a través de su degradación. No obstante, se ha visto que p27 tiene funciones importantes fuera de su papel en el ciclo celular, como promover neurogénesis en la corteza cerebral, inhibir el factor de transcripción Sox2 (marcador de precursores neurales) y promover la diferenciación de neuroesferas de ND.

En el contexto del mesencéfalo ventral (MV), hemos visto que la deficiencia de p27 tiene un efecto específico en la producción de las ND, disminuyendo de manera significativa la diferenciación de estas neuronas tanto *in vivo* como *in vitro.* Estas diferencias van acompañadas con un aumento en el numero de precursores neurales, aumentando la expresión de factores como Sox2 y Ngn2. Sin embargo, a pesar de ver un incremento en el número de precursores, dianas "downstream" de Ngn2, como sería el marcador NeuroD1 (que es necesario para promover la progresión de progenitores hacía ND maduras), está disminuido. Por lo tanto, nuestro trabajo sugiere un papel nuevo de p27 en la regulación del ciclo celular para promover y activar los genes necesarios para neurogénesis. Estos resultados podrían ser importantes para ayudar a mejorar los protocolos actuales de diferenciación de ND, y para futuras terapias de reemplazo celular en la EP.

TABLE OF CONTENTS

ABBREVIATIONS

- **α-MEM:** Minimum essential medium with α-modification
- **α-syn:** α-synuclein
- **AA:** Ascorbic acid
- **Ascl1 or Mash1:** Achaete scute homolog
- **BDNF:** Brain derived neurotrophic factor
- **bHLH:** Basic helix loop helix
- **BSA:** Bovine serum albumin
- **CDK:** Cyclin dependent kinase
- **CKI:** Cyclin/cyclin dependent kinase inhibitor
- **CNS:** Central nervous system
- **DA:** Dopaminergic neurons
- **DAT:** Dopamine transporter
- **DBS:** Deep brain stimulation
- **DM:** Dorsal mesencephalon
- **DMEM:** Dulbecco's modified eagle medium
- **DNA:** Deoxyribonucleic acid
- **dNTP:** Deoxyribonucleotide triphosphate
- **DRD2:** Dopamine d2 receptor
- **DTT:** Dithiothreitol
- **EB:** Embryoid body
- **EDTA:** Ethylenediaminetetraacetic acid
- **EP:** Enfermedad de Parkinson
- **ESC:** Embryonic stem cell
- **FBS:** Fetal bovine serum
- **Ferd31:** Fer3 like bHLH transcription factor
- **FGF2:** Fibroblast growth factor 2
- **FGF8:** Fibroblast growth factor 8
- **Foxa2:** Forkhead box A2
- **FP:** Floor plate
- **G1:** Growth phase 1
- **G2:** Growth phase 2

- **Gbx2:** Gastrulation homeobox 2
- **GDNF:** Glial-cell derived neurotrophic factor
- **HBSS:** Hank's buffered saline solution
- **Hes1:** Hairy and enhancer of split-1
- **Hes5:** Hairy and enhancer of split-5
- **ICC:** Immunocytochemistry
- **IHC:** Immunohistochemistry
- **iPSC:** Induced pluripotent stem cell
- **IsO:** Isthmic organizer
- **IZ:** Intermediate zone
- **KID:** Kinase inhibitory domain
- **KO-DMEM:** Knock-out Dulbecco's modified eagle medium
- **L-dopa:** Levodopa
- **LB:** Lysogeny broth
- **LD:** Linker domain
- **Lif:** Leukemia inhibitory factor
- **Lmx1a:** LIM homeobox transcription factor 1, alpha
- **Lmx1b:** LIM homeobox transcription factor 1, beta
- **M:** Mitosis
- **MEF:** Mouse embryonic fibroblast
- **MeSC:** Mesenchymal stem cell
- **MHB:** Midbrain/hindbrain boundary
- **miPSC:** Mouse induced pluripotent stem cell
- **MSC:** Multipotent stem cell
- **Msx1:** Msh homeobox 1
- **MV:** Mesencéfalo ventral
- **MZ:** Mantle zone
- **ND:** Neuronas dopaminérgicas
- **NEAA:** Non-essential amino acids
- **NES:** Nuclear export signal
- **Ngn2:** Neurogenin 2
- **NHS:** Normal horse serum

- **NLS:** Nuclear localization signal
- **NSC:** Neural stem cell
- **Nurr1:** Nuclear receptor related protein-1
- **Otx2:** Orthodenticle homeobox 2
- **P/S:** Penicillin/streptomycin
- **p21:** $p21^{Cip1}$
- **p27:** $p27^{Kip1}$
- **p57:** $p57^{Kip2}$
- **PBS:** Phosphate-buffered saline
- **PCR:** Polymerase chain reaction
- **PD:** Parkinson's Disease
- **PFA:** Paraformaldehyde
- **Pitx3:** Pituitary homeobox 3
- **PNS:** Peripheral nervous system
- **PSC:** Pluripotent stem cell
- **Rb:** Retinoblastoma
- **RNA:** Ribonucleic acid
- **RrF:** Retrorubral area
- **RT-qPCR:** Real time-quantitative polymerase chain reaction
- **S:** Synthesis phase
- **SB:** Sodium butyrate
- **SCF Complex:** Skp, Cullin, F box containing complex
- **Shh:** Sonic hedgehog
- **Skp1:** S-phase kinase associated protein 1
- **Skp2:** S-phase kinase associated protein 2
- **SN:** Substantia nigra
- **Sox2:** SRY-box 2
- **SR:** Serum replacement
- **Subdomain D1:** Cyclin binding subdomain D1
- **Subdomain D2:** Cyclin binding subdomain D2
- **TBS:** Tris buffered saline
- **TGF-ß:** Transforming growth factor beta

- **TH:** Tyrosine hydroxylase
- **USC:** Unipotent stem cell
- **VM or midbrain:** Ventral mesencephalon
- **Vmat2:** Vesicular monoamine transporter 2
- **VTA:** Ventral tegmental area
- **VZ:** Ventricular zone
- **WB:** Western blot
- **Wnt1:** Wingless-int1

INTRODUCTION

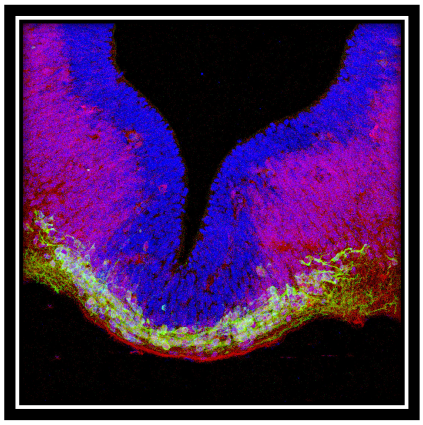

1. PARKINSON'S DISEASE

Parkinson's Disease (PD) is a chronic neurodegenerative disorder, first described by James Parkinson in his article *An Essay on the Shaking Palsy* (Parkinson 1817). This marked the beginning of what became, and remains to this day, an intense area of research, as we race against time trying to understand the molecular and pathophysiological mechanism leading to the development of PD and to discover new and effective treatment options that can repair these pathological processes.

PD is the second most common neurodegenerative disorder, affecting 1-2% of the population over the age of 65 (Poewe et al 2017). Age is the main risk factor, where the prevalence and incidence increase almost exponentially with age, and peaks after the age of 80 (Poewe et al 2017). There are an estimated 6.1 million cases worldwide, with about 700,000 cases in the United States, 830,000 cases in Western Europe and almost 100,000 cases in Spain (García Ramos et al 2016, GBD 2016 Parkinson's Disease Collaborators, 2018). With an aging population, the impact of this disease becomes a major public health issue, and the incidence is expected to double by 2050 (Rocca 2018). Therefore, there is an urgent need for research focused on finding new preventative treatments to halt, alter or reverse the progression of PD.

1.1 Pathology and Etiology

Today, PD is commonly characterized by the loss of A9 nigrostriatal dopaminergic (DA) neurons in the midbrain (González et al 2015, Poewe et al 2017) and the presence of α-synuclein (α-syn) rich protein aggregates known as Lewy bodies (Braak et al 2003). Although the histopathological features of the disease have been well defined, the etiology remains unknown. PD is generally considered an idiopathic disease, with the majority of cases being of sporadic origin. Certain risk factors (aside from age) have been identified, including specific environmental factors such as the exposure to pesticides and certain heavy metals, rural living and previous head injury (Olanow and Tatton 1999, Ascherio and Schwarzschild 2016). 5-10% of cases have been associated to certain genes, which demonstrate both autosomal dominant and autosomal recessive inheritance (Klein and Westenberger 2012, Blesa and Przedborski 2014, Kouli et al 2018).

However, it is now known that PD is a heterogenous disease, and the pathological changes begin years before it is diagnosed. It is a slow, progressive, multifactorial disease, gradually affecting several neuroanatomical areas, caused by a complex interplay between environmental, lifestyle and genetic factors (Figure I.1; Kalia and Lang 2015, Poewe et al 2017). Furthermore, due to the heterogenous and multifactorial nature of PD, patients exhibit

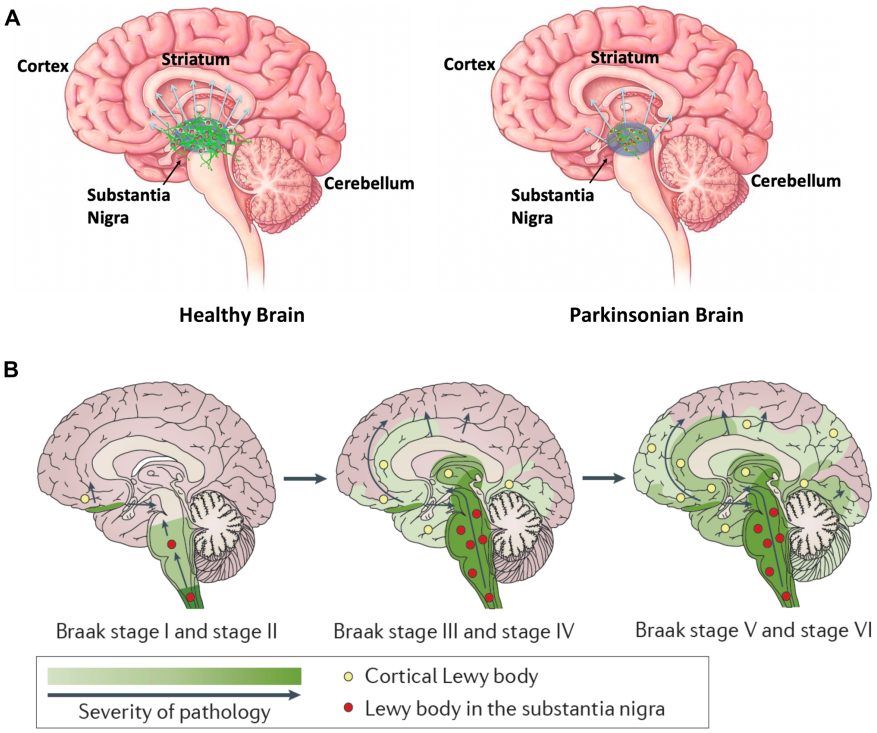

Figure I.1: Parkinson's Disease. PD is characterized by the loss of DA neurons in the SN. A) In healthy individuals, DA neurons project to the striatum where they release dopamine and are involved in motor function, and this is the population of neurons that is most affected in PD. B) Braak's hypothesis of disease pathology and spread of α-synuclein in PD (Braak et al 2003). According to this theory, α-synuclein inclusions begin in the lower brainstem (Braak Stage I and II) during early disease onset, before motor symptoms appear, although non-motor symptoms may be present. In Braak Stage III and IV, these inclusions infiltrate the midbrain and motor symptoms appear. In Braak Stages V and VI, α-synuclein aggregates spread to the limbic and neocortical brain regions in advanced stages of the disease (Braak et al 2003, Poewe et al 2017).

varying symptomatology and neuropathology, and there is great variation in the degree of responsiveness to currently available treatment options.

1.2 Symptoms and Current Treatment Options

PD is recognized by its distinctive primary motor symptoms: resting tremor, rigidity, slow movements known as bradykinesia and postural instability. However, although PD is best known for the symptoms that arise due to the death of DA neurons, it is known that non-dopaminergic systems are also affected. Furthermore, PD is characterized by the histopathological presence of α-syn protein aggregates in both the central and peripheral nervous systems (CNS and PNS) (Pollanen et al 1993, Forno 1995, Spillantini et al 1998). It is believed that the pathological changes that accompany the formation of these protein aggregates not only contribute to motor dysfunction but also lead to several non-motor symptoms (Marinus et al 2018), which can include cognitive impairment, dementia, hallucinations, anxiety,

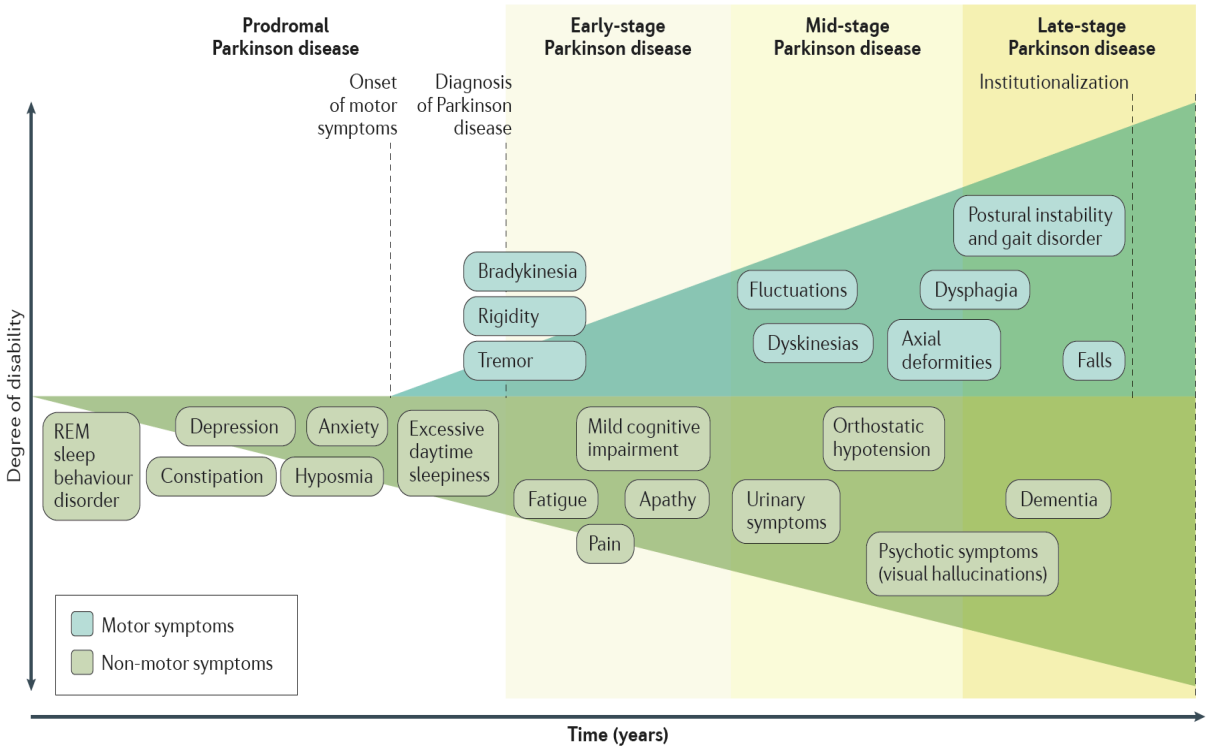

Figure I.2: Symptoms associated with PD. Non-motor symptoms are known to precede a clinical diagnosis by several years in what is called prodromal PD. The onset of motor symptoms in early-stage PD leads to a clinical diagnosis. As the disease progresses, both motor and non-motor symptoms worsen, both of which leads to further disability. Side effects of long term L-dopa use also become apparent, leading to fluctuations and dyskinesias. At later stages, some patients disability becomes so severe, they require full-time assistance from family members or caretakers (Poewe et al 2017).

depression, sleep disturbances (excessive daytime sleepiness and insomnia), constipation, olfactory loss and impulse control disorders (Figure I.2; Lang 2011, Marinus et al 2018). These non-motor symptoms can have an equally debilitating effect on the patient's quality of life (Chaudhuri and Schapira 2009, Lindvall 2015a).

Fortunately, several treatment options have been developed, based on the replacement of dopamine levels in the striatum. This includes administering levodopa (L-dopa), dopamine agonists, and/or enzyme inhibitors to reduce dopamine breakdown (including monoamine oxidase and catechol-O-methyl transferase inhibitors). L-dopa is currently the most effective, and considered the gold standard treatment (Fahn 2006, Brichta et al 2013, Lindvall 2015b). Furthermore, surgical interventions such as deep brain stimulation (DBS) have also been shown to be effective in certain patients (Lindvall and Kokaia 2009).

However, these treatments are only effective for a limited time, as prolonged use leads to severe side effects. Furthermore, none of the current treatments can modify the disease, prevent its progression or relieve non-motor symptoms. For this reason, there is tremendous

interest in developing alternative strategies to slow down or repair the underlying process, especially in the form of stem cell replacement therapies.

1.3 Current Objectives of PD Research

Due to the main challenges presented by PD (including late diagnosis, heterogenous etiology, multifactorial progression and varying degrees of patient response to treatment options, as described above), there is urgent need for new treatment options. To achieve this, one of the main objectives of PD research is a firm understanding of the pathophysiological changes leading to disease, in order to identify new biomarkers, allowing for an earlier diagnosis and the development of more preventative therapies. However, in addition to this, a solid understanding of the proper physiological development of DA neurons is also fundamental. This understanding could allow a more accurate replication of these neurons using stem cell technology *in vitro,* for cell replacement therapies, disease modeling and drug discovery. The focus of the present work is based on improving our current knowledge of proper DA neuron development, where we investigate new factors that might be important in this process, which could then be used to improve current protocols for stem cell replacement therapies and disease modeling to aid in the search of new treatments for PD.

2. DOPAMINERGIC NEURONS

DA neuros have been extensively studied due to their implication in PD, with the idea of developing cell replacement therapies as new treatment options for this disease. However, obtaining DA neurons that are biologically, chemically and physiologically equivalent to those found in the brain is a complicated process, combining and coordinating the precise expression of numerous signaling molecules and transcription factors. Therefore, in order to be able to grow fully mature and correctly functioning DA neurons *in vitro*, a comprehensive understanding of the proper physiological development of these neurons is an essential aspect of PD research.

2.1 Definition

DA neurons are capable of releasing the catecholaminergic neurotransmitter dopamine and are best characterized by the presence of tyrosine hydroxylase (TH), the enzyme involved in the limiting step of dopamine synthesis (Arenas et al 2015). There are several dopamine containing neuronal cell groups found throughout the mammalian brain, with three commonly recognized nuclei in the ventral mesencephalon (VM, midbrain): the A8 (retrorubral area, RrF), A9 (substantia nigra, SN), and the A10 (ventral tegmental area, VTA) DA neuron clusters

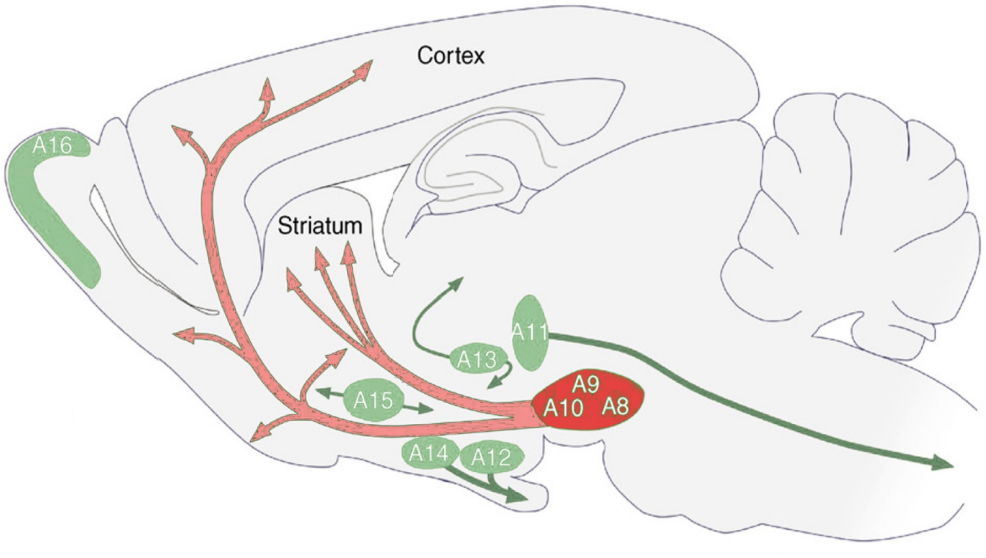

Figure I.3: DA projections in the rodent brain. Several DA-containing neuronal cell groups are found throughout the mammalian brain. The DA neuron nuclei located in the VM include A8, A9 and A10. A9 dopaminergic neurons project to the striatum via the nigrostriatal pathway, whereas A8 and A10 DA neurons project to the prefrontal cortex via the mesolimbic and mesocortical pathways (in red) (Adapted from Björklund and Dunnett 2007).

(Figure I.3; Björklund and Dunnett 2007, Roeper 2013). A9 DA neurons of the SN project to the striatum forming the nigrostriatal pathway, where they release dopamine and are involved in motor function (Hegarty et al 2013). A8 and A10 neurons project to the prefrontal cortex, forming the mesolimbic and mesocortical systems, where they are involved in emotion and reward (Hegarty et al 2013, Arenas et al 2015). Although it is now known that several different neuronal systems are affected in PD, the cells most affected are DA neurons in the SN, which are responsible for the majority of motor symptoms, and therefore become a main target for cell replacement therapies and disease modeling.

2.2 DA Neuron Development

The earliest stages of DA neuron development begin with the formation of the isthmic organizer (IsO) and the floor plate (FP), whose combined actions initiate and coordinate multiple functions of proper DA neuron development, including regional identity & patterning, specification & proliferation of progenitors, neurogenesis and survival (Figure I.4, I.5; Arenas et al 2015).

2.2.1 Early Regionalization and Patterning

Proper regionalization of the VM begins with formation of the IsO, which defines the midbrain/hindbrain boundary (MHB) based on the coordinated expression of two transcription

factors: Otx2 (orthodenticle homolog 2) and Gbx2 (gastrulation brain homeobox 2). A concentration gradient is formed from the expression of Otx2 in the midbrain and Gbx2 in the hindbrain, where each transcription factor mutually represses the other, and defines the sharp border and proper positioning of the MHB (Wasserman et al 1997, Millet et al 1999, Rhinn and Brand 2001). This activates the expression of two morphogens, Wnt1 (Wingless-int1) and Fgf8 (Fibroblast growth factor 8), but only Fgf8 is necessary and sufficient to induce the IsO (Martinez et al 1999). The MHB is formed based on the interaction of concentration gradients created by Fgf8 signaling (Arenas et al 2015). At about the same time as the formation of the IsO, a second patterning event takes place, which depends on the expression of Shh (Sonic hedgehog) to specify the most ventral region of the neural plate, forming the floor plate (FP) (Roelink et al 1995). The expression of Shh in the neural plate induces the expression of Foxa2, which is required for FP development and correct ventral patterning (Ang and Rossant 1994, Ang 2009). Foxa2, in turn, upregulates Shh, forming a positive-feedback loop between Shh and Foxa2 to regulate the proper patterning of the FP (Epstein et al 1999).

The importance of Shh and Fgf8 signaling (Shh for ventral FP patterning and Fgf8 for maintenance of IsO patterning) have made them key components in protocols for the directed differentiation of DA neurons *in vitro* (discussed below).

2.2.2 Specification

Upon the establishment of the MHB and the Shh-Foxa2 signaling network in the FP, Foxa2 begins to regulate the expression of two LIM homeobox transcription factors: Lmx1a and Lmx1b (Arenas et al 2015). Lmx1b is needed to promote the differentiation of DA neuron precursors (Smidt et al 2000) and Lmx1a is needed for the specification of DA neurons in the FP (Andersson et al 2006b). Lmx1a has been shown to upregulate Wnt1, and Wnt1 in turn upregulates Lmx1a and Otx2 via ß-catenin. In addition to specification of DA neurons, the formation of this autoregulatory loop has important functions in inhibiting alternative fates (Chung et al 2009). Furthermore, Lmx1a has also been shown to directly upregulate markers important for DA neuron differentiation: Nurr1 and Pitx3 (discussed below), which have important functions in the maintenance and survival of these neurons (Chung et al 2009). Therefore, the proper specification of DA neurons is controlled by the combined actions of the Shh-Foxa2 and Otx2-Wnt1-Lmx1a networks (Arenas et al 2015).

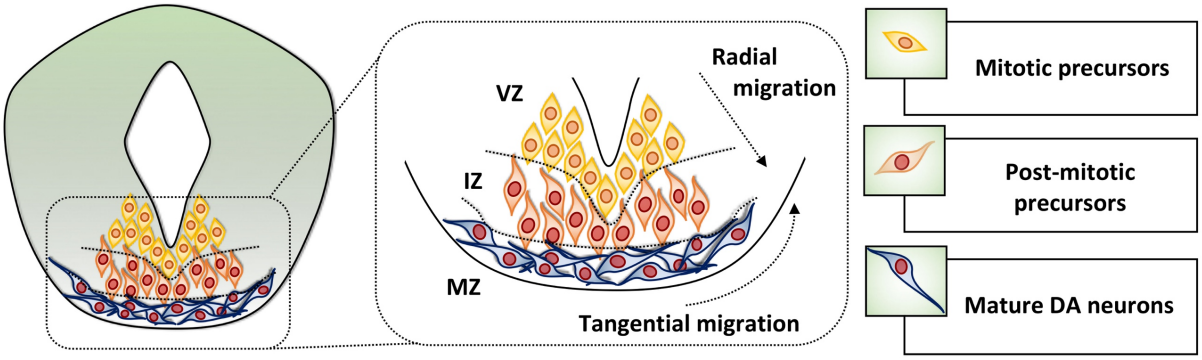

Figure I.4: Neurogenesis in the developing VM. DA neurons are born in the VZ (yellow cells), where they are considered mitotic precursors, expressing markers such as Sox2. As these precursors begin to migrate through the IZ (orange cells), they become post-mitotic precursors expressing markers such as Ngn2 and some Nurr1. DA neurons are considered mature upon reaching the MZ (blue cells) where they express markers such as TH, Nurr1 and Pitx3. Early markers important for regionalization of the FP such as Foxa2 and specification of DA precursors such as Lmx1a are expressed in all three zones (yellow, orange and blue cells) throughout development and into adulthood.

2.2.3 Neurogenesis

DA precursors are born in the ventricular zone (VZ) of the developing FP, and as they become post-mitotic, they begin migrating radially outwards, gradually losing progenitor identity as they pass through the intermediate zone (IZ). Upon reaching the mantle zone (MZ), these neurons migrate tangentially until they reach the SN and express mature DA identity markers, including TH, Nurr1 and Pitx3. This process is mainly regulated by two basic-helix-loop-helix (bHLH) transcription factors, Neurogenin2 (Ngn2) and Mash1 (Ascl1), though only Ngn2 is required for DA neurogenesis (Andersson et al 2006a, Kele et al 2006). The two regulatory networks described above (Shh-Foxa2 and Otx2-Wnt1-Lmx1a) are direct and indirect regulators of Ngn2, where Foxa2 suppresses pro-neural gene inhibitors (such as Hes1 via Ferd3l) to promote neurogenesis (Ferri et al 2007, Metzakopian et al 2012) and Lmx1a upregulates Ngn2 via Msx1 (Andersson et al 2006b). Although Ngn2 is expressed throughout the developing brain, in the context of the developing VM, cells positive for Ngn2 are considered DA precursors (Kele et al 2006).

During embryonic development, it is important to keep in mind the importance of proper cell cycle exit of proliferating precursors to give rise to post-mitotic neuroblasts. In this context, Sox2, a general marker of neural precursors in the developing brain, has been shown to interact with Ngn2 to drive cell cycle exit and promote neurogenesis (Graham et al 2003). In the developing VM, cells expressing the marker Sox2 make up the population of proliferating precursors in the VZ, and Ngn2 has been shown to be co-expressed in some Sox2-expressing

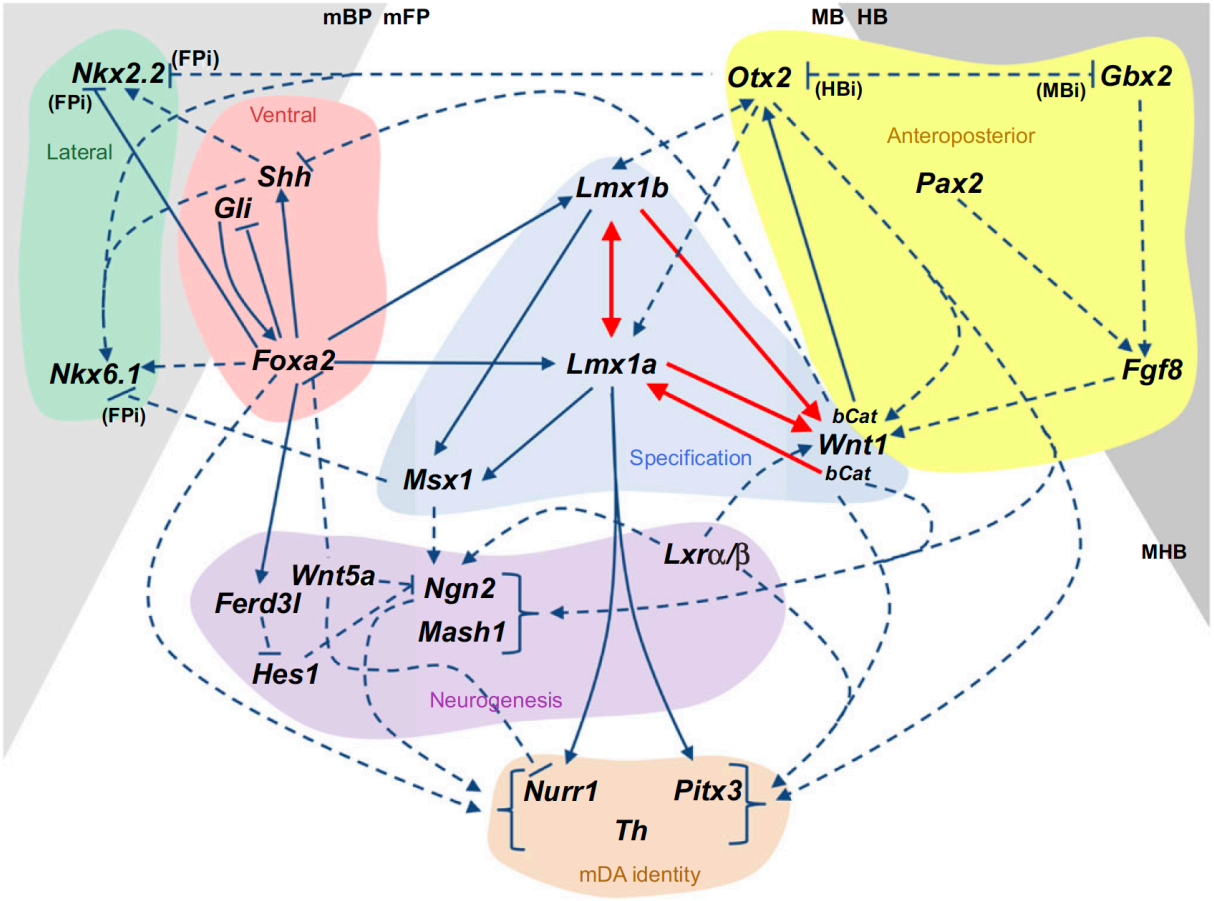

Figure I.5: Network of known factors controlling DA neuron development. DA neuron development begins with the formation of the MHB, controlled by Otx2 (yellow area) and the IsO (pink and green area), which establishes the two signaling centers that later secrete Fgf8 and Shh. Shh forms an autoregulatory loop with Foxa2 (pink area) and is responsible for the proper regionalization and patterning of the FP. Otx2 also forms a regulatory loop with Wnt1 and Lmx1a to specify DA neuron precursors (blue area). The collaborative actions of the Shh-Foxa2 and Otx2-Wnt1-Lmx1a networks control the expression of Ngn2 (purple area) to initiate neurogenesis of DA neuron precursors. Neurogenesis of DA neurons takes place as precursors migrate through the VM to their final destination in the SN, and express the mature DA neuron markers TH, Nurr1 and Pitx3, which become important in maintaining phenotype stability and functionality (Arenas et al 2015).

proliferating precursors. As these cells exit the cell cycle, Ngn2 expressing cells that have lost Sox2 expression make up the IZ, and these cells continue migrating, gradually gaining the expression of mature DA neuron markers such as Nurr1 and TH. The coordinated expression of these markers indicates the importance of proper spatiotemporal control during DA development, although the exact interaction between Sox2 and Ngn2 remains poorly understood (Kele et al 2006).

2.2.4 Differentiation and Survival

After neurogenesis, the post-mitotic precursors located in the IZ begin to differentiate into DA neurons, which continue to migrate until they reach their final destination in the MZ (Arenas et al 2015). Nurr1 is the first post-mitotic marker of DA precursors, which is necessary for the survival of DA neuroblasts, proper neurotransmitter identity and maintenance of a mature DA neuron phenotype (Zetterström et al 1997, Kadkhodaei et al 2009). Of particular importance, Nurr1 has been shown to induce the expression of TH, the gold-standard marker for DA neurons, and is the first mature marker that appears in the developing VM (Smits et al 2003). Another important marker of mature DA neurons is Pitx3, which appears to be independent of the Nurr1-TH cascade (Smidt et al 2000). Pitx3 is required for terminal DA neuron differentiation and phenotype maintenance (Li et al 2009).

Furthermore, both Pitx3 and Nurr1 have been shown to have important functions in acquiring phenotypic markers of DA functionality such as dopamine transporter (DAT), vesicular monoamine transporter 2 (Vmat2), dopamine D2 receptor (Drd2) and glial-cell line derived neurotrophic factor (Gdnf) (Saucedo-Cardenas et al 1998, Jacobs et al 2009, Kadkhodaei et al 2009, Arenas et al 2015).

Although a great deal is known about factors important and necessary for the proper development of these neurons, it remains a highly complex and complicated process. This is caused, in part, by the fact that there are most likely several other factors involved that have yet to be described. Previous evidence supports the idea that the cell cycle protein $p27^{Kip1}$ (p27) has important functions in driving neurogenesis, which was described for cortical neurons (Nguyen et al 2006). Furthermore, it was also shown that p27 overexpression could promote the differentiation of VM neurospheres to DA neurons (Sacchetti et al 2009).

3. $P27^{KIP1}$ AND DOPAMINERGIC NEURONS

p27 is a cyclin/cyclin-dependent kinase inhibitor (CKI) belonging to the Cip/Kip family of proteins. p27 and its family members $p21^{Cip1}$(p21) and $p57^{Kip2}$ (p57) share a conserved N-terminal domain that facilitates binding to cyclin and cyclin dependent kinase (CDK) complexes (Besson et al 2008). These conserved structures make up the kinase inhibitory domains (KID), which include three subdomains: the cyclin-binding subdomain (D1), the CDK-binding subdomain (D2), and a linker domain (LH) that links the D1 and D2 subdomains (Lacy et al 2004, Otieno et al 2011, Bachs et al 2018). The inhibitory action of CKIs occurs when a portion of the D2 subdomain is introduced into the catalytic center of CDKs, directly competing with and inhibiting ATP binding (Russo et al 1996). Interestingly, the D1 and D2

subdomains are mostly unfolded in isolated p27, but quickly fold upon the association with CDKs, and the KID is known to contain a nuclear export signal (NES) (Bachs et al 2018).

Despite these conserved regions, CKIs are generally considered intrinsically disordered proteins due to their lack of tertiary structure in isolation (Dyson and Wright 2005, Huang et al 2015). The C-terminal domain, in particular, is an intrinsically disordered region which includes a nuclear localization signal (NLS) and differences observed in the remainder of their sequences indicate that p27, p21 and p57 may each have individual functions (Besson et al 2008).

p27 is best known for its cell cycle-dependent functions and promoting cell cycle exit. However, in recent years it has been demonstrated that p27 also has cell-cycle independent functions, which implicates this protein in a broad range of processes, including neurogenesis. Currently, no link between p27 and PD has been described, but it has been suggested that p27 may regulate α-syn expression, and our results show an important function of p27 in the development of DA neurons.

3.1 Cell-Cycle Dependent Functions of p27

Cyclins and CDKs are a group of proteins whose coordinated activities are involved in the regulation of the cell cycle (Sherr and Roberts 2004). The cell cycle is composed of 4 phases, including: G1 (when the cell is preparing for DNA synthesis), S (when the cell is actively synthesizing DNA), G2 (when the cell is preparing for mitosis) and M (mitosis, or cell division) (Schafer 1998). Progression through G_1 phase is dependent on Cyclin D-Cdk4/6 complexes, while Cyclin E/A-Cdk2 signals for the G_1/S transition. Cyclins B combined with Cdk1 are required for the advancement of G_2/M (Sherr and Roberts 1999; Bilodeau et al 2009).

p27 is best known for its function in promoting cell cycle exit, which it primarily does by binding to the catalytic cleft of Cyclin E/A-Cdk2 complexes, inhibiting ATP binding and the phosphorylation of retinoblastoma (Rb) proteins. In a hypo-phosphorylated state, Rb remains bound to E2F, thereby preventing E2F-mediated transcription of genes necessary to drive the cell cycle (Ludlow et al 1990). The control of p27 in the cell cycle is further supported by evidence suggesting that D-type cyclins sequester p27, preventing p27 from inhibiting Cyclin E/A-Cdk2 complexes, leading to phosphorylated Rb and E2F-mediated transcription that promotes the G_1/S transition (Sherr and Roberts 1999). Furthermore, it has been shown that in mitogen rich conditions, p27 stabilizes Cyclin D-Cdk4/6 complexes, promoting G1 phase progression, whereas in mitogen starved conditions, these complexes disassemble,

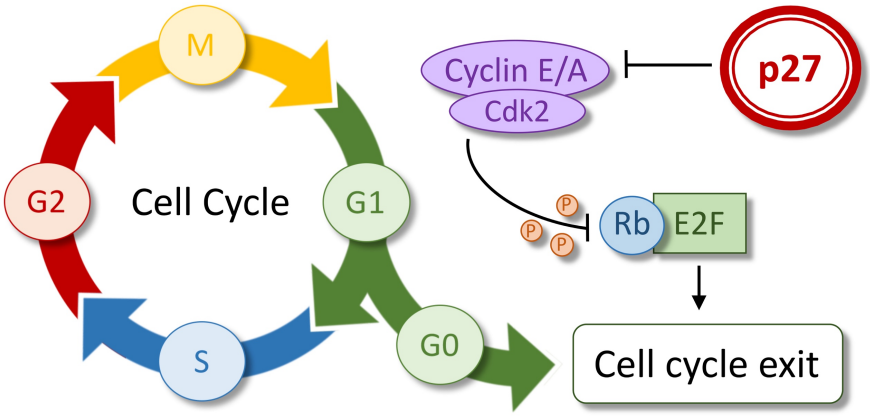

Figure I.6: Cell cycle and inhibition by p27. The cell cycle is composed of 4 phases (G1, S, G2 and M) controlled by the coordinated expression of cyclins and CDKs. p27 inhibits the progression from G1 to S by binding to the catalytic cleft of Cyclin E/A-Cdk2 complexes, preventing its ability to phosphorylate Rb complexes. Rb associated to E2F renders E2F unable to mediate the transcription of genes controlling cell cycle progression.

preventing Cyclin D-Cdk4/6 from promoting cell cycle progression, leaving p27 free to associate with and inhibit Cyclin E/A-Cdk2 complexes (Figure I.6; Sherr and Roberts 1999).

3.2 Cell-Cycle Independent Functions of p27

As mentioned before, p27 is classified as an intrinsically disordered protein, and in addition to its function in regulating the cell cycle, important roles of p27 have been found linked to apoptosis, transcriptional regulation, cell fate determination, cell migration and cytoskeletal dynamics (Besson et al 2008). p27 has been found to regulate processes directly related to neurogenesis as well, such as promoting the differentiation and radial migration of cortical projection neurons, where neural differentiation was promoted by the stabilization of Ngn2 at the N-terminal half of p27, and neural migration was promoted by blocking RhoA activity at the C-terminal half (Nguyen et al 2006). p27 has been shown to directly repress Sox2 (a neural precursor in the context of DA neuron development) during stem cell differentiation, indicating a possible role of p27 in DA neuron differentiation (Li et al 2012) and it has been demonstrated that p27 promotes tangential migration through its association to microtubules that promote polymerization in extending neurites (Godin et al 2012). In recent years, increased interest in p27 as a transcriptional regulator has shown important functions of p27 in association with several different transcription factors to promote gene expression important in functions such as: promoting the cell cycle (via p130-E2F), neurogenesis (via Ngn2), muscle differentiation (via MyoD) and to promote cell adhesion, ion transport and cell signaling (via both PCAF and Pax5) (Bachs et al 2018). Recently, loss of p27 was associated with increased

α-syn expression in the cerebellum of p27 KO mice, implicating p27 as a possible participant in the induction of PD (Gallastegui et al 2018).

3.3 Transcriptional and post-translational regulation of p27

p27 is ubiquitously expressed and is maximal in quiescent cells (Chu et al 2007). Its expression is regulated by both transcriptional and post-translational processes, and certain transcriptional regulators have been identified that can either activate or repress the transcription of p27 (Bachs et al 2018). However, p27 is mainly regulated by controlling its degradation, which is primarily stimulated by phosphorylation at specific threonine and serine sites, marking it for ubiquitin-dependent proteolysis (Shirane et al 1999, Hnit et al 2015). The most studied process of p27 regulation is the polyubiquitylation and subsequent degradation by the SCF^{SKP2}-complex, specifically S-phase kinase associated protein 1 (Skp1) and S-phase kinase associated protein 2 (Skp2). Cyclin E/A-Cdk2 complexes, the same complexes inhibited by p27, are known to phosphorylate p27 at T187, targeting it for SCF^{SKP2}-mediated degradation, and thereby promoting cell-cycle progression (Nakayama and Nakayama 2006, Chu et al 2008, Teixeira and Reed 2013). p27 degradation can also take place without T187 phosphorylation, mediated by both Skp2 dependent and independent pathways (Hara et al 2001, Kossatz et al 2001, Chu et al 2007). Furthermore, phosphorylation of p27 at T74, T88, and T89 has been shown to greatly decrease its ability to inhibit Cyclin E/A-Cdk2 complexes, thereby reducing its cell cycle inhibitory function (Besson et al 2008), further indicating the importance of post-translational modifications in the regulation of p27 function.

3.4 Subcellular localization of p27

The subcellular localization of p27 has important implications. In the nucleus, p27 can act as a transcriptional regulator and can be directly involved in gene expression, as briefly described above (Sherr and Roberts 1999, Bachs et al 2018). Cytoplasmic localization tends to be associated with dysregulation and degradation of the protein, which may be implicated in pathologies such as cancer and neurodegenerative diseases (Besson et al 2008, Bachs et al 2018). The implication of p27 in cancer has been very well described, and decreased levels of p27 or a cytoplasmic localization has been associated with higher malignancy and poorer prognostic outcome (Chu et al 2008, Lee and Kim 2009, De Almeida et al 2015, Yang and Al-Hendy 2018).

3.5 Application of p27 in neurodegeneration and PD

p27 has been identified as an important biological regulator of neuronal differentiation (Ngyuen et al 2006, Biçer et al 2017, Perearnau et al 2017), and several transcriptional programs have been shown to be related to different neurodegenerative diseases, including PD (Bachs et al 2018). Furthermore, p27 has been shown to repress α-syn expression in a mechanism involving p130-E2F, suggesting an important implication of p27 in the etiology of the disease (Gallastegui et al 2018). The main focus of this work is to elucidate the possible role of p27 on DA neurogenesis. *In vivo*, we are investigating the differences in the developing midbrain of p27-deficient and wild-type mice. *In vitro*, we are comparing the effects of p27 deficient, p27-recovery and p27-overexpressing pluripotent stem cells. This knowledge could expand our understanding of DA neuron development, which would be of interest for improving current protocols of DA neuron differentiation *in vitro* from different types of stem cells and help develop a reliable source of these cells for clinical use in cell replacement therapies for the treatment of PD.

4. STEM CELLS AND THEIR APPLICATION IN PD

Stem cells are unspecialized cells with the ability to self-renew. In specific conditions, these cells begin to differentiate, and depending on the context, give rise to more specialized cell types and can be classified into different types based on their differentiation potential. Pluripotent stem cells (PSCs) are cells that can give rise to any cell of the organism, from the three germ layers (endoderm, mesoderm and ectoderm). Multipotent stem cells (MSCs) are more specialized cells that can give rise to all the cells of a given lineage (for example, neural stem cells can give rise to all the cells of the nervous system). Unipotent stem cells (USCs) are the most specialized stem cell which can give rise to cells of a certain tissue. Due to their properties, PSCs and MSCs are currently considered the best sources for developing new treatment options for PD (reviewed in Palmer and Liste 2016, Palmer et al 2018).

4.1 Stem Cell Technology and PD

In PD research, the two main types of stem cells currently being investigated as potential treatment options are PSCs and MSCs. The type of PCSs being used are embryonic stem cells (ESCs) and induced PSCs (iPSCs), while the type of MSCs include neural stem cells (NSCs) and mesenchymal stem cells (MeSCs). DA neurons have been efficiently derived from ESCs (Chambers et al 2009, Kriks et al 2011, Kirkeby et al 2012, Grealish et al 2014), iPSCs and NSCs, (Villa et al 2009, Courtois et al 2010) while MeSCs are currently being investigated for

their potential neuroprotective qualities (Glavaski-Joksimovic and Bohn 2013, Palmer et al 2018). In this work, we focus on the use of ESCs, iPSCs and NSCs.

4.1.1 Embryonic Stem Cells

ESCs are naturally pluripotent cells obtained from the inner cell mass of the blastocyst that forms about one week after fertilization of the human embryo (Thomson et al 1998). The discovery of these cells offered a new approach to biomedical research and regenerative medicine, and provided new ways to overcome issues of donor tissue shortage and implant rejection, as well as the possibility to obtain and purify specific cell types to be used for cell

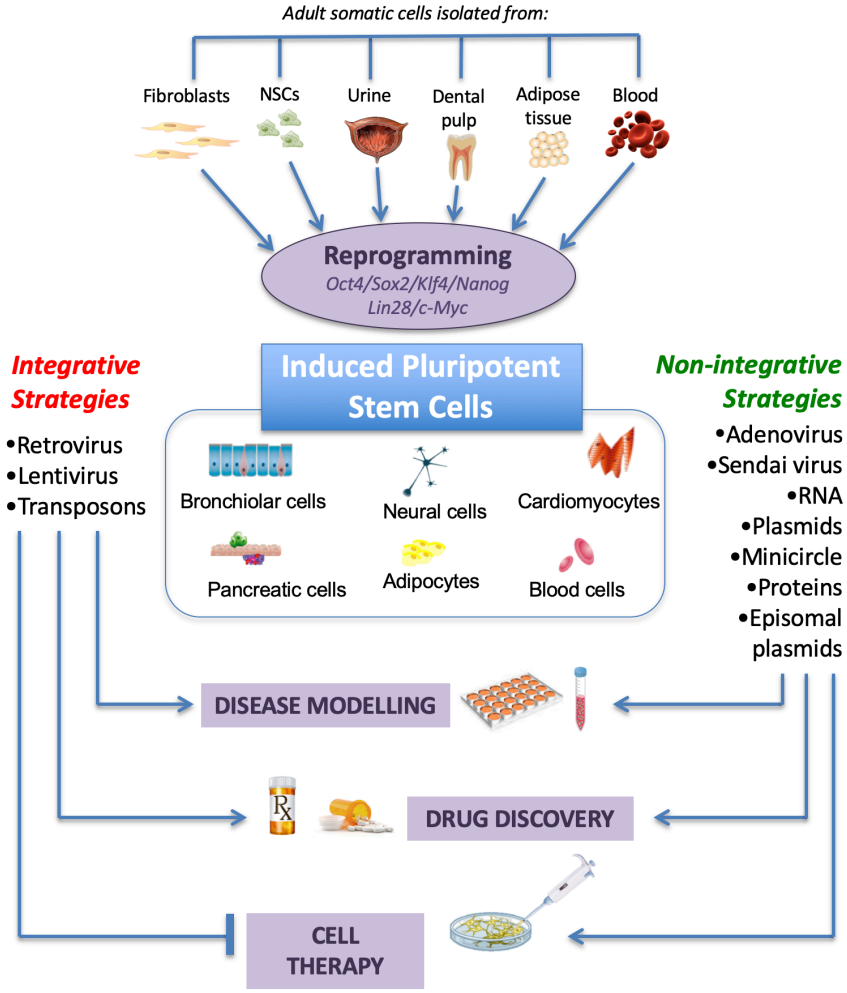

Figure I.7: Application of iPCSs in disease modeling, drug discovery and cell therapy. Adult somatic cells can be reprogrammed using specific genes to induce pluripotency. Once cells express these genes endogenously, they can be used to obtain any cell from the three germ layers. iPSCs have incredible value and potential, as they can be sourced from adult somatic cells with no associated ethical issues. Strategies using integrative vectors can be used for disease modeling and drug discovery, while non-integrative strategies are also being explored for their potential use as cell replacement therapies (Adapted from Revilla et al 2015).

replacement therapies, disease modeling and drug screening (He et al 2003). However, despite their promise and potential, the main limitation of their widespread use is the high ethical concern associated with their isolation from aborted embryos. For this reason, finding a new source of PSCs was intensely researched for almost two decades.

4.1.2 Induced Pluripotent Stem Cells

In 2006, Takahashi and Yamanaka made a remarkable breakthrough in stem cell research with the discovery of what we now know as iPCSs. These cells were adult somatic cells that, upon the addition of the four factors Oct4, Sox2, Klf4 and c-myc, Yamanaka and his team were able to reprogram the differentiated state of these adult cell, reverse their specification and return them to a pluripotent state (Figure I.7; Takahashi and Yamanaka 2006, Takahashi et al 2007, Yu et al 2007). These new cells showed characteristics almost identical to ESCs, including: cell morphology, the expression of pluripotency markers, epigenetic changes, ability to generate cells of all three germ layers *in vitro* and *in vivo* (by forming teratomas) and the ability to generate viable chimeras (Takahashi and Yamanaka 2006).

Today, a variety of strategies and protocols have been developed based on the basic concept of differentiating pluripotent stem cells to neuroprogenitor cells, expanding the population and finally guiding differentiation to DA neurons with specific factors implicated in proper DA development (Freed et al 2011, Kirkeby et al 2012, Grealish et al 2014). The most effective protocols involve early dual SMAD inhibition (Chambers et al 2009), high levels of Shh for early induction of FP specification (Fasano et al 2010), GSK3-ß inhibition (Kriks et al 2011) and the addition of certain transcription factors such as Lmx1a (Friling et al 2009) and Wnts (Andersson et al 2013).

However, an optimized differentiation protocol for the development of safe and viable dopaminergic neurons for large-scale cell replacement clinical application is still lacking. The work in our lab is aimed towards improving the development of such protocols, by studying novel factors that might be important for proper DA neuron development.

4.1.3 Neural Stem Cells

NSCs are a type of multipotent stem cells frequently used in PD research. These cells are more differentiated than PSCs and have a more limited differentiation capacity. Specifically, NSCs give rise to precursors that grow and differentiate into cells making up neural tissue, including neurons and glia. NCSs can be acquired from the fetal, neonatal and adult brain or

from the directed differentiation of pluripotent stem cells. (Martínez-Morales and Liste 2012). Neural precursor cells obtained from the human VM are considered the best candidates for cell therapies in PD, but as mentioned above, their widespread use for large scale clinical application is limited. Apart from high ethical concerns, these cells have unstable phenotypes, present reduced growth potential, and survive poorly after grafting (Villa et al 2009, Martínez-Serrano and Liste 2010, Martínez-Morales and Liste 2012).

4.2 Stem Cell Therapy for PD in Clinical Trials

Several open-label clinical trials involving the intrastriatal transplantation of human fetal mesencephalic tissue has provided proof of principle that stem cell replacement therapy can be a clinically competitive treatment option for PD (Barker et al 2013, Palmer et al 2016, Björklund and Lindvall 2017). These trials showed that transplanted tissue is able to generate DA neurons capable of re-innervating the denervated striatum, restoring striatal dopamine

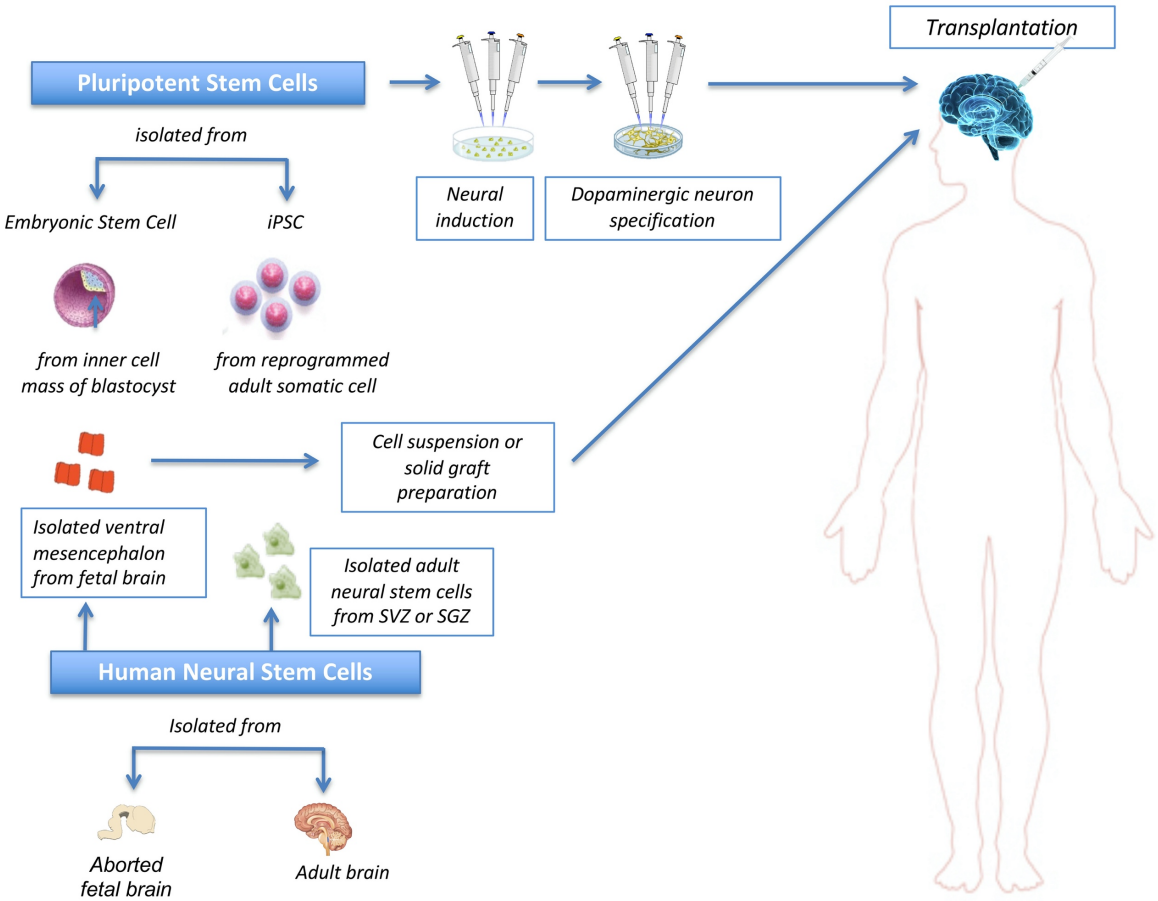

Figure I.8: Stem cell therapies in PD. PSCs such as ESCs and iPSCs can be used to obtain DA neurons, by first inducing a neural identity and later specifying these cells towards a DA neuron phenotype. NSCs sourced from the fetal brain are currently the best option for cell replacement therapies in PD, and can be administered as cell suspensions or as solid grafts. However, high ethical concerns with using fetal tissue limits their widespread clinical use. (Adapted from Palmer et al 2018).

release and providing significant symptomatic relief in some patients (Figure I.8; Lindvall et al 1989, Lindvall et al 1990, Freed et al 1992, Spencer et al 1992, Piccini et al 2000, Kefalopoulou et al 2014). The success and excitement that emanated from these initial trials led the NIH to approve two double-blind, placebo-controlled studies (Freed et al 2001, Olanow et al 2003). Neither of these trials, however, were successful in meeting their primary end-point, and the inconsistent results, both between and within trials, has made it difficult for further transplantation trials to be approved. Currently, the TRANSEURO trial funded by the European Union is ongoing, whose main objective is to standardize transplant procedures using fetal tissue in order to create a template protocol for clinical trials, and hopefully prove the efficacy of such treatment options for PD with improved patient selection, tissue preparation, tissue delivery and immunosuppressive treatments (transeuro.org.uk).

However, the use of fetal tissue is limited for large-scale clinical use, due to technical issues with tissue procurement and high ethical concerns. For this reason, a more reliable source of cells for replacement therapies must be found, with the goal of developing a uniform source of dopaminergic neurons (discussed above).

4.3 Advantages and Challenges

The discovery of stem cells has revolutionized biomedical research, as it has provided us a tool that can be manipulated in an unlimited number of ways to study specific disease processes, test new drugs and to investigate new therapeutic alternatives, based on the use of these cells to replace those damaged or lost due to pathological processes.

However, before stem cells can be approved for clinical applications in PD, they must first meet several strict safety requirements. A general target of using stem cell technology to obtain DA neurons is to obtain cells equivalent to those of human VM. When transplanted, these cells must be able to survive, integrate into the host circuitry by re-innervating the striatum without tumor formation or evoking an immune response. Furthermore, they need to significantly improve motor symptoms, not cause side effects including the development of involuntary movements such as dyskinesias (Lindvall and Kokaia 2009, Barker 2014, Lindvall 2015b).

Although great advancements have been made in the field of stem cell therapies for PD and in our knowledge of fundamental processes involved in DA neuron development, there is still no optimized protocol for the development of these neurons *in vitro* for large scale clinical applications. The focus of this thesis has been studying novel factors involved in DA neuron development, with the general goal of contributing to the improvement of current protocols, by

increasing homogeneity of DA neuron production. Based on previous results, including one study showing that increased levels of p27 in VM neurospheres favored the differentiation of these cells (Sacchetti et al 2009), this work has studied the effects this cell cycle protein has on the development and differentiation of DA neurons, both *in vivo* and *in vitro,* whose effects in the context of the VM have not yet been described.

O B J E C T I V E S

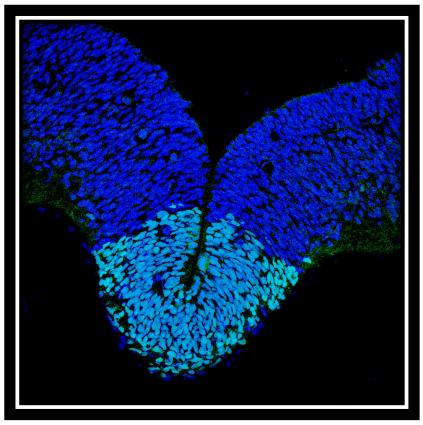

OBJECTIVES

Our general objective is to improve the knowledge of DA neuron development, which could assist in improving the differentiation of these neurons *in vitro* for possible future therapies to help treat PD.

The presented work had two main objectives: 1) to study the effects of p27 deficiency on the development of DA neurons *in vivo* and 2) develop cellular models to study the effects of p27 on the differentiation of DA neurons *in vitro*.

In order to study these objectives in detail, the specific objectives were as follows:

1.) Establish an expression pattern for p27 in the developing embryonic mouse midbrain in relation to factors important for proper DA neuron development.

2.) Study the effects of p27 deficiency on different stages of embryonic mouse midbrain development.

3.) Study possible mechanisms to explain the observed effects of p27 deficiency *in vivo*.

4.) Study the effects of p27 deficiency on VM primary cultures.

5.) Generate and establish a cell line of mouse induced pluripotent stem cells (miPSC) from p27 deficient and p27 control mouse embryonic fibroblasts to study the effects of p27 deficiency on DA neuron development *in vitro.*

6.) Generate and establish a cell line of miPSCs to study the re-introduction of p27 into p27 deficient cells (from here on “p27 recovery”) and its effect on DA neuron development *in vitro*.

7.) Generate and establish a cell line of miPSCs to study p27 overexpression in p27 control cells and its effect on DA neuron development *in vitro*.

MATERIALS & METHODS

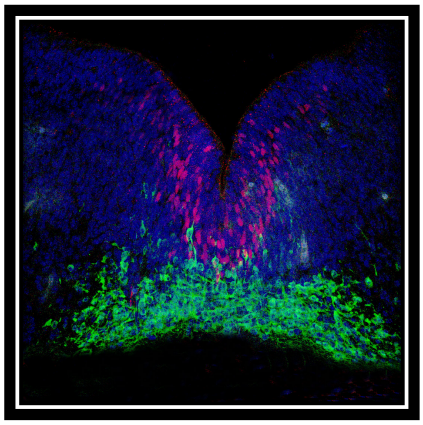

1. *IN VIVO*

1.1 Ethics statement

Mice were housed, bred and treated in accordance with protocols approved by local ethics committees at the Instituto de Salud Carlos III (CBA-PA-97-2010). p27 null mice were obtained as previously described (Fero et al 1996) and animal work was done in accordance with national and European legislation regarding the use of laboratory animals.

1.2 Genotyping

Standard PCR analysis was performed to confirm genotypes of mice born to maintain the p27-null mouse line. DNA was extracted from tail samples by first adding 2M NaOH + 0.5M EDTA in H_2O, and placed in a thermal block set to 95˚C for 1 hour. Then, 1M Tris-HCl (pH 7.5) in H_2O was added, samples were centrifuged at 2000 rpm for 10 minutes (or until a pellet formed) and the supernatant was recovered. PCR was carried out using specifically designed primers (Table 1) in a SimpliAmp^{TM} Thermal Cycler (Applied Biosystems), with the following optimized program: 1 cycle of 94˚C for 3 minutes, 40 cycles of 94˚C for 30 seconds, 59˚C for 30 seconds and 72˚C for 1 minute, 1 cycle of 72˚C for 10 minutes and finally cooled to a holding temperature of 4˚C. The samples were then subjected to electrophoresis on a 1.5% Agarose (Lonza) gel at 80V. p27+/- females were mated with p27+/- males to generate p27-/- embryos, and PCR was also needed to confirm the genotypes of embryos obtained for analysis. For this purpose, DNA was extracted from embryo tissue by adding 2M NaOH + 0.5M EDTA in H_2O, then placed in a thermal block set to 95˚C, and tissue dissociation was checked every 10 minutes. Once the tissue had dissociated, 1M Tris-HCl (pH 7.5) in H_2O was added, samples were centrifuged at 2000 rpm for 10 minutes (or until a pellet formed) and the supernatant was recovered. The PCR was then carried out as described above.

Table 1: Primers used for genotyping

Primer Pair	Sequence
p27+/+ Forward	5’-TGGAACCCTGTGCCATCTCTAT -3’
p27+/+ Reverse	5’-AACCCAGCCTGATTGTCTGACGAG-3’
p27-/- Forward	5’-TGGAACCCTGTGCCATCTCTAT -3’
p27-/- Reverse	5’-CCTTCTATCGCCTTCTTGACG -3’

1.3 Embryo brain section preparation

For analysis of embryonic brains, mice were mated overnight, and at noon the following day, observed plugs were considered E0.5. Mothers were sacrificed at days equivalent to embryonic ages E11.5, E12.5, E13.5 and E14.5 at which time embryos were dissected out of the uterine horns and cleaned with cold Phosphate buffered saline (PBS) 1X. Brains were left in the developing skull to preserve morphology, and fixed in 4% paraformaldehyde (PFA) for 2 hours. Brains were then washed 3 x 10 minutes in PBS 1X and transferred to 30% sucrose for at least 24 hours. Finally, brains were included in a solution consisting of 15% sucrose + 7.5% gelatin, and frozen at -80ºC with isopentane (Sigma) until used. 15µm serial coronal brain sections were obtained on a cryostat (Leica) and mounted on Superfrost Ultra Plus® microscope slides (Thermo Scientific). Heterozygous (p27+/-) females were crossed with heterozygous males to generate p27-/- embryos, which were carefully genotyped as described above. p27+/+ embryos were used as controls.

2. *IN VITRO:* PRIMARY CULTURES

2.1 Mouse Embryonic Fibroblast (MEF) extraction

Time mated females were sacrificed at days equivalent to embryonic ages E13.5 or E14.5, when embryos were extracted from the uterine horns and cleaned with cold PBS 1X. Internal organs and heads were removed and saved for genotyping. The remaining skin was cleaned and rinsed, and manually dissociated with the help of a sterile razor blade. Each embryo was added to a separate 15mL centrifuge tubes containing 500µL trypsin-EDTA 0.25% (Thermo Scientific) and left for 30 minutes at 37ºC. Trypsin was deactivated by adding 2mL of MEF medium (Table 2), and the cells were resuspended until completely dissociated. The cells were then centrifuged for 2 minutes at 900 rpm and the supernatant removed. 2mL of fresh MEF medium was added, and the process of centrifugation was repeated 2 more times. The last centrifugation was left for 5 minutes at 900 rpm. Cells were then seeded at a density of one embryo per 60-120cm^2 depending on the size of the pellet and maintained in an incubator set to 37ºC and 5% CO_2. MEFs that were not needed were frozen at -80ºC for future use and only early-passage MEFs (less than 5 passages) were used for our experiments.

2.2 VM primary culture

Primary cultures of VM precursors were dissected directly from the E13.5 embryonic brain with the aid of a magnifier under sterile conditions in a horizontal laminar-flow hood. In the developing rodent brain, the midbrain is a tube recognized by it characteristic curve behind the

cortex, which was removed and placed in cold, sterile PBS 1X with 0.05% glucose. Straight surgical micro-scissors were then used to remove the upper curve of the midbrain, corresponding to the dorsal mesencephalon (DM). The bottom curve, corresponding to the VM was flattened and recognized by its "butterfly" shape, from which the edges were trimmed with a sterile razor blade, if necessary. Each dissected VM was kept separate and manually dissociated. Bodies were saved for genotyping. Cells were seeded on poly-L-lysine (10µg/mL, Sigma) and laminin (1.5µg/mL, Sigma) treated plastic culture plates. In the case of using glass cover slips, these were treated with 30µg/mL poly-L-lysine and 1.5µg/mL laminin. 150,000 cells were initially seeded in 30µL drops for 15 minutes to promote adhesion, and later maintained in a chemically defined medium (N2:B27 medium) consisting of N2 medium (Table 3) in a 1:1 ratio with NB:B27 medium (Table 4) supplemented with Shh (200ng/µL, Peprotech), Fgf8 (25ng/µL, Peprotech) and Fgf2 (10ng/µL, Preprotech) for 3 days and maintained in an incubator set to 37ºC and 5% CO_2.

Table 2: MEF Medium

Component	Final Concentration	Source	Reference
DMEM*	1X	Lonza	12-604F
Fetal Bovine Serum (FBS)	10%	Biological Industries	04-007-1A
200 mM L-Glutamine	1%	Lonza	17-605E
P/S**	0.5%	Lonza	SV30010

*Dulbecco's modified eagle medium **Penicillin/Streptomycin

Table 3: N2 Medium

Component	Final Concentration	Source	Reference
DMEM:F12 with GlutaMAX-I	1X	Gibco	31331-028
20% AlbuMAX in DMEM:F12	0.26%	Gibco	11020-021
1M HEPES	5mM	Gibco	15630-056
30% glucose in DMEM:F12	0.6%	Merck	1.04074.1000
N2 supplement	1%	Gibco	17502-048
NEAA*	1%	Gibco	11140-035
P/S	0.5%	Lonza	SV30010

*Non-essential amino acids

Table 4: NB:B27 Medium

Component	Final Concentration	Source	Reference
Neurobasal	1X	Gibco	21103-049
B27 Supplement	1%	Gibco	17504-044
200 mM L-Glutamine	1%	Lonza	17-605E
P/S	0.5%	Lonza	SV30010

3. *IN VITRO:* CELL LINES

3.1 Cells and culture conditions

3.1.1 PA6 stromal cells

PA6 mouse stromal cells were maintained as monolayer cultures in PA6 medium (Table 5) on plates pre-treated with 0.1% gelatin. For neural induction, they were inactivated with Mitomycin (Roche) at 1µg/mL overnight and seeded at a density of 50 x 10^3 cell/cm^2. Cells were maintained in an incubator set to 37ºC and 5% CO_2.

Table 5: PA6 medium

Component	Final Concentration	Source	Reference
α-MEM*	1X	Gibco	22571-038
FBS	10%	Biological Industries	04-007-1A
200 mM L-Glutamine	1%	Lonza	17-605E
P/S	0.5%	Lonza	SV30010

*Minimum essential medium with α-modification

3.1.2 mESCs and miPSCs

mESCs and miPSCs were grown as monolayer cultures in SRM medium (Table 6) supplemented with Leukemia inhibitory factor (Lif, 1000U/mL; Millipore). Cells were allowed to grow until ~80% confluence, at which time they would be passed. Cells were grown in culture plates pre-treated with 0.1% gelatin and maintained in an incubator set to 37ºC and 5% CO_2.

Table 6: SRM Medium

Component	Final Concentration	Source	Reference
KO-DMEM*	1X	Gibco	10829-018
Serum replacement (SR)	15%	Gibco	11520366
200 mM L-Glutamine	1%	Lonza	17-605E
NEAA	1%	Gibco	11140-035
ß-mercaptoethanol	0.1 mM	Sigma	M6250-250M
P/S	0.5%	Lonza	SV30010

*Knock Out-DMEM

3.2 Reprogramming MEFs to miPSCs

After extracting MEFs and properly genotyping the embryos, mouse iPSC p27+/+ (miPSC WT) and mouse iPSC p27-/- (miPSC p27KO) cells were reprogrammed from MEFs by retroviral infection (kindly provided by Dr. Han Li and Manuel Serrano, Li et al 2012) or reprogrammed using the CoMIP plasmid according to the diagram in Figure M.1. CoMIP is an

optimized mini-intronic plasmid containing the four pluripotency genes *Sox2*, *Oct4, Klf4* and *c-Myc* allowing for efficient reprogramming after a single transfection (Diecke et al 2015). 5 x 10^6 cells were co-nucleofected with the CoMIP and pMax-GFP plasmids using the A-23 program of the Amaxa Nucleofector system (Lonza), according to the manufacturers instruction. After nucleofection, MEFs were seeded in MEF medium (Table 2) supplemented with ascorbic acid (AA; 50µg/mL; Sigma) and sodium butyrate (SB; 0,2 mM; Tocris). Two days after nucleofection, the medium was changed to SRM medium (Table 6) supplemented with Lif (1000U/mL), AA (50µg/mL) and SB (0,2 mM). Once colonies began to form, cells were passed and left in SRM medium supplemented with Lif (1000U/mL).

MEFs from p27-/- embryos E13.5(1) and E13.5(9) were reprogrammed to become miPSC p27KO(1) and miPSC p27KO(9), respectively. MEFs from p27+/+ embryos were reprogrammed to become miPSC WT controls.

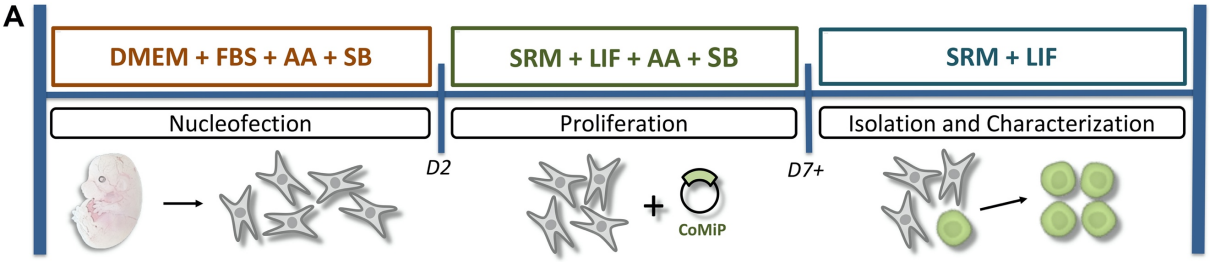

Figure M.1: Reprogramming Protocol. Diagram representing the reprogramming protocol followed. MEFs were isolated from p27+/+ and p27-/- embryos and subjected to nucleofection with the CoMIP plasmid until stem cell colonies began to appear.

3.3 Nucleofection with pBabep27

miPSC p27KO$^{p27\ recovery}$, R1 mESC$^{p27\ overexpression}$ and miPSC WT$^{p27\ overexpression}$ cells were obtained by nucleofection with the plasmids pBabe-p27Kip1-puromycin (Li et al 2012) and pMax-GFP into 2 x 10^6 cells using the A-13 program of the Amaxa Nucleofector system (Lonza), according to the manufacturer's instruction. The empty vector pBabe-puromycin was used to obtain control cells. Cells were subject to selection for two weeks with puromycin (2µg/mL medium, Apollo Scientific Limited) to eliminate non-resistant cells, forming a heterogeneous cell line, according to the diagram in Figure M.2. A limiting dilution protocol was then followed to obtain homogenous cell populations, from which several clones were obtained and at least two clones were selected for each experiment. Once selected, these cells were maintained in ordinary SRM medium (Table 6) supplemented with Lif (1000U/mL).

3.4 Nucleofection with pCX-NeuroD1

miPSC p27KO^{NeuroD1} cells were obtained by nucleofection with the plasmids pCX-NeuroD1-neomycin (Boutin et al 2010) and pMax-GFP into 2 x 10^6 cells using the A-13 program of the Amaxa Nucleofector system (Lonza), according to the manufacturer's instruction. The empty vector pCX-neomycin was used to obtain control cells. Cells were subject to selection for two weeks with neomycin (150µg/mL medium, Gibco) forming a heterogenous cell line, according to the diagram in Figure M.2. A limiting dilution protocol was followed as described above, and two p27KO^{NeuroD1} clones were chosen. After selection, these cells were maintained in ordinary SRM medium (Table 6) supplemented with Lif (1000U/mL).

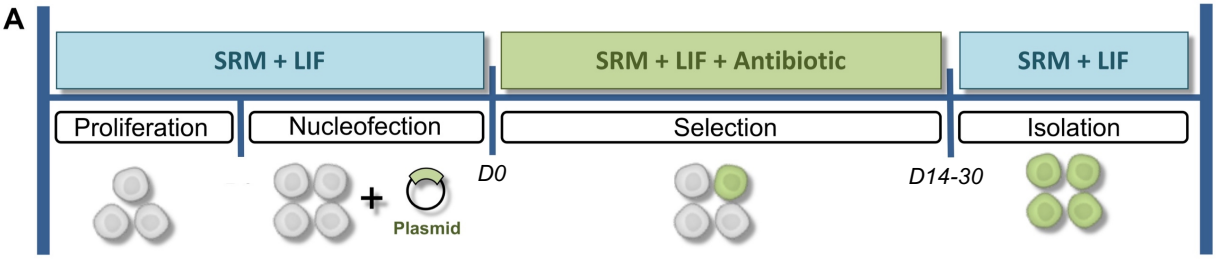

Figure M.2: Nucleofection Protocol. Diagram representing the nucleofection protocol followed. miPSCs were nucleofected with the appropriate plasmids, and subject to selection with the corresponding antibiotic treatment (puromycin or neomycin). After selection, individual colonies were isolated .

3.5 Embryoid Body formation and differentiation

Embryoid bodies (EBs) were formed by seeding 500 cells in 20µL drops consisting of SRM medium (Table 6) and left in suspension for 3 days. On day 3, EBs were transferred individually to plates pre-treated with 0.1% gelatin for at least 30 minutes. Once transferred, EBs were left in SRM medium, an un-specified differentiation medium, in order to promote spontaneous differentiation and confirm the differentiation potential of our iPSCs.

3.6 Differentiation of DA neurons

The differentiation of miPSCs to DA neurons was achieved by adapting the protocol described by Barberi et al 2003, consisting of SRM medium (Table 6) supplemented with Shh (200ng/µL, Peprotech) and Fgf8 (25ng/µL, Peprotech), N2 medium (Table 3) supplemented with Shh (200ng/µL, Peprotech), Fgf8 (25ng/µL, Peprotech) and Fgf2 (10ng/µL, Preprotech) and N2 medium (Table 3) supplemented with AA (100uM), BDNF (Brain derived neurotrophic factor; 20ng/µL) and GDNF (20ng/µL) according to the timeline presented in Figure M.3. Cells

were seeded at low density (60 cells/cm^2) in order to promote the formation of colonies, and grown over previously inactivated PA6 stromal cells.

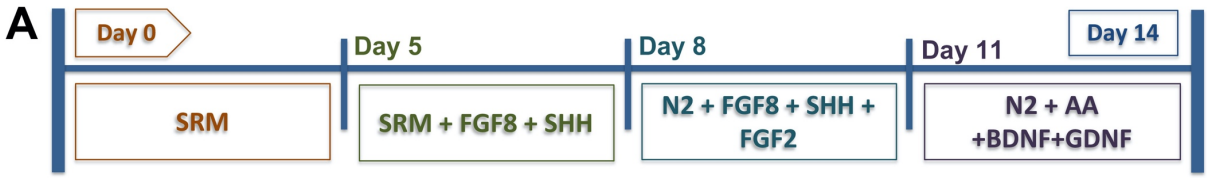

Figure M.3: PA6 Differentiation Protocol. Diagram representing the differentiation protocol adapted from Barberi et al 2003.

4. EXPERIMENTAL TECHNIQUES

4.1 Bacterial transformation for plasmid expansion and purification

1 vial of TOP10 competent bacterial cells (Thermo Scientific) was added to previously chilled, individual polystyrene tubes and maintained on ice for 15 minutes. 50ng of plasmid was added to each tube and left on ice for another 15 minutes. All tubes were then subject to thermic shock by being placed in a water bath set to 42ºC for 45 seconds to introduce the plasmid into the bacteria. After 45 seconds, tubes were placed on ice for 2 minutes. Lysogeny broth (LB) agar previously heated to room temperature was added to each tube for a final volume of 1mL. Tubes were then incubated with agitation for 1 hour at 37ºC. Each tube was then seeded on LB agar plates containing ampicillin (50µg/mL) at a concentration of 1/10 (100µL of bacterial mixture) or 9/10 (900µL of bacterial mixture centrifuged to eliminate excess supernatant) and left at 37ºC for 24 hours. The following day individual colonies were isolated and placed in 50mL centrifuge tubes containing 6mL LB agar with ampicillin (50-100µg/mL). Tubes were then incubated with agitation at 37ºC for 24 hours. The following day, plasmids were isolated using the Plasmid Mini Kit (Qiagen) according to the manufacturer's instruction.

4.2 Immunohistochemistry (IHC) and image analysis

Frozen microscope slides were allowed to dry at room temperature for at least 1 hour, de-gelatinized at 37˚C for 20 minutes and placed in a humidity chamber. Sections were then washed with PBS 1X, left in blocking solution (Table 7) at room temperature for 1 hour and incubated with primary antibody diluted in blocking solution overnight at 4˚C. After removal of the primary antibody, slides were rinsed in washing solution (Table 8) and incubated with the corresponding secondary antibody diluted in blocking solution for 2 hours at room temperature. All primary antibodies used are listed in Table 9 and secondary antibodies are

listed in Table 10. After washing with PBS 1X, the slides were incubated with Hoechst 33258 (0.2µg/mL, Invitrogen) diluted in PBS 1X for 10 minutes and mounted using Mowiol (Sigma) with DAPCO (Sigma) to preserve fluorescence. A confocal microscope (Leica SP5) was used for image capture. Total number positive cells for each marker were counted using Adobe Photoshop CC, and total areas were calculated using ImageJ Fiji.

Table 7: Blocking Solution for IHC

Component	Final Concentration	Source	Reference
PBS	1X	Lonza	BE17-515Q
10% Triton X100	0.3%	BioRad	161-0407
Normal Horse Serum (NHS)	5%	Gibco	16050-130
10% Bovine Serum Albumin (BSA)	0.1%	Sigma	A7906

Table 8: Washing Solution for IHC

Component	Final Concentration	Source	Reference
PBS	1X	Lonza	BE17-515Q
10% Triton X100	0.3%	BioRad	161-0407

Table 9: Primary Antibodies used for IHC

Marker	Host	Dilution	Source	Reference
p27	Mouse	1:100	BD Biosciences	610241
TH	Rabbit	1:300	Pel Freez	P40101-150
TH	Sheep	1:300	Pel Freez	P60101-150
Nurr1	Rabbit	1:100	Santa Cruz	SC-5568
Pitx3	Rabbit	1:1000	Gift; M. Smidt (UVA, NL)	N/A
Ki67	Rabbit	1:100	Invitrogen	MA5-14520
Sox2	Rabbit	1:300	Millipore	AB5603
Ngn2	Goat	1:100	Santa Cruz	SC-19233
Foxa2	Goat	1:50	Santa Cruz	SC-6554
Lmx1a	Rabbit	1:300	Millipore	AB10533

Table 9 Continued: Primary Antibodies used for IHC

Marker	Host	Dilution	Source	Reference
Casp3	Rabbit	1:500	Cell Signaling	9664
BIII-Tub	Mouse	1:1000	Biolegend	801202
Gfap	Mouse	1:300	BD Pharmagen	556327
NeuroD1	Rabbit	1:750	Millipore	ABE991

Table 10: Secondary Antibodies

Antibody	Host	Dilution	Source	Reference
Alexa Flour 555 (red)	Donkey α-mouse	1:500	Life Technologies	A31570
Alexa Flour 555 (red)	Donkey α-rabbit	1:500	Life Technologies	A31572
Alexa Flour 555 (red)	Donkey α-goat	1:500	Life Technologies	A21432
Alexa Flour 488 (green)	Donkey α-mouse	1:500	Life Technologies	A21202
Alexa Flour 488 (green)	Donkey α-rabbit	1:500	Life Technologies	A21206

4.3 Immunocytochemistry (ICC) and image analysis

Cells were fixed in 4% PFA for 10 minutes, washed 3 x 10 minutes with PBS 1X and left in blocking solution (Table 11) at room temperature for 30 minutes and incubated with primary antibody diluted in antibody solution (Table 12) overnight at 4˚C using the primary antibodies listed in Table 13. Primary antibodies were revealed with the corresponding secondary antibody (Table 10) diluted in antibody solution for 1 hour at room temperature. Nuclei were stained with Hoechst 33258 (0.2µg/mL, Invitrogen) diluted in PBS 1X for 10 minutes. A fluorescence microscope (Leica DM IL LED) equipped with a digital camera (Leica DFC345FX) was used for image capture. For analysis, 6 separate fields were captured from at least 3 individual wells, per experiment. Each experiment was replicated at least 3 times (n=3).

Table 11: Blocking solution for ICC

Component	Final Concentration	Source	Reference
PBS	1X	Lonza	BE17-515Q
Triton X100 (10%)	0.3%	BioRad	161-0407
NHS	5%	Gibco	16050-130

Table 12: Antibody solution for ICC

Component	Final Concentration	Source	Reference
PBS	1X	Lonza	BE17-515Q
Triton X100 (10%)	0.3%	BioRad	161-0407
NHS	5%	Gibco	16050-130

Table 13: Antibodies used for ICC

Marker	Host	Dilution	Source	Reference
p27	Mouse	1:100	BD Biosciences	610241
TH	Rabbit	1:300	Pel Freez	P40101-150
TH	Sheep	1:300	Pel Freez	P60101-150
Nurr1	Rabbit	1:100	Santa Cruz	SC-5568
Ki67	Rabbit	1:100	Invitrogen	MA5-14520
Sox2	Rabbit	1:300	Millipore	AB5603
Casp3	Rabbit	1:500	Cell Signaling	9664
BIII-Tub	Mouse	1:1000	BioLegend	801202

4.4 BrdU Treatment

For proliferation studies, we used the thymidine analog 5-bromo-2'-deoxyuridine (BrdU) that incorporates into newly synthesized DNA of actively dividing cells. For *in vivo* studies, we injected pregnant females with 50µg BrdU/g of body weight at days equivalent to E11.5 and sacrificed 24 hours later at E12.5. Tissue was then processed as described above (Section 1.3). For IHC studies, slides were prepared as described in Section 4.2. After de-gelatinizing, slides were treated with 2M HCl for 30 minutes at 37ºC. Slides were washed 3 x 10 minutes with PBS 1X to equilibrate the pH and IHC was completed as normal. HCl treatment was repeated if necessary. For double IHC studies, slides were treated with HCl after incubating

with the first primary antibody. For *in vitro* studies, BrdU was added to the medium of differentiating cells (V_f = 5µM BrdU) and left for 4 hours. After fixing the cells with 4% PFA (described above, Section 4.3), cells were treated with 2M HCl for 30 minutes at 37ºC and washed 3 x 10 minutes with PBS 1X to equilibrate the pH. ICC was performed as described in Section 4.3. HCl treatment was repeated if necessary. For double ICC studies, cells were treated with HCl after incubating with the first primary antibody.

4.5 Western Blot

For western blot (WB) analysis, 25µg of protein sample was boiled for 5 minutes and subjected to electrophoresis on a 10% SDS-PAGE gel using the Mini-PROTEAN Tetra Cell system, according to the manufacturer's instruction. Gels were transferred to nitrocellulose membranes (GE Healthcare), blocked in 5% nonfat-milk with 0.05% Tween 20 (Sigma) in Tris buffered saline (TBS) for 1 hour at room temperature and incubated with primary antibody (Table 14) at 4˚C overnight. The blots were developed using peroxidase-conjugated horse anti-mouse (HAMPO 1:2500, Atom) or peroxidase-conjugated goat anti-rabbit (GARPO 1:2000, Atom). Chemiluminescent HRP substrate (Millipore) was used to visualize the secondary antibody according to the manufacturer's instruction.

Table 14: Antibodies used for WB

Marker	Host	Dilution	Source	Reference
B-actin	Mouse	1:1000	Sigma	A5441
p27	Mouse	1:1000	BD Biosciences	610241
TH	Rabbit	1:500	Pel-Freez	P40101-150
NeuroD1	Rabbit	1:1000	Millipore	ABE991
Sox2	Rabbit	1:100	Millipore	AB5603
Oct4	Rabbit	1:500	Santa Cruz	SC-9081

4.6 RNA extraction

For *in vivo* studies, VM tissue was dissected directly from the brain of E11.5, E12.5, E13.5 and E14.5 embryos with the aid of a magnifier under sterile conditions. As described above (Section 2.2), the midbrain of the developing rodent brain is a tube recognized by its characteristic curve behind the cortex, which was removed and placed in cold, sterile PBS 1X.

Straight surgical micro-scissors were then used to remove the upper curve of the midbrain, corresponding to the dorsal mesencephalon (DM). The bottom curve, corresponding to the VM was flattened and recognized by its "butterfly" shape, from which the edges were trimmed with a sterile razor blade, if necessary. Each dissected VM was maintained separately and bodies were saved for genotyping. Due to the smaller size of the midbrain at E11.5, after genotyping, at least 2 VMs of the same genotype were combined in order to provide enough tissue for RNA extraction.

For *in vitro* studies, cells in feeder-free conditions (such as cells in proliferation and EBs) were collected for RNA extraction directly from the well, first by washing 2-3 times with PBS 1X and then by adding RLT lysis buffer. Cells with feeders were left in a solution of Hank's Buffered Saline Solution (HBSS) with HEPES for at least 30 minutes, and colonies were later lifted from the feeder layer with the aid of a syringe.

Total RNA extraction was performed using RNeasy Mini Isolation Kit (Qiagen), following manufacturer's instruction. RNA was quantified using the Nanodrop (Tecan) system, and the 260/280 ratio measure was used to ensure pure RNA samples.

4.7 RT-qPCR analysis

1µg of total RNA was reverse-transcribed in a two-step process, starting with a 12.8µL reaction mixture (containing 1µg RNA, 0.5µL 25mM dNTPs, 150ng random hexamer and H_20) placed in a SimpliAmp^{TM} Thermal Cycler (Applied Biosystems) set to 65ºC for 5 minutes. These tubes were then placed directly on ice for 2 minutes and 4µL 5x buffer, 2µL 0.1M DTT, 0.2µL RNasin and 1µL SuperScriptIII-RT (Life Technologies) was added to each tube, reaching a final volume of 20µL, and again placed in the thermal cycler in a program consisting of 25ºC for 10 minutes, 50ºC for 60 minutes and finally 75ºC for 10 minutes before cooling to a holding temperature of 4ºC. cDNA was analyzed by RT-qPCR using the SYBR-green system (Applied Biosystems) according to the manufacturer's instruction. 10ng total cDNA and 10µM of primers were used in a 15µL reaction mixture. Primers were specifically designed to span exon sequences for relative mRNA level quantification. All primers used are listed in Tables 15-22. An initial trial was performed testing various housekeeping genes, with *Gapdh* providing the most consistent results. All experiments were therefore normalized to *Gapdh* expression levels. Relative RNA levels were estimated using the $2^{-\Delta\Delta Ct}$ relative quantification method. RNA was extracted from 4-8 animals per genotype (n=4-8) or from at least 3 separate *in vitro* experiments (n=3).

Table 15: RT-qPCR primers-Housekeeping genes

Marker	Primer pair	Amplicon length
Actb Forward *Actb* Reverse	5'-CTAAGGCCAACCGTGAAAAG-3' 5'-ACCAGAGGCATACAGGGACA-3'	104 base pairs
Gapdh Forawrd *Gapdh* Reverse	5'-AATGTGTCCGTCGTGGATCT-3' 5'-CTGCTTCACCACCTTCTTGA-3'	78 base pairs
Tbp1 Forward *Tbp1* Reverse	5'-GGCGGTTTGGCTAGGTTT-3' 5'-TCTGGGTTATCTTCACACACCA-3'	86 base pairs
Pgk1 Forward *Pgk1* Reverse	5'-TACCTGCTGGCTGGATGG-3' 5'-CACAGCCTCGGCATATTTC-3'	65 base pairs
Hprt1 Forward *Hprt1* Reverse	5'-GGAGCGGTAGCACCTCCT-3' 5'-AACCTGGTTCATCATCGCTAA-3'	119 base pairs
Rplp0 Forward *Rplp0* Reverse	5'- ACTGGTCTAGGACCCGAGAAG -3' 5'-CTCCCACCTTGTCTCCAGTC-3'	124 base pairs

Table 16: RT-qPCR primers-DA neuron developmental markers

Marker	Primer pair	Amplicon length
p27 Forward *p27* Reverse	5'-GTTAGCGGAGCAGTGTCCA-3' 5'-TCTGACGAGTCAGGCATTTG-3'	84 base pairs
Th Forward *Th* Reverse	5'-CCCAAGGGCTTCAGAAGAG-3' 5'-GGGCATCCTCGATGAGACT-3'	106 base pairs
Nurr1 Forward *Nurr1* Reverse	5'-AGTGCCTAGCTGTTGGGATG-3' 5'-CCTCTCCGGCCTTTTAAACT-3'	64 base pairs
Pitx3 Forward *Pitx3* Reverse	5'-ACCCTCCGCTTCCAGAAC-3' 5'-GAGGCCTTCTCCGAGTCAC-3'	104 base pairs
Foxa2 Forward *Foxa2* Reverse	5'-AAGTAGCCACCACACTTCAGG-3' 5'-TGTGGCCCATCTATTTAGGG-3'	71 base pairs
Lmx1a Forward *Lmx1a* Reverse	5'-CAGCAACAGGACCAACAGAA-3' 5'-CCCACTACCATTTGTCTGAGC-3'	60 base pairs
Ki67 Forward *Ki67* Reverse	5'-TCAAGACAATCATCAAGGAACG-3' 5'-GGCGTTATCCCAGGAGACT-3'	65 base pairs
Sox2 Forward *Sox2* Reverse	5'-TCAAAGAGATACAAGGGAATTGG-3' 5'-TTTCCTTTTGAGCATTATCAGATTT-3'	76 base pairs
Ngn2 Forward *Ngn2* Reverse	5'-GACATTCCCGGACACACAC-3' 5'-AGTCTCAGATTTGACGAACATCC-3'	82 base pairs

Table 17: RT-qPCR primers-Pluripotency markers

Marker	Primer pair	Amplicon length
Sox2 Forward *Sox2* Reverse	5'-TCAAAGAGATACAAGGGAATTGG-3' 5'-TTTCCTTTTGAGCATTATCAGATTT-3'	76 base pairs
Oct4 Forward *Oct4* Reverse	5'-CTGGGCGTTCTCTTTGGA-3' 5'-GTTGTCGGCTTCCTCCAC-3'	129 base pairs
Klf4 Forward *Klf4* Reverse	5'-CGGGAAGGGAGAAGACACT-3' 5'-GAGTTCCTCACGCCAACG-3'	62 base pairs
Nanog Forward *Nanog* Reverse	5'-TTCTTGCTTACAAGGGTCTGC-3' 5'-CAGGGCTGCCTTGAAGAG-3'	95 base pairs

Table 18: RT-qPCR primers-NeuroD proteins

Marker	Primer pair	Amplicon length
NeuroD1 Forward *NeuroD1* Reverse	5'-CGCAGAAGGCAAGGTGTC-3' 5'-TTTGGTCATGTTTCCACTTCC-3'	90 base pairs
NeuroD2 Forward *NeuroD2* Reverse	5'-CGCCAAGCCAGTGTCTCT-3' 5'-CTTGACCTCAGCCAACGTG-3'	64 base pairs
NeuroD3 Forward *NeuroD3* Reverse	5'-GACCTGTCCAGCTTCCTCAC-3' 5'-TGGAGGCTAGGGGCTGTAG-3'	61 base pairs
NeuroD4 Forward *NeuroD4* Reverse	5'-CTCTTCGACTGGCAAGGAAC-3' 5'-TCTACAAATCCCTTCCCTTCAA-3'	85 base pairs
NeuroD6 Forward *NeuroD6* Reverse	5'-TCCTTCGAGGAAAGAGCATT-3' 5'-TCCTCCTCTTCTTTCTCGGTTT-3'	61 base pairs

Table 19: RT-qPCR primers-Cyclins and CDKs

Marker	Primer pair	Amplicon length
Cyclin D1 Forward *CyclinD1* Reverse	5'-TTTCTTTCCAGAGTCATCAAGTGT-3' 5'-TGACTCCAGAAGGGCTTCAA-3'	78 base pairs
Cyclin D2 Forward *Cyclin D2* Reverse	5'-GCTGTGCATTTACACCGACA-3' 5'-TCAGCTTACCCAACACTACCAG-3'	77 base pairs
Cyclin D3 Forward *Cyclin D3* Reverse	5'-GGCATACTGGATGCTGGAG-3' 5'-CCAGGTAGTTCATAGCCAGAGG-3'	77 base pairs
Cdk4 Forward *Cdk4* Reverse	5'-CCGGTTGAGACCATTAAGGA-3' 5'-GAACAATGCAGTTTGCATG-3'	76 base pairs
Cdk6 Forward *Cdk6* Reverse	5'-TTTCAGATGGCCCTTACCTC-3' 5'-ACAGGGGTGGCATAGCTG-3'	86 base pairs
Cyclin A Forward *Cyclin A* Reverse	5'-GCTCTCTACACAGTCACAGGACA-3' 5'-AAGGTCCACAAGACAAGGCTTA-3'	96 base pairs
Cyclin E Forward *Cyclin E* Reverse	5'-TTTCTGCAGCGTCATCCTC-3' 5'-TCTCTGTGGAGCTTATAGACTTCG-3'	86 base pairs
Cdk2 Forward *Cdk2* Reverse	5'-TGGTGTACAAAGCCAAAAACA-3' 5'-ACTGGGTACACCTTCAGTCTCAG-3'	89 base pairs

Table 19 Continued: RT-qPCR primers-Cyclins and CDKs

Marker	Primer Pair	Amplicon Length
Cyclin B Forward *Cyclin B* Reverse	5'-GTGTGTGAACCAGAGGTGGA-3' 5'-GGCTTGGAGAGGGATTATCA-3'	72 base pairs
Cdk1 Forward *Cdk1* Reverse	5'-CTCTATTAAAAGAACTTCGACATCCA-3' 5'-CCATGGACAGGAACTCAAAGA-3'	99 base pairs

Table 20: RT-qPCR primers-Germ layers

Marker	Primer pair	Amplicon length
Acta2 Forward *Acta2* Reverse	5'-TAACCCTTCAGCGTTCAGC-3' 5'-ACATAGCTGGAGCAGCGTCT-3'	99 base pairs
Brachyury Forward *Brachyury* Reverse	5'-CAGCCCACCTACTGGCTCTA-3' 5'-GAGCCTGGGGTGATGGTA-3'	72 base pairs
Afp Forward *Afp* Reverse	5'-GTTCTGGCATGCTGCAAA-3' 5'-CCTTTGCAATGGATGCTCTC-3'	70 base pairs
Hnf4a Forward *Hnf4a* Reverse	5'-TCCTGCAGGCAGAGGTTC-3' 5'-TCGCCATTGATCCCAGAG-3'	61 base pairs
Nestin Forward *Nestin* Reverse	5'-CTGCAGGCCACTGAAAAGTT-3' 5'-TCTGACTCTGTAGACCCTGCTTC-3'	73 base pairs
BIII-Tub Forward *BIII-Tub* Reverse	5'-GCGCATCAGCGTATACTACAA-3' 5'-TTCCAAGTCCACCAGAATGG-3'	73 base pairs

Table 21: RT-qPCR primers-Alternative phenotypes

Marker	Primer pair	Amplicon length
BIII-Tub Forward *BIII-Tub* Reverse	5'-GCGCATCAGCGTATACTACAA-3' 5'-TTCCAAGTCCACCAGAATGG-3'	73 base pairs
Gfap Forward *Gfap* Reverse	5'-ATCTTGCTCCGTTCCGAGA-3' 5'-TGGCCATTGTCATTTCTTCTT-3'	67 base pairs
GABA Forward *GABA* Reverse	5'-CCATTTCCTGGTTTTATGGTG-3' 5'-CACAGCTTCCACCAGATGC-3'	88 base pairs
Gad1 Forward *Gad1* Reverse	5'-CTGGGCCTGAAGATCTGTG-3' 5'-CAGGAAAGCAGGTTCTTGGA-3'	110 base pairs
Vglut1 Forward *Vglut1* Reverse	5'-GCAGGAGGAGTTTCGGAAG-3' 5'-CCTGCCGCTTCTCCAGTA-3'	71 base pairs
Vglut2 Forward *Vglut2* Reverse	5'-ATGGGATATGGAGCAAGTGG-3' 5'-TGACTGCTCCAGCATAGGAA-3'	87 base pairs
Glul Forward *Glul* Reverse	5'-ATGGGATATGGAGCAAGTGG-3' 5'-TGACTGCTCCAGCATAGGAA-3'	90 base pairs
Sert Forward *Sert* Reverse	5'-ACCTGGACACTCCATTCCAC-3' 5'-CCTGGAGTCCCTTTGACTGA-3'	88 base pairs
Tph2 Forward *Tph2* Reverse	5'-GAGCTTGATGCCGACCAT-3' 5'-TGGCCACATCCACAAAATAC-3'	76 base pairs

Table 22: RT-qPCR primers-Miscellaneous

Marker	Primer pair	Amplicon length
Hes1 Forward *Hes1* Reverse	5'-TGCCAGCTGATATAATGGAGAA-3' 5'-CCATGATAGGCTTTGATGACTTT-3'	126 base pairs
Hes5 Forward *Hes5* Reverse	5'-CCCAAGGAGAAAAACCGACT-3' 5'-TGCTCTATGCTGCTGTTGATG-3'	77 base pairs
Dll1 Forward *Dll1* Reverse	5'-GGGACAGAGGGGAGAAGATG-3' 5'-TCCATGTTGGTCATCACACC-3'	92 base pairs
Pax5 Forward *Pax5* Reverse	5'-GACGCTGACAGGGATGGT-3' 5'-GGGGAACCTCCAAGAATCAT-3'	94 base pairs
Mash1 Forward *Mash1* Reverse	5'-GCTCTCCTGGGAATGGACT-3' 5'-CGTTGGCGAGAAACACTAAAG-3'	70 base pairs
p57 Forward *p57* Reverse	5'-CAGGACGAGAATCAAGAGCA-3' 5'-GCTTGGCGAAGAAGTCGT-3'	118 base pairs
P21 Forward *p21* Reverse	5'- AACATCTCAGGGCCGAAA -3' 5'- TGCGCTTGGAGTGATAGAAA -3'	62 base pairs

5. STATISTICAL ANALYSIS

Statistical tests were run using GraphPad Prism 6.0. Results are shown as the average ± S.E.M. of data from 3-8 animals (n=3-8) or from 3 separate *in vitro* experiments (n=3). Mean values between two groups were compared using a two-tailed Student's t-test for independent samples. Mean values between more than two groups were compared using a one-way analysis of variance (ANOVA) followed by Tukey's post-hoc test. P-values <0.05 were considered statistically significant ($p<0.05$*, $p<0.01$**, $p<0.001$***, $p<0.0001$****).

RESULTS

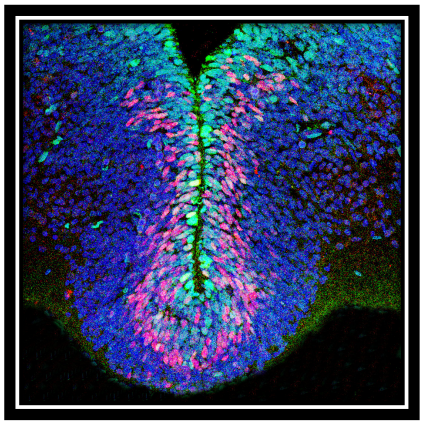

SECTION I:

EXPRESSION PATTERN OF P27 IN THE DEVELOPING MOUSE BRAIN

The main purpose of this thesis is studying the effects of the protein p27 on the development of DA neurons. Since functions of p27 have yet to be described in the midbrain, we first established an expression pattern of p27 in the developing VM from E11.5 to E14.5, which is when DA neurogenesis is known to take place (Arenas et al 2015).

1.1 Dissecting the VM

In order to establish an expression pattern for p27 in the developing midbrain, we first dissected the VM directly from the brain for RNA or protein extraction, as indicated by the line through the recognizable curve present during embryonic mouse brain development (Figure 1.1 A). We then obtained coronal sections of embryo brains for IHC studies in order to establish expression patterns of factors known to be present in different developmental areas that arise during DA neuron development (Figure 1.1 A'-A"), and specifically studied the co-expression of these factors with p27.

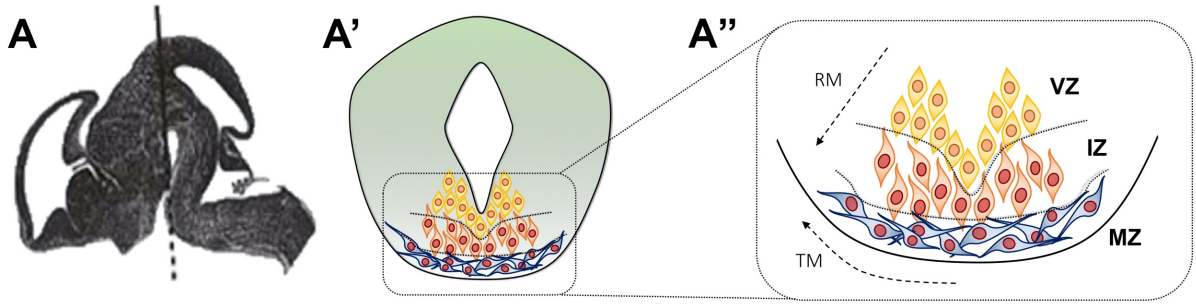

Figure 1.1 Dissecting the VM: A) Embryonic mouse brain at E13.5. A'-A") Diagram of DA neuron development.

1.2 p27 Expression pattern in the VM

First, we studied the expression of p27 and TH, using TH as a positive control of VM tissue (Figure 1.2). We saw a steady increase in the mRNA expression of both markers from E11.5 to E14.5 (Figure 1.2 A,B), indicating that we had correctly dissected tissue of the VM, that p27 is present in the developing midbrain and that its expression increases as development progresses. These results were confirmed by WB studies (Figure 1.2 C).

Next, we sectioned brains for IHC studies to see the expression pattern of p27 in the developing VM. At E11.5, we saw a clear pattern for p27, whose expression was restricted to the IZ and MZ, and completely absent from the VZ (Figure 1.2 D). As development progressed, the percentage of p27 expression increased in relation to Hoechst expression (Figure 1.2 F),

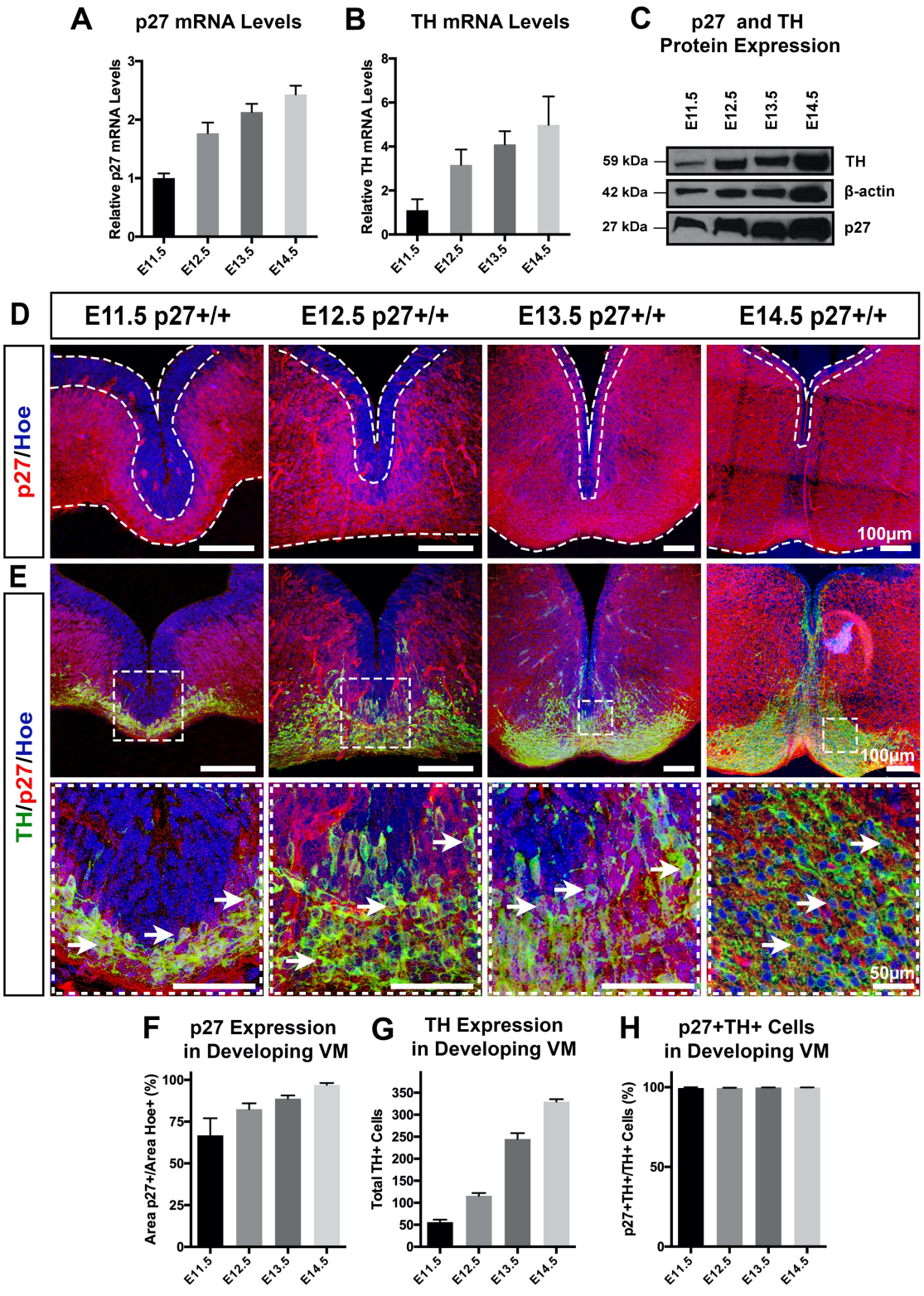

Figure 1.2: p27 expression pattern in the VM. A) *p27* mRNA levels in the developing VM. B) *TH* mRNA levels in the developing VM. C) TH and p27 protein expression in the developing VM. D) IHC of p27 expression pattern in the developing VM; scale bars = 100µm. E) p27 and TH co-expression in the developing VM; scale = bars 100µm (top panels) and 50µm (bottom panels).

which was accompanied by a progressive decrease in the area of the VZ. The expression of TH was shown to increase as development progressed, with only 56.0 ± 5.6 total TH+ cells per section at E11.5 which increased to 637.2 ± 17.3 total TH+ cells per section at E14.5 (Figure 1.2 E,G). These results are expected, and also serve as a positive control of midbrain tissue. When studying the co-expression of p27 with TH, we saw that all TH+ cells were p27+TH+ double positive from E11.5 to E14.5 (Figure 1.2 H).

These results allow us to conclude that p27 is expressed in the developing VM and increases as development progresses. Furthermore, the expression pattern of p27 is restricted to the IZ and MZ, and completely absent from the VZ.

1.3 p27 co-expression with DA neuron markers

Next, we studied the co-expression of p27 with the early DA neuron marker Nurr1 and the mature DA neuron marker Pitx3. The expression of Nurr1 increased as development progressed, from 152.0 ± 29.6 total Nurr1+ cells per section at E11.5 to 669.6 ± 54.4 total Nurr1+ cells per section at E14.5 (Figure 1.3 A,C). In almost all cases, Nurr1+ cells were p27+Nurr1+ double positive (Figure 1.3 D).

Lastly, we studied the co-expression of p27 with the late DA neuron marker Pitx3. At E11.5 there was very little Pitx3 expression, with 38.4 ± 6.4 total Pitx3+ cells per section at E11.5, which increased to 492.2 ± 5.3 total cells per section at E14.5 (Figure 1.3 B,E). As in the case with TH, all Pitx3+ cells were p27+Pitx3+ double positive (Figure 1.3 F).

These results allow us to conclude that we have successfully located VM sections based on appropriate TH, Nurr1 and Pitx3 expression, and that p27 is co-expressed with all three, indicating a possible function of p27 in the development of these markers and thereby DA neurons.

1.4 p27 co-expression with DA neuron developmental markers

Knowing that p27 was co-expressed with markers of mature DA neurons, we next studied the co-expression of p27 with two markers important during their early development: Foxa2 which is necessary for proper regionalization and patterning of the FP (Ang and Rossant 1994, Ang 2009) and Lmx1a which is necessary for the proper specification of DA neurons (Andersson et al 2006b).

We saw that Foxa2 expression appeared to reach a consistent level, with approximately 90% of cells in the VM expressing Foxa2 (Figure 1.4 A,C). Foxa2 is expressed in all three developmental zones (VZ, IZ and MZ), and it therefore makes sense to see an increase in the

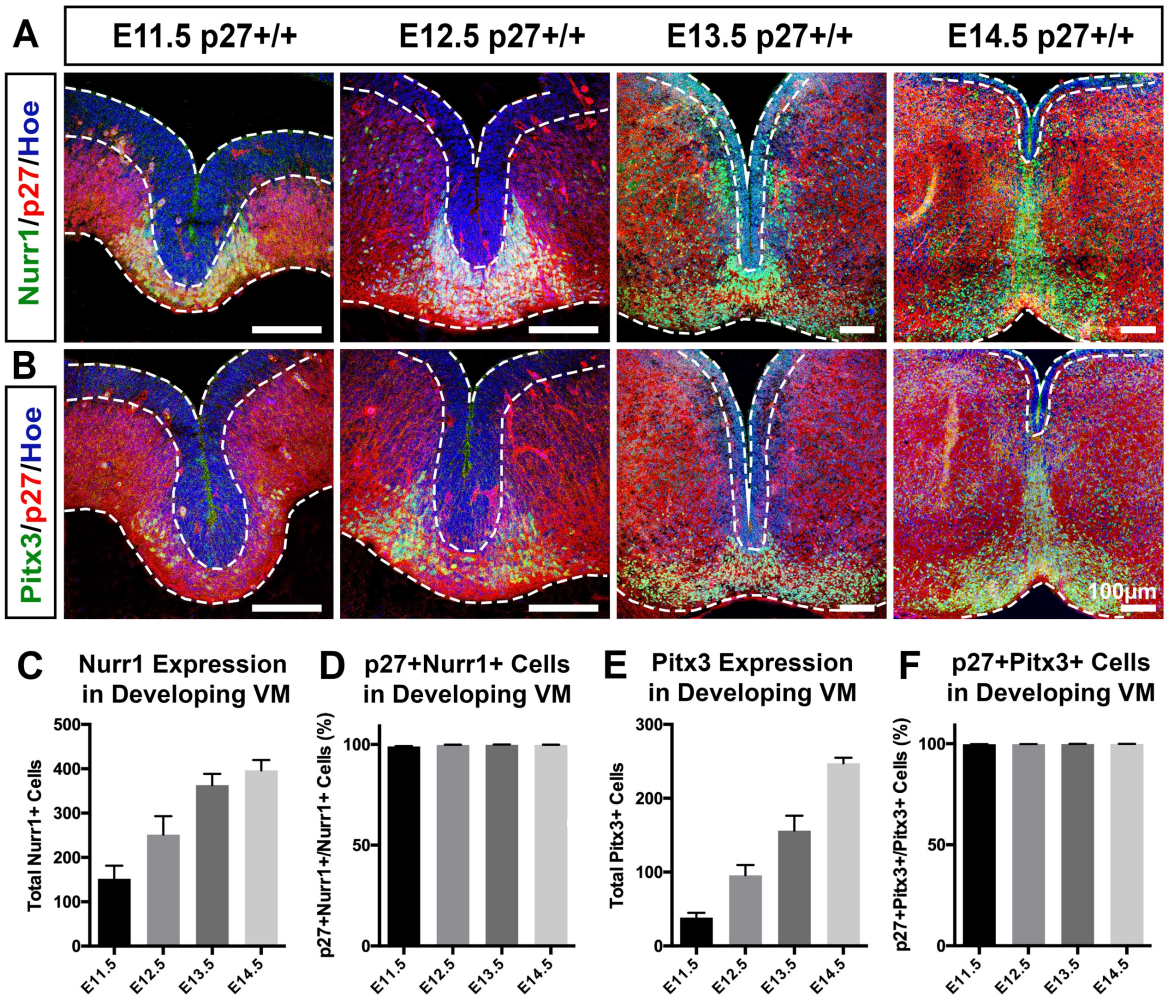

Figure 1.3: p27 co-expression with DA neuron markers. Co-expression and quantification of DA neuron markers with p27 from E11.5 to E14.5: A) IHC of Nurr1 and p27 co-expression. B) IHC of Pitx3 and p27 co-expression. C) Quantification of total Nurr1+ cells. D) Quantification of p27+Nurr1+ double positive cells. E) Quantification of total Pitx3+ cells. F) Quantification of p27+Pitx3+ double positive cells. Scale bars = 100µm.

number of p27+Foxa2+ double positive cells (from 42.6% ± 15.5 at E11.5 to 94.8% ± 1.8 at E14.5, Figure 1.4 D), consistent with an increased number of proliferating precursors exiting the cell cycle at later developmental stages.

When studying Lmx1a expression, we saw a peak of total Lmx1a+ cells at E12.5-E13.5 (378.1 ± 10.9 total Lmx1a+ cells at E12.5 and 350.6 ± 19.3 total Lmx1a+ cells at E13.5, Figure 1.4 B,E). Similar to Foxa2, we saw that Lmx1a expression spanned the three developmental zones and the number of p27+Lmx1a+ double positive cells increased from E11.5 to E14.5, again consistent with an increased number of proliferating precursors exiting the cell cycle at later developmental stages (Figure 1.4 F).

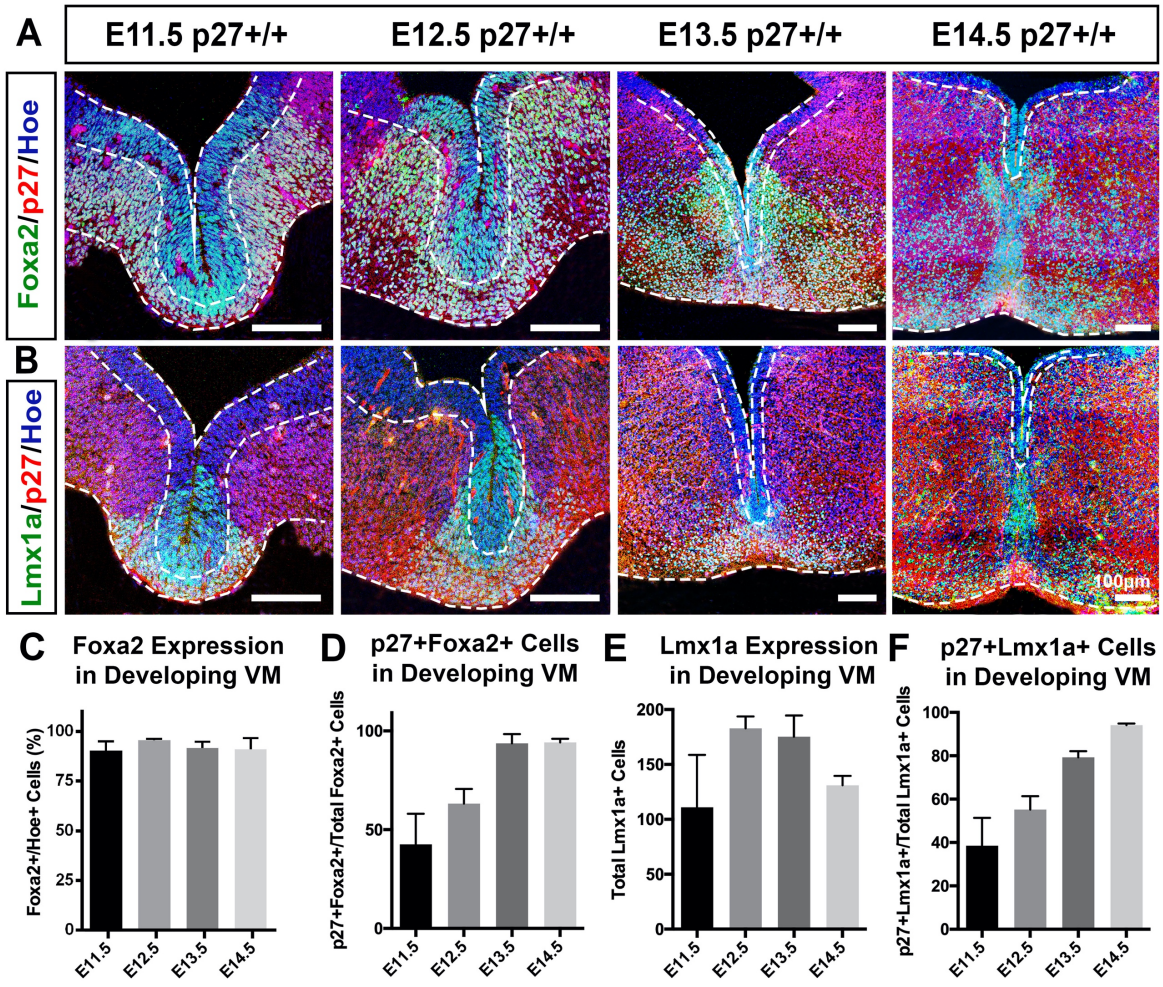

Figure 1.4: p27 co-expression with DA neuron developmental markers. Co-expression and quantification of DA neuron developmental markers with p27 from E11.5 to E14.5: A) IHC of Foxa2 and p27 co-expression. B) IHC of Lmx1a and p27 co-expression. C) Quantification of Foxa2+ cells in relation to Hoescht. D) Quantification of p27+Foxa2+ double positive cells. E) Quantification of total Lmx1a+ cells. F) Quantification of p27+Lmx1a+ double positive cells. Scale bars = 100µm.

1.5 p27 co-expression with DA precursor markers

In the context of the VM, we know that Ngn2+ cells are DA neuron specific precursors (Kele et al 2006). Ngn2 expression was high at early stages of development (101.4 ± 19.8 Ngn2+ cells at E11.5) and steadily decreased until it was completely absent by E14.5 (Figure 1.5 A,B). Ngn2 expression was mainly restricted to the VZ, with some Ngn2+ cells also present in the IZ. The IZ can be distinguished in these sections, as it is composed of the small region where we see both Ngn2+ and p27+ cells, although there was very little co-expression of these markers (Figure 1.5 C).

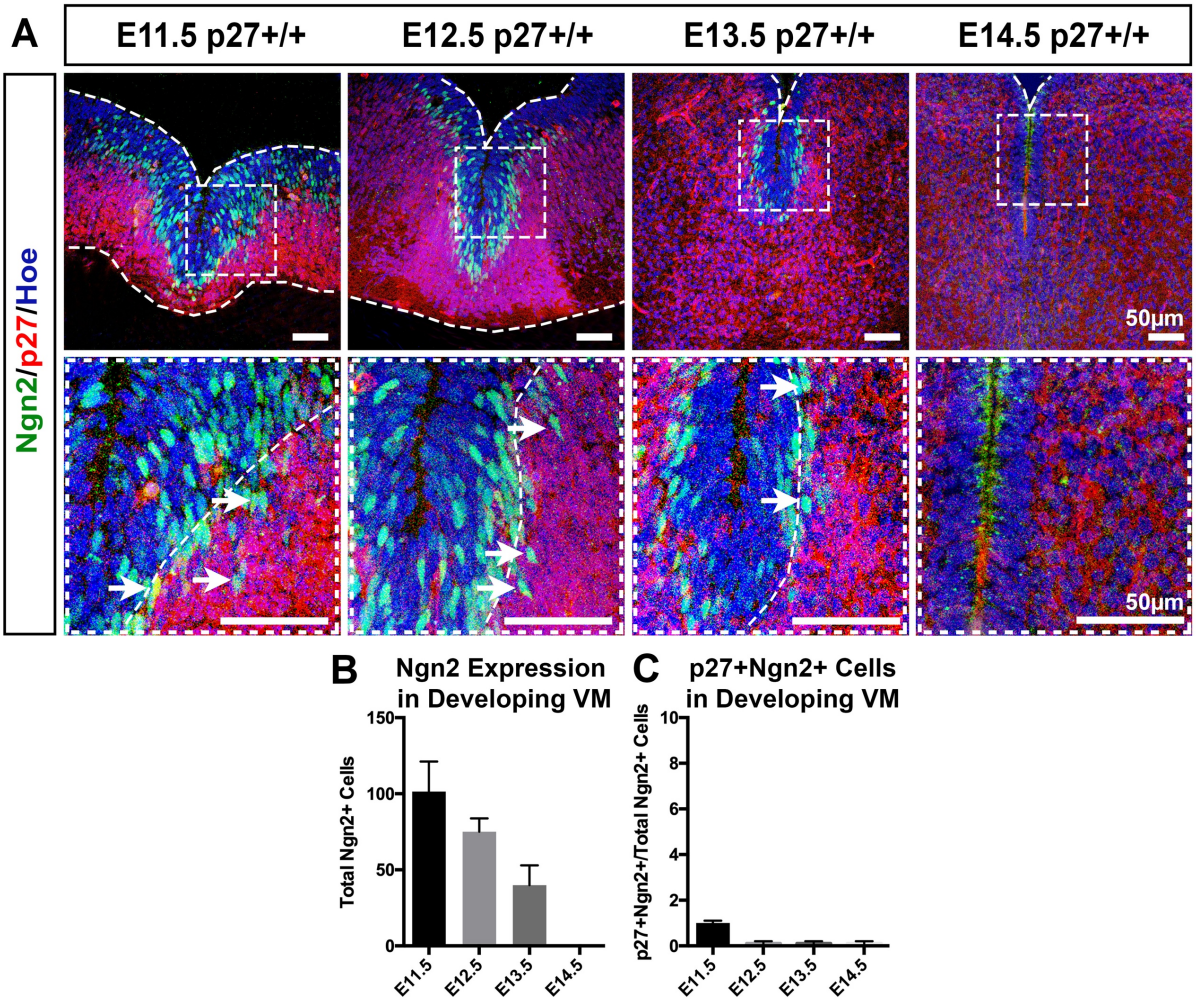

Figure 1.5: p27 co-expression with DA precursor markers. Co-expression and quantification of DA neuron precursor markers with p27 from E11.5 to E14.5: A) IHC of Ngn2 and p27 co-expression. B) Quantification of total Ngn2+ cells. C) Quantification of p27+Ngn2+ double positive cells. Scale bars = 50µm.

1.6 p27 co-expression with mitotic cell markers in the VM

Knowing the importance of proper cell cycle exit in promoting the correct transition from proliferating precursors to differentiating neurons, we next studied the expression of the cell cycle marker Ki67 and the general neural precursor Sox2.

Ki67 expression was exclusively restricted to the VZ, with expression decreasing from 42.9% ± 9.1 at E11.5 to 3.0% ± 1.7 at E14.5 (Figure 1.6 A,C). This expression was entirely complementary to p27, with no p27+Ki67+ double positive cells present during the development of the VM (Figure 1.6 D).

Sox2+ expression was similar to Ki67 expression, where we see an expression pattern exclusively restricted to the VZ. Sox2 expression decreased from 47.0% ± 4.3 at E11.5 to 2.9%

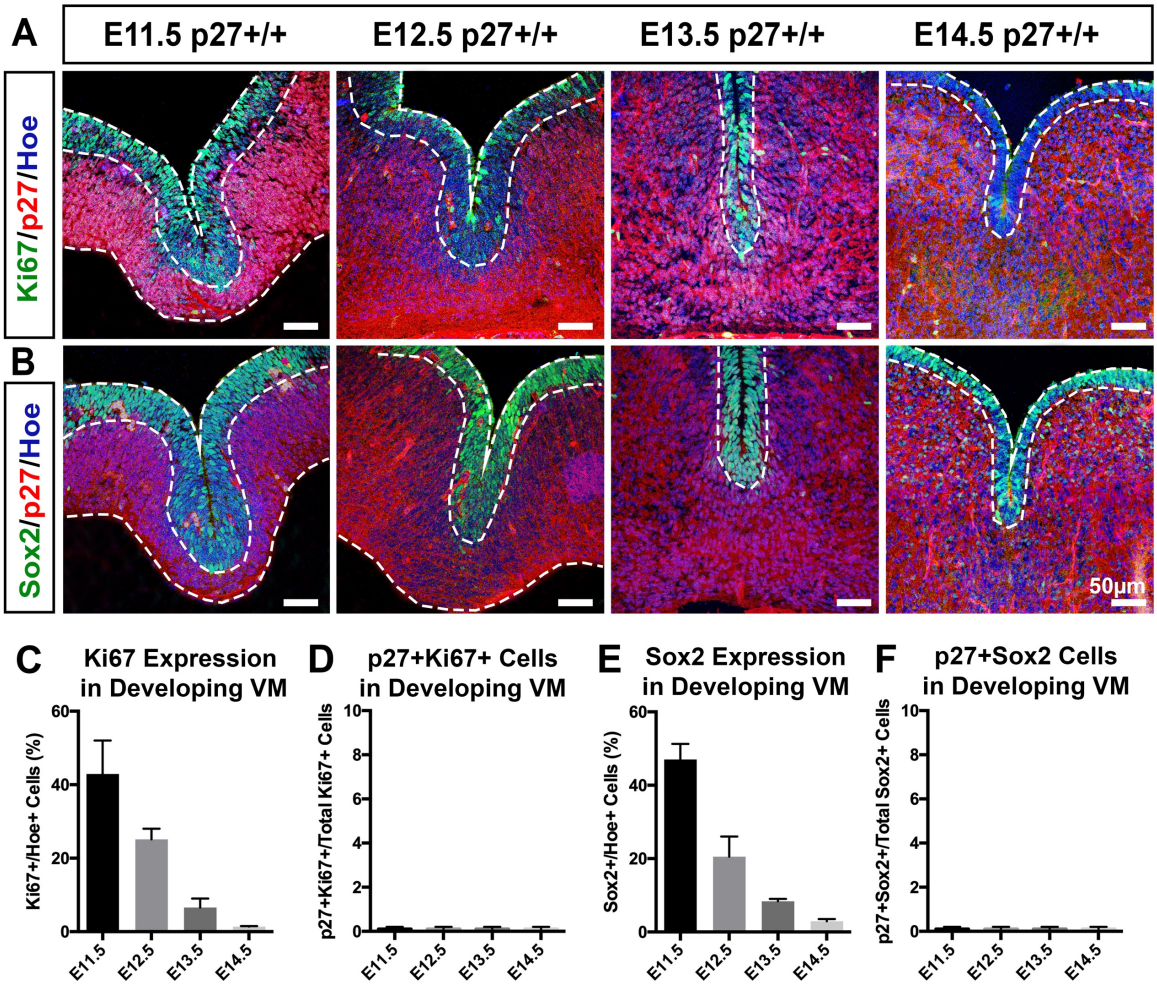

Figure 1.6: p27 co-expression with mitotic cell markers in the VM. Co-expression and quantification of mitotic cell markers and p27 from E11.5 to E14.5: A) IHC of Ki67 and p27 co-expression. B) IHC of Sox2 and p27 co-expression. C) Quantification of Ki67+ cells in relation to Hoescht. D) Quantification of p27+Ki67+ double positive cells. E) Quantification of Sox2+ cells in relation to Hoescht. F) Quantification of p27+Sox2+ double positive cells. Scale bars = 50µm.

± 0.6 at E14.5 (Figure 1.6 B,E). Again, we saw no p27+Sox2+ double positive cells during the development of the VM (Figure 1.6 F)

In summary, we have established an expression pattern for p27 in the developing VM, where p27 is restricted to the IZ and MZ, and its expression increases as development progresses. p27 is co-expressed with DA neuron markers throughout development, its co-expression increases with the developmental markers Foxa2 and Lmx1a as development progresses, and p27 expression is entirely complementary to the cell cycle marker Ki67 and the neural precursor marker Sox2. p27 was not shown to be co-expressed with the DA precursor marker Ngn2, though there was some overlap in their spatiotemporal expression.

SECTION II:

EFFECTS OF P27 DEFICIENCY ON THE DEVELOPING MOUSE BRAIN

After establishing an expression pattern for p27 in the VM, and an expression pattern for the co-expression of key markers important during DA neuron development, we studied the effects of p27 deficiency on the developing mouse midbrain by comparing the embryonic brain of p27 deficient (p27-/-) mice to wild type (p27+/+) controls, from E11.5 to E14.5.

2.1 p27 deficiency decreases early DA neuron development

We first wanted to examine the effects of p27 deficiency on TH development in the midbrain. At E11.5, we saw a significant decrease in TH expression in brain sections (28.0 ± 3.0 TH+ cells in p27-/- mice compared to 56.6 ± 5.6 TH+ cells in controls; p<0.001***) as well as decreased mRNA levels (0.77 ± 0.16 relative *TH* mRNA levels in p27-/- mice compared to 1.02 ± 0.25 in controls; p<0.05*) (Figure 2.1 A-A"). These results were maintained at E12.5, where we again saw a significant decrease in TH expression in brain sections (73.6 ± 6.7 TH+ cells in p27-/- mice compared to 116 ± 6.3 TH+ cells in controls; p<0.01**) and decreased mRNA levels (0.71 ± 0.18 relative *TH* mRNA levels in p27-/- mice compared to 1.02 ± 0.24 in controls;

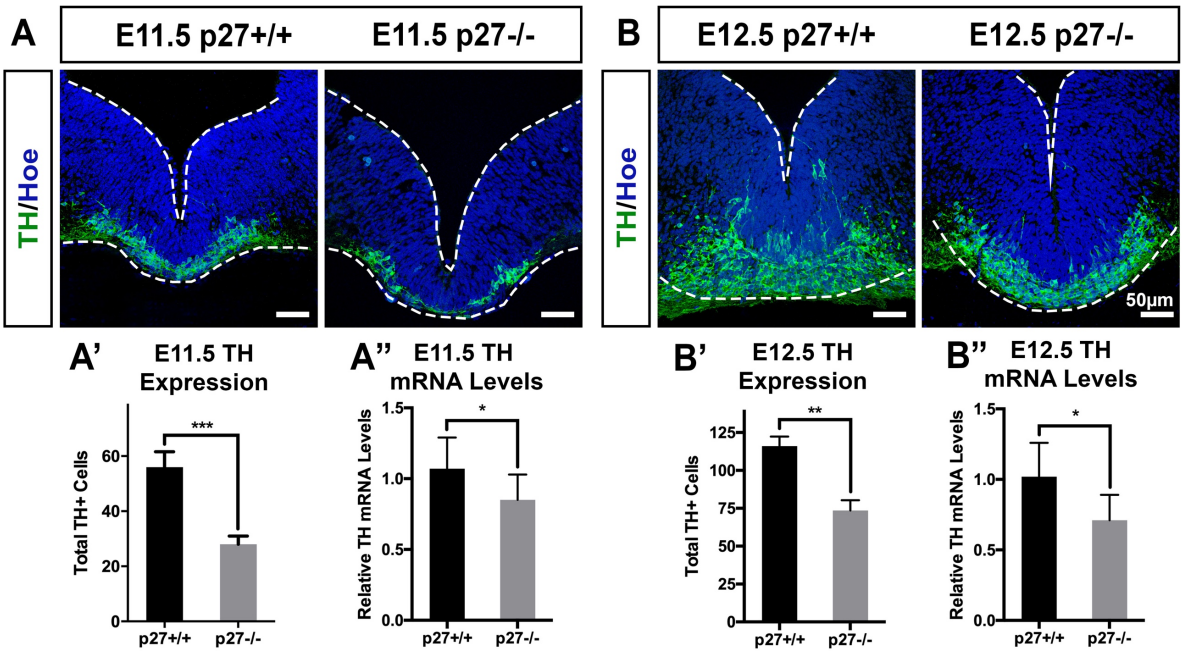

Figure 2.1: p27 deficiency decreases early DA neuron development. A-A') Coronal sections of E11.5 VM showing decreased TH expression in p27 deficient mice as compared to control and A") decreased *TH* mRNA levels. B-B') Coronal sections of E12.5 VM showing decreased TH expression in p27 deficient mice as compared to control and B") decreased *TH* mRNA levels. Data represents mean ± S.E.M. (n=4-8 for each experiment). Statistical analysis was performed using Student's t-test between control and p27 deficient mice; p<0.05*; p<0.01**; p<0.001***. Scale bars = 50µm.

p<0.05*) (Figure 2.1 B-B"). These results allow us to conclude that p27 deficiency significantly decreases DA neuron production at early stages of development.

2.2 p27 deficiency decreases expression of DA neuron markers

We further examined the effects of p27 deficiency on DA neuron development by studying the effects of p27 deficiency on the DA neuron markers Nurr1 and Pitx3. We saw a significant decrease in Nurr1 (68.6 ± 16.7 Nurr1+ cells in p27-/- mice compared to 152.0 ± 29.6 Nurr1+ cells in controls; p<0.01**; Figure 2.2 A-A') and Pitx3 (2.3 ± 3.9 Pitx3+ cells in p27-/- mice compared to 38.4 ± 6.4 Pitx3+ cells in controls; p<0.0001****; Figure 2.2 C-C') at E11.5, which was confirmed by RT-qPCR studies (0.54 ± 0.37 relative *Nurr1* mRNA levels in p27-/- mice compared to 1.01 ± 0.13; p<0.001**; Figure 2.2 A" and 0.49 ± 0.14 relative *Pitx3* mRNA levels in p27-/- mice compared to 1.02 ± 0.39 in controls; p<0.01**; Figure 2.2 C").

Similar results were obtained at E12.5, where p27 deficiency, again caused a significant decrease in the expression of both Nurr1 (165.3 ± 43.6 Nurr1+ cells in p27-/- mice compared to 274.8 ± 13.1 in controls; p<0.05*; Figure 2.2 B-B') and Pitx3 (105.2 ± 3.2 Pitx3+ cells in p27-/- mice compared to 191.1 ± 14.1 in controls; p<0.001**; Figure 2.2 D-D'). These results were confirmed by RT-qPCR studies (0.83 ± 0.14 relative *Nurr1* mRNA levels in p27-/- mice compared to 1.04 ± 0.07 in controls: p<0.01**; Figure 2.2 B" and 0.62 ± 0.19 relative *Pitx3* mRNA levels in p27-/- mice compared to 1.05 ± 0.19 in controls; p<0.001**; Figure 2.2 D")

These results further confirm that p27 deficiency significantly decreases the production of DA neurons during early developmental stages.

2.3 p27 deficiency does not affect early regionalization or specification

Since we saw that p27 co-expression with the regionalization marker Foxa2 and the specification marker Lmx1a increased as development progressed, we wanted to see the effects p27 deficiency had on the early expression of these markers. We saw no significant differences in the expression of Foxa2 in p27 deficient mice compared to controls in brain sections (90.6% ± 1.4 Foxa2 expression in p27-/- mice compared to 90.3% ± 4.7 in controls) or at the mRNA level (0.93 ± 0.26 relative *Foxa2* mRNA levels in p27-/- mice compared to 1.04 ± 0.29 in controls) (Figure 2.3 A-A"). Similarly, we saw no significant differences in the expression of Lmx1a in p27 deficient mice compared to controls, as IHC studies showed 264.3 ± 15.1 Lmx1a+ cells in p27 deficient mice compared to 272.7 ± 4.7 Lmx1a+ cells in controls (Figure 2.3 C-C'). This was confirmed by RT-qPCR studies (1.02 ± 0.2 relative *Lmx1a* mRNA levels

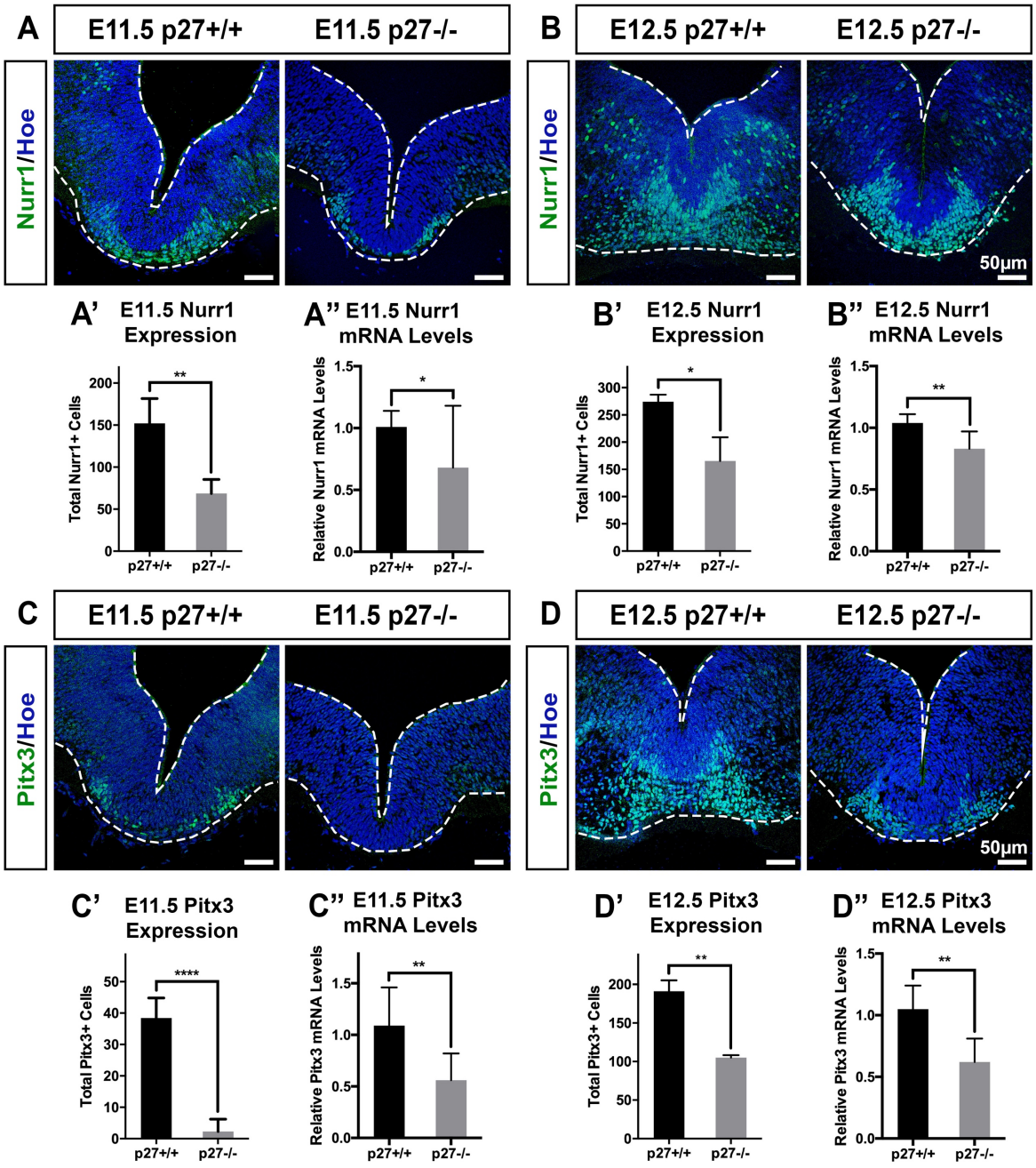

Figure 2.2: p27 deficiency decreases expression of DA neuron markers. A-A') Coronal sections of E11.5 VM showing decreased Nurr1 expression in p27 deficient mice as compared to control and A") decreased *Nurr1* mRNA levels. B-B') Coronal sections of E12.5 VM showing decreased Nurr1 expression in p27 deficient mice as compared to control and B") decreased *Nurr1* mRNA levels. C-C') Coronal sections of E11.5 VM showing decreased Pitx3 expression in p27 deficient mice as compared to control and C") decreased *Pitx3* mRNA levels. D-D') Coronal sections of E12.5 VM showing decreased Pitx3 expression in p27 deficient mice as compared to control and D") decreased *Pitx3* mRNA levels. Data represents mean ± S.E.M. (n=4-8 for each experiment). Statistical analysis was performed using Student's t-test between control and p27 deficient mice; $p<0.05$*; $p<0.01$**; $p<0.0001$****. Scale bars = 50µm.

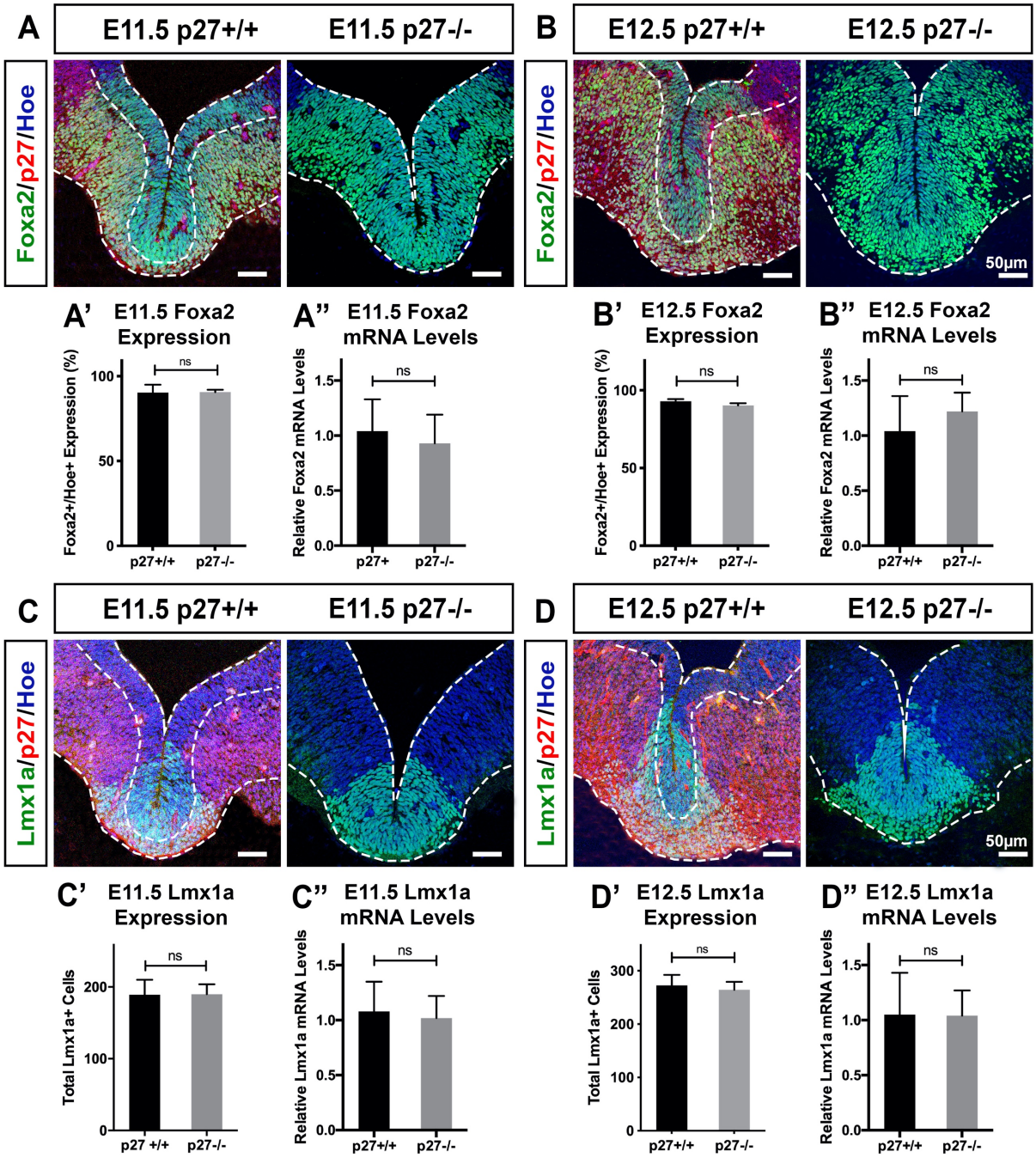

Figure 2.3: p27 deficiency does not affect early regionalization or specification markers. A-A') Coronal sections of E11.5 VM showing unaltered Foxa2 expression and A") unaltered *Foxa2* mRNA levels in p27 deficient mice compared to controls. B-B') Coronal sections of E12.5 VM showing unaltered Foxa2 expression and B") unaltered *Foxa2* mRNA levels in p27 deficient mice compared to controls. C-C') Coronal sections of E11.5 VM showing unaltered Lmx1a expression and C") unaltered *Lmx1a* mRNA levels in p27 deficient mice compared to controls. D-D') Coronal sections of E12.5 VM showing unaltered Lmx1a expression and D") unaltered *Lmx1a* mRNA levels in p27 deficient mice compared to controls. Data represents mean ± S.E.M. (n=4-8 for each experiment). Statistical analysis was performed using Student's t-test between control and p27 deficient mice. Scale bars = 50µm.

in p27-/- mice compared to 1.08 ± 0.27 in controls; Figure 2.3 C").

These results were maintained at E12.5, with no significant differences in Foxa2 expression in brain sections (90.2% ± 1.4 Foxa2 expression in p27-/- mice compared to 92.9% ± 1.4 in controls) or at the mRNA level (1.22 ± 0.17 relative *Foxa2* mRNA levels in p27-/- mice compared to 1.04 ± 0.32 in controls) (Figure 2.3 B-B"). Again, we did not observe significant differences in Lmx1a expression in brain sections (189.9 ± 13.8 Lmx1a+ cells in p27-/- mice compared to 189.1 ± 21 in controls) or at the mRNA level (1.04 ± 0.23 relative *Lmx1a* mRNA levels in p27-/- mice compared to 1.05 ± 0.38 in controls) (Figure 2.3 D-D").

These results allow us to conclude that p27 deficiency does not decrease DA neuron development by affecting early regionalization (Foxa2) or specification (Lmx1a) in the developing midbrain.

2.4 p27 deficiency increases mitotic precursors in the VM

Since we saw no effect on early developmental markers, we next investigated the effects of p27 deficiency on the cell cycle marker Ki67 and the neural precursor marker Sox2. At E11.5, there was a significant increase in the expression of Ki67 in the VM of p27 deficient mice (70.5% ± 3.5 Ki67 expression in p27-/- mice compared to 42.9% ± 9.8 in controls; p<0.001***), which was confirmed by RT-qPCR studies (1.22 ± 0.16 relative *Ki67* mRNA levels in p27-/- mice compared to 1.02 ± 0.12 in controls; p< 0.01**) (Figure 2.4 A-A"). Similar results were obtained for Sox2 expression (73.1% ± 1.0 Sox2 expression in p27-/- mice compared to 40.6% ± 9.5 in controls; p<0.001***), which was also confirmed by RT-qPCR studies (2.27 ± 1.13 relative *Sox2* mRNA levels in p27-/- mice compared to 1.13 ± 0.49 in controls; p<0.05*) (Figure 2.4 C-C").

The results observed at E11.5 were maintained at E12.5, where we saw a significant increase in both Ki67 expression (35.7% ± 6.8 Ki67 expression in p27-/- mice compared to 14.8% ± 3.8 in controls; p<0.01*; Figure 2.4 B-B") and Sox2 expression (40% ± 7.8 Sox2 expression in p27-/- mice compared to 20.5% ± 5.5 in controls; p<0.05*; Figure 2.4 D-D'). These results were further conformed by RT-qPCR studies (1.41 ± 0.2 relative *Ki67* mRNA levels in p27-/- mice compared to 1.02 ± 0.23 in controls; p<0.05*; Figure 2.4 C" and 1.51 ± 0.24 relative *Sox2* mRNA levels in p27-/- mice compared to 1.03 ± 0.28 in controls; p<0.05*; Figure 2.4 D"). This allows us to conclude that p27 deficiency significantly increases the number of cells still in the cell cycle (Ki67+ cells) and the pool of neural precursors (Sox2+ cells).

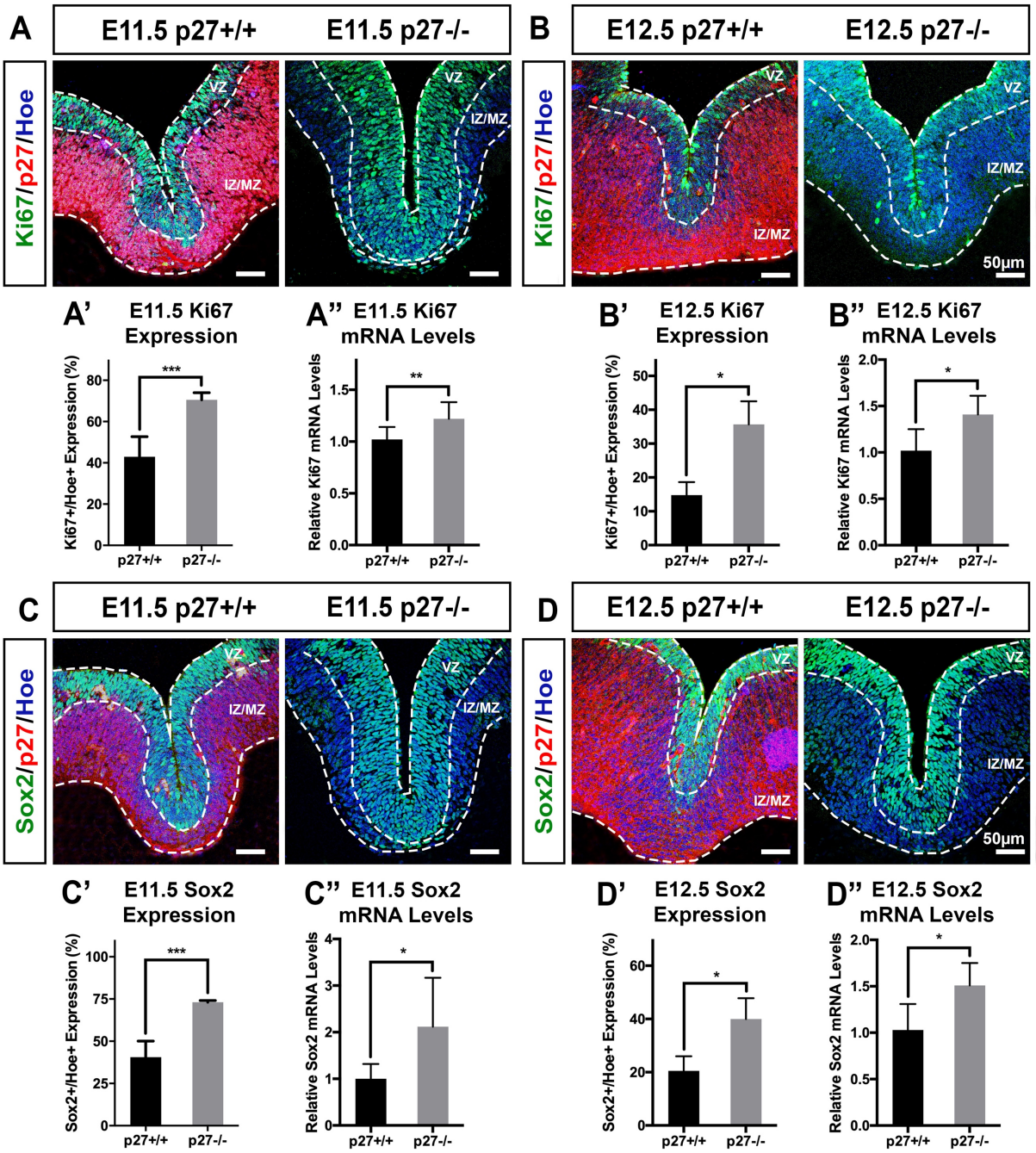

Figure 2.4: p27 deficiency increases mitotic precursors in the VM. A-A') Coronal sections of E11.5 VM showing increased Ki67 expression in p27 deficient mice as compared to control and A") increased *Ki67* mRNA levels. B-B') Coronal sections of E12.5 VM showing increased Ki67 expression in p27 deficient mice as compared to control and B") increased *Ki67* mRNA levels. C-C') Coronal sections of E11.5 VM showing increased Sox2 expression in p27 deficient mice as compared to control and C") increased *Sox2* mRNA levels. D-D') Coronal sections of E12.5 VM showing increased Sox2 expression in p27 deficient mice as compared to control and D") increased *Sox2* mRNA levels. Data represents mean ± S.E.M. (n=4-8 for each experiment). Statistical analysis was performed using Student's t-test between control and p27 deficient mice; $p<0.05$*; $p<0.01$**; $p<0.001$***. Scale bars = 50µm.

2.5 p27 deficiency increases cell proliferation

After seeing an increase in the cell cycle marker Ki67, we wanted to check the effect of p27 deficiency on proliferation. We injected pregnant females at E11.5 with BrdU and extracted the embryos 24 hours later. We saw a significant increase in BrdU expression in p27 deficient mice as compared to controls (32.5% ± 4.4 BrdU+ cells in p27-/- mice compared to 20.8% ± 5.5 BrdU+ cells in controls; $p<0.05$*; Figure 2.5 A,B). These results were confirmed by looking at the marker PCNA at E12.5 (Figure 2.5 C,D). Therefore, p27 deficiency increases cell proliferation in the developing midbrain.

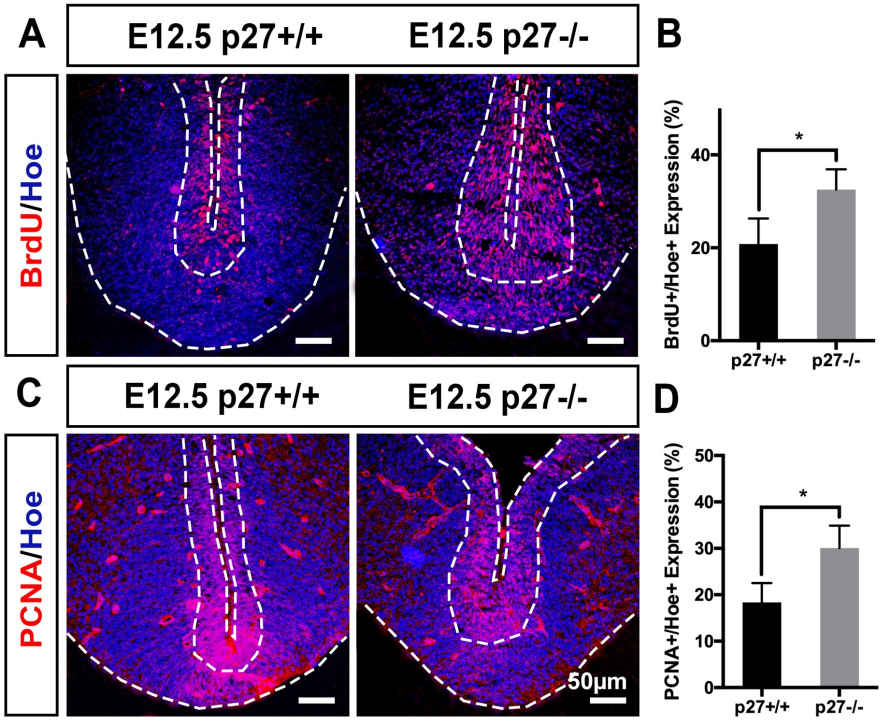

Figure 2.5: p27 deficiency increases proliferation in the VM. A,B) Coronal sections of E12.5 VM showing increased BrdU expression in p27 deficient mice as compared to control. C,D) Coronal sections of E12.5 VM showing increased PCNA expression in p27 deficient mice as compared to control. Data represents mean ± S.E.M. (n=3 for each experiment). Statistical analysis was performed using Student's t-test between control and p27 deficient mice; $p<0.05$*. Scale bars = 50µm.

2.6 p27 deficiency increases pool of proliferating precursors

We next double stained sections from BrdU-treated mice with either Ki67 or Sox2 and quantified the co-expression of these markers. Since we saw increased expression of Ki67 and BrdU separately, we can expect to see an increase in the co-expression of these markers. We saw that the number of total BrdU+Ki67+ double positive cells increased significantly in p27 deficient mice (120.0 ± 1.4 BrdU+Ki67+ double positive cells) compared to controls (58.0 ± 2.8 BrdU+Ki67+ double positive cells; $p<0.0001$****; Figure 2.6 A-A'), consistent with our previous results. When calculating Ki67+BrdU+ double positive cells in relation to total Ki67+ cells, we did not see any differences between p27 deficient mice and controls (97.4% ± 1.5 BrdU+Ki67+/Total Ki67+ cells in p27-/- mice compared to 96.1% ± 0.9 BrdU+Ki67+/Total Ki67+ cells in controls; Figure 2.6 A,A").

Similar results were obtained for total BrdU+Sox2+ cells (183.5 ± 30.4 total BrdU+Sox2+ cells in p27-/- mice compared to 100.5 ± 3.5 in controls; $p<0.05$*; Figure 2.6 C-C'). Again, upon calculating BrdU+Sox2+ cells in relation to Sox2+ cells, we see no differences between p27 deficeint mice and controls (95.4% ± 2.9 BrdU+Sox2+/Total Sox2+ cells in p27-/- mice compared to 97.3% ± 0.7 in controls; Figure 2.6 C,C").

To confirm these results, we studied another marker of proliferation: PCNA. Again, we saw significant differences between p27 deficient mice and controls when comparing total PCNA+Ki67+ double positive cells (110.0 ± 1.4 PCNA+Ki67+ double positive cells in p27-/- mice compared to 73.5 ± 20.5 in controls; $p<0.05$*; Figure 2.6 B-B'), but not when comparing PCNA+Ki67+/Total Ki67 cells (97.4% ± 1.1 PCNA+Ki67+/Total Ki67 in p27-/- mice compared to 96.3% ± 2.8 in controls; Figure 2.6 B,B"). Similar results were obtained for total PCNA+Sox2+ double positive cells (148.5 ± 14.8 total PCNA+Sox2+ double positive cells in p27-/- mice compared to 92.5 ± 17.7 in controls; Figure 2.6 D-D') and PCNA+Sox2+/Total Sox2+ (97.5% ± 1.4 double positive cells in p27-/- mice compared to 97% ± 0.1 in controls; Figure 2.6 D,D"). Though the increase observed for total PCNA+Sox2+ double positive cells was not significant, this is most likely due to lack of sufficient biological replicates. However, in all cases, the total double-positive expression is near 100%, meaning that Ki67 and Sox2 can be considered indirect measures of proliferation, and that p27 deficiency increases the number of proliferating precursors in the developing VM.

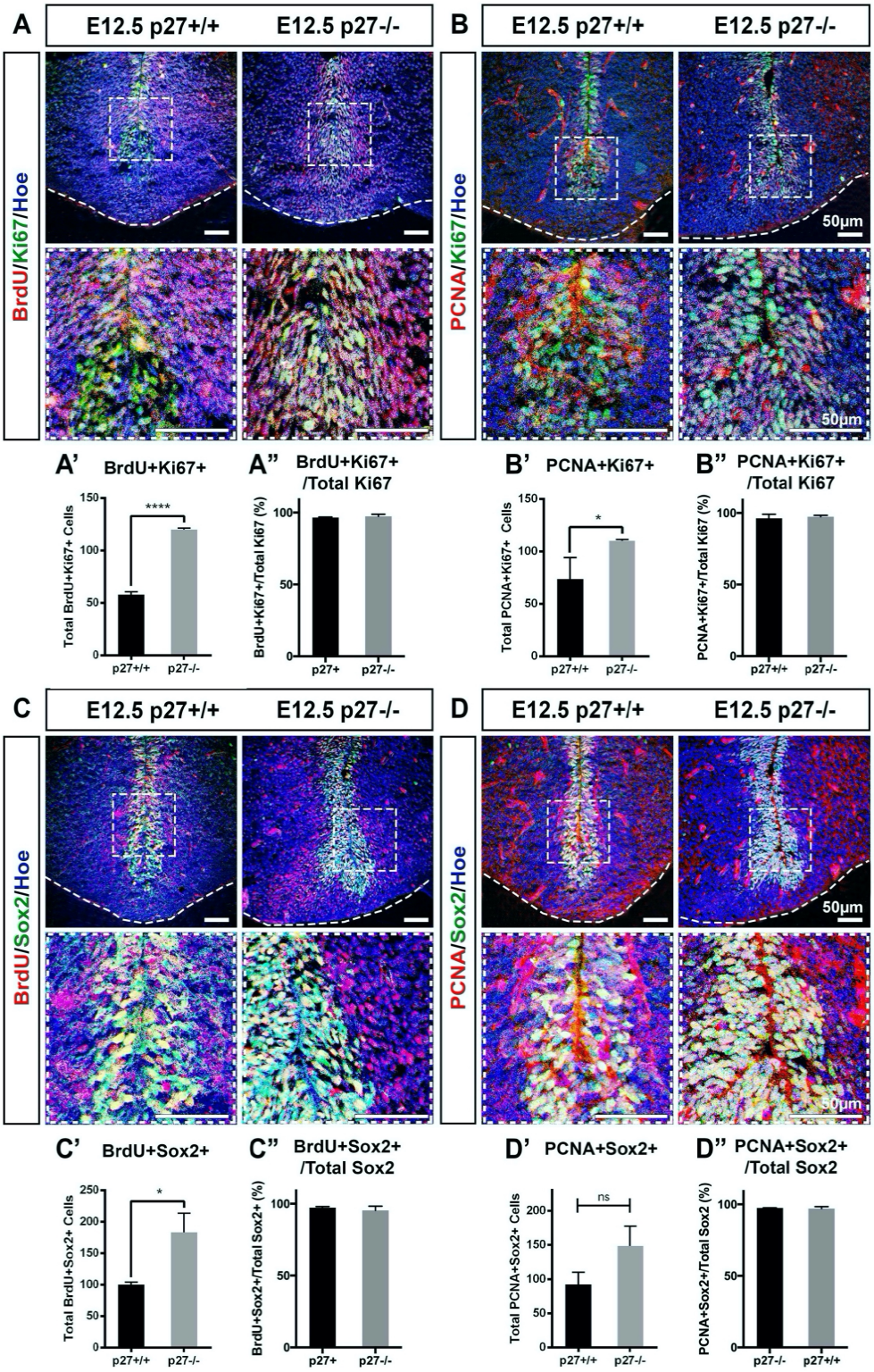

Figure 2.6: p27 deficiency increases pool of proliferating precursors. A-A") Coronal sections of E12.5 VM showing BrdU and Ki67 co-expression and how all Ki67+ cells are also BrdU+. B-B") Coronal sections of E12.5 VM showing PCNA and Ki67 co-expression and how all Ki67+ cells are also PCNA+. C-C") Coronal sections of E12.5 VM showing BrdU and Sox2 co-expression and how all Sox2+ cells are also BrdU+. D-D") Coronal sections of E12.5 VM showing PCNA and Sox2 co-expression and how all Sox2+ cells are also PCNA+. Data represents mean ± S.E.M. (n=3 for each experiment). Statistical analysis was performed using Student's t-test between control and p27 deficient mice; $p<0.05$*; $p<0.0001$****. Scale bars = 50µm.

2.7 p27 deficiency increases DA neuron precursors

We have seen that p27 deficiency significantly decreases DA neurons at early developmental stages, yet, we have also seen a significant increase in proliferating neural precursors. In order to study this effect in more detail, we analyzed the expression of Ngn2, a DA neuron precursors-specific marker in the context of the VM. We initially believed that p27 could have an effect on increasing the general pool of neural progenitors but decreasing the number of DA neuron-specific precursors. Contrary to what we expected, we saw a significant increase in Ngn2+ expression in p27 deficient mice at E11.5 as compared to controls (150.4 ± 15 Ngn2+ cells in p27-/- mice compared to 101.3 ± 16.2 in controls; $p<0.01$**; Figure 2.7 A-A'). These results were confirmed by RT-qPCR studies (1.29 ± 0.12 relative *Ngn2* mRNA levels in p27-/- mice compared to 1.02 ± 0.27 in controls; $p<0.05$*; Figure 2.7 A"), and were maintained at E12.5 (196.7 ± 10.4 Ngn2+ cells in p27-/- brains compared to 75 ± 8.8 in controls; $p<0.001$***; Figure 2.7 B-B' and 1.49 ± 0.4 relative *Ngn2* mRNA levels in p27-/- mice compared to 1 ± 0.29 in controls; $p<0.05$*; Figure 2.7 B").

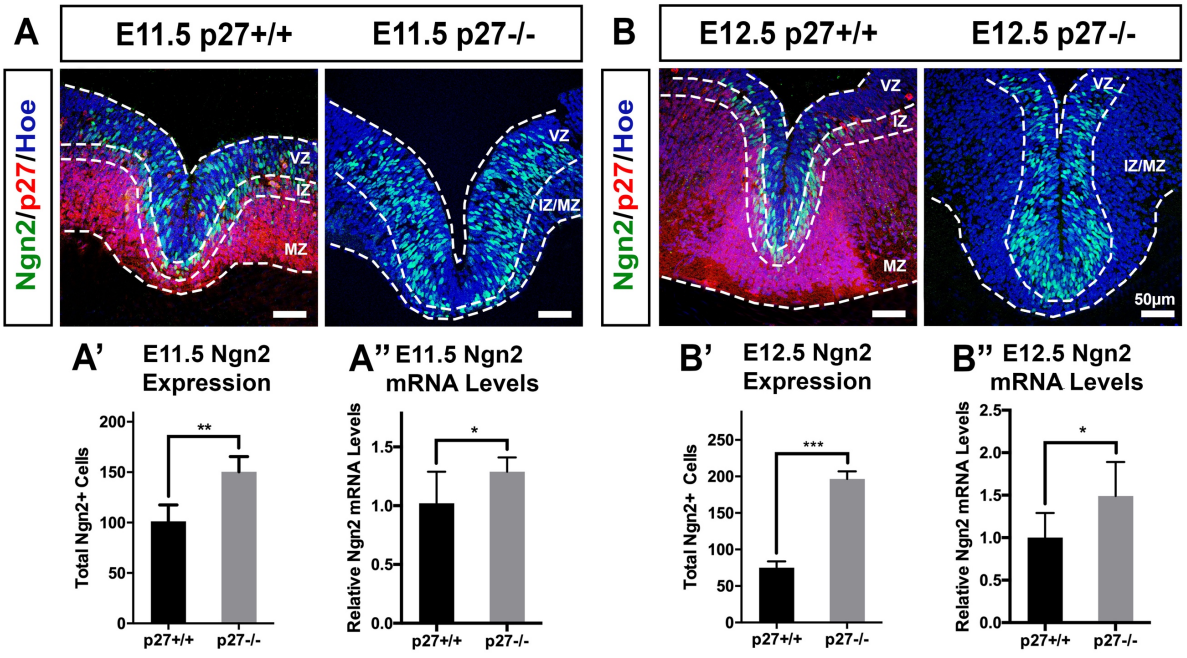

Figure 2.7: p27 deficiency increases DA neuron precursors. A-A') Coronal sections of E11.5 VM showing increased Ngn2 expression in p27 deficient mice as compared to control and A") increased *Ngn2* mRNA levels. B-B') Coronal sections of E12.5 VM showing increased Ngn2 expression in p27 deficient mice as compared to control and B") increased *Ngn2* mRNA levels. Data represents mean ± S.E.M. (n=4-8 for each experiment). Statistical analysis was performed using Student's t-test between control and p27 deficient mice; $p<0.05$*; $p<0.01$**; $p<0.001$***. Scale bars = 50µm.

2.8 p27 deficiency alters the distribution of DA neuron precursors

After seeing an increase in DA neuron precursors, we did a more in-depth study of their distribution in the midbrain. We studied the expression of Ngn2+Sox2+ double positive cells, which represents the population of precursors destined to become DA neurons. At E11.5, we saw a significant increase in Ngn2+Sox2+ double positive cells in p27 deficient mice (170 ± 19.5 Ngn2+Sox2+ cells) compared to controls (88 ± 14 Ngn2+Sox2+ cells; $p<0.01$**; Figure 2.8 A,B). These results were confirmed at E12.5 (86.7 ± 7 Ngn2+Sox2+ cells in p27-/- mice compared to 30.3 ± 1.5 in controls; $p<0.001$***; Figure 2.8 C,D).

This result is expected, as we saw an increase in both of these markers individually. We therefore decided to study the number of Ngn2+Sox2+ double positive cells with respect to the total number of Sox2+ cells, which would tell us the number of DA neuron precursors in relation to total neural progenitors. Again, we saw a significant increase in the number of Ngn2+Sox2+ double positive cells in relation to total Sox2+ cells in p27 deficient mice at E11.5 (37.7 ± 4.8 Ngn2+Sox2+/Total Sox2+ cells) compared to controls (25.2 ± 1.3 Ngn2+Sox2+/Total Sox2+ cells; $p<0.05$*; Figure 2.8 B').

These results were also confirmed at E12.5 (29.4 ± 2.3 Ngn2+Sox2+/Total Sox2+ cells in p27-/- mice compared to 21.5 ± 3.7 in controls; $p<0.05$*; Figure 2.8 D'). These results confirm that p27 deficiency increases the number of DA neuron precursors in the developing midbrain. We therefore studied the distribution of these cells, and saw that in control mice, Ngn2+Sox2+ double positive cells were centered around the border between the VZ and IZ, whereas in p27 deficient brains, these precursors were mainly interspersed in the VZ.

Seeing this expression pattern, we studied the expression of Ngn2+Sox2- cells, which are DA neuron precursors that have exited the cell cycle, and reside mainly in the IZ. At E11.5, we saw no differences in Ngn2+Sox2- cells in p27 deficient mice (39.7 ± 9.1 Ngn2+Sox2- cells) compared to controls (39.7 ± 6.5 Ngn2+Sox2- cells; Figure 2.8 B") and these results were maintained at E12.5 (25.3 ± 6.0 Ngn2+Sox2- cells in p27-/- mice compared to 23.0 ± 4.1 in controls; Figure 2.8 D"). These results allow us to conclude that p27 deficiency increases the number of DA neuron precursors, and alters their distribution in the VZ, without affecting their distribution in the IZ.

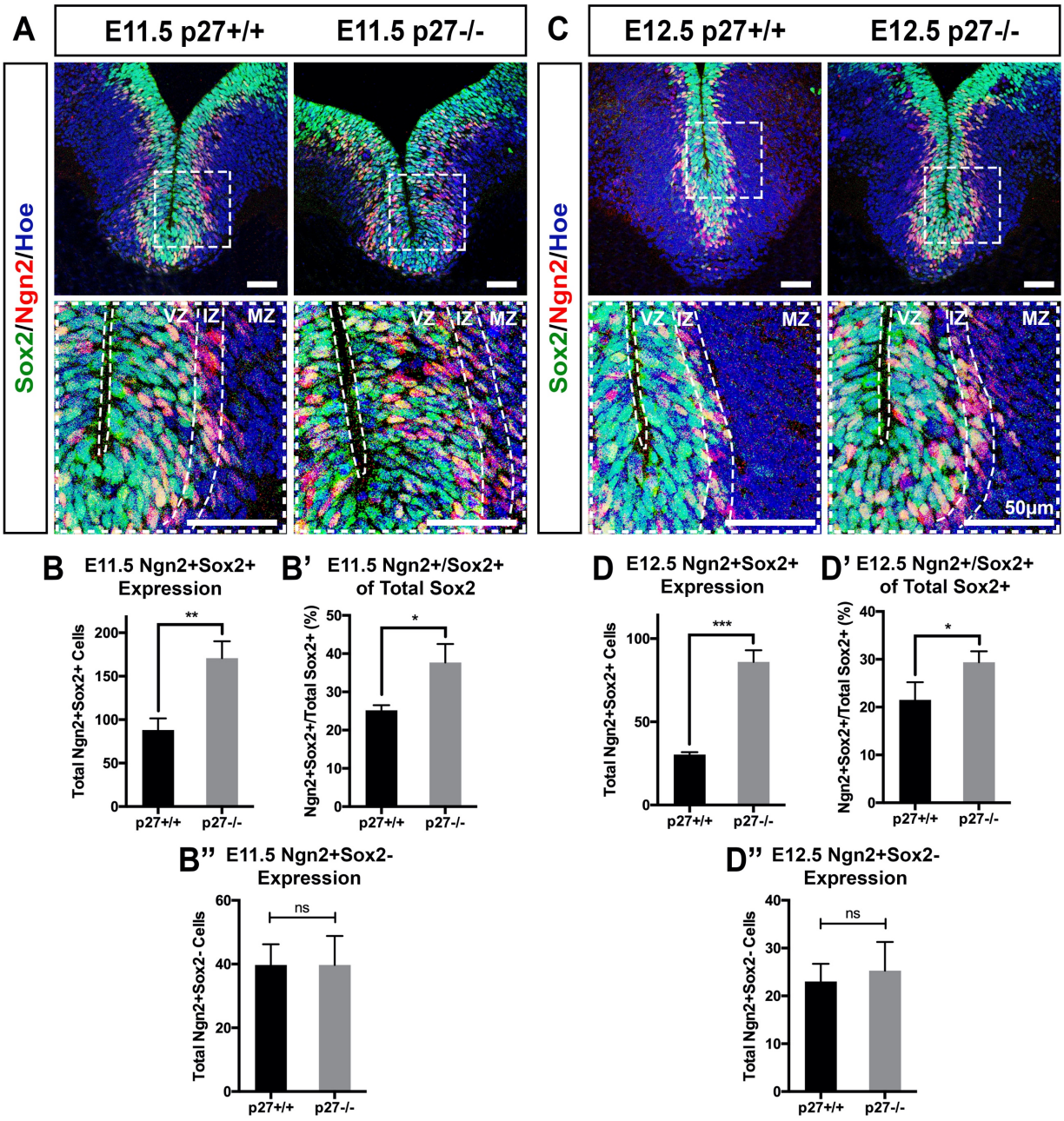

Figure 2.8: p27 deficiency alters the distribution of DA neuron precursors. A) Coronal sections of E11.5 VM showing co-expression of Ngn2 and Sox2. B-B") Quantification of Ngn2+Sox2+ double positive cells of the VZ and Ngn2+Sox2- cells of the IZ at E11.5. C) Coronal sections of E12.5 VM showing co-expression of Ngn2 and Sox2. D-D") Quantification of Ngn2+Sox2+ double positive cells of the VZ and Ngn2+Sox2- cells of the IZ at E12.5. Data represents mean ± S.E.M. (n=3 for each experiment). Statistical analysis was performed using Student's t-test between control and p27 deficient mice; $p<0.05$*; $p<0.01$**; $p<0.001$***. Scale bars = 50µm.

2.9 Effects of p27 deficiency are maintained at later stages of development

Seeing an increased number of precursors suggests that these cells later differentiate, thereby giving rise to an increased number of DA neurons in the midbrain. To check this, we looked at the expression of the mature DA neuron markers TH and Pitx3 at later developmental stages. At E13.5, we saw that both TH expression (173.6 ± 40.6 TH+ cells in p27-/- mice compared to 244.7 ± 13.0 TH+ cells in controls $p<0.05$*; Figure 2.9 A-A') and Pitx3 expression (199.7 ± 7.3 Pitx3+ cells in p27-/- mice compared to 238.2 ± 20.0 in controls; $p<0.05$*; Figure 2.8 C-C') remained decreased, and these results were confirmed by RT-qPCR experiments (0.75 ± 1.70 relative *TH* mRNA levels in p27-/- mice compared to 1.01 ± 0.11 in controls; $p<0.05$; Figure 2.9 A" and 0.53 ± 0.14 relative *Pitx3* mRNA levels in p27-/- mice compared to 1.02 ± 0.20 in controls; $p<0.001$***; Figure 2.9 C"). Similar results were obtained at E14.5, both in brain sections (261.1 ± 17.0 TH+ cells in p27-/- mice compared to 318.7 ± 17.3 in controls; $p<0.05$*; Figure 2.9 B-B' and 215.1 ± 14.2 Pitx3+ cells in p27-/- mice compared to 246.1 ± 5.3 in controls; $p<0.05$*; Figure 2.9 D-D') and in RT-qPCR studies (0.70 ± 0.10 relative *TH* mRNA levels in p27-/- mice compared to 1.23 ± 0.44 in controls; $p<0.05$*; Figure 2.9 B" and 0.63 ± 0.20 relative *Pitx3* mRNA levels in p27-/- mice compared to 1.14 ± 0.39 in controls; $p<0.05$*; Figure 2.9 D"). These results confirm that the effect p27 deficiency has on increasing proliferating precursors at early developmental stages does not increase DA neuron differentiation at later stages.

2.10 Effects of p27 deficiency begin to recover at later stages of development

Although the effects of p27 deficiency were maintained for mature DA neuron markers, we saw that by E13.5, the expression of Nurr1 was recovered in p27 deficient mice as compared to control, in both brain sections (252.0 ± 28.6 Nurr1+ cells in p27-/- mice compared to 289.8 ± 55.7 in controls) and RT-qPCR experiments (0.95 ± 0.23 relative *Nurr1* mRNA levels in p27-/- mice compared to 1.03 ± 0.28 in controls) (Figure 2.10 A-A"). These results were further confirmed at E14.5 (314.3 ± 59.7 Nurr1+ cells in p27-/- mice compared to 334.8 ± 54.4 in controls and 1.04 ± 0.15 relative *Nurr1* mRNA levels in p27-/- mice compared to 1.05 ± 0.33 in controls) (Figure 2.10 B-B").

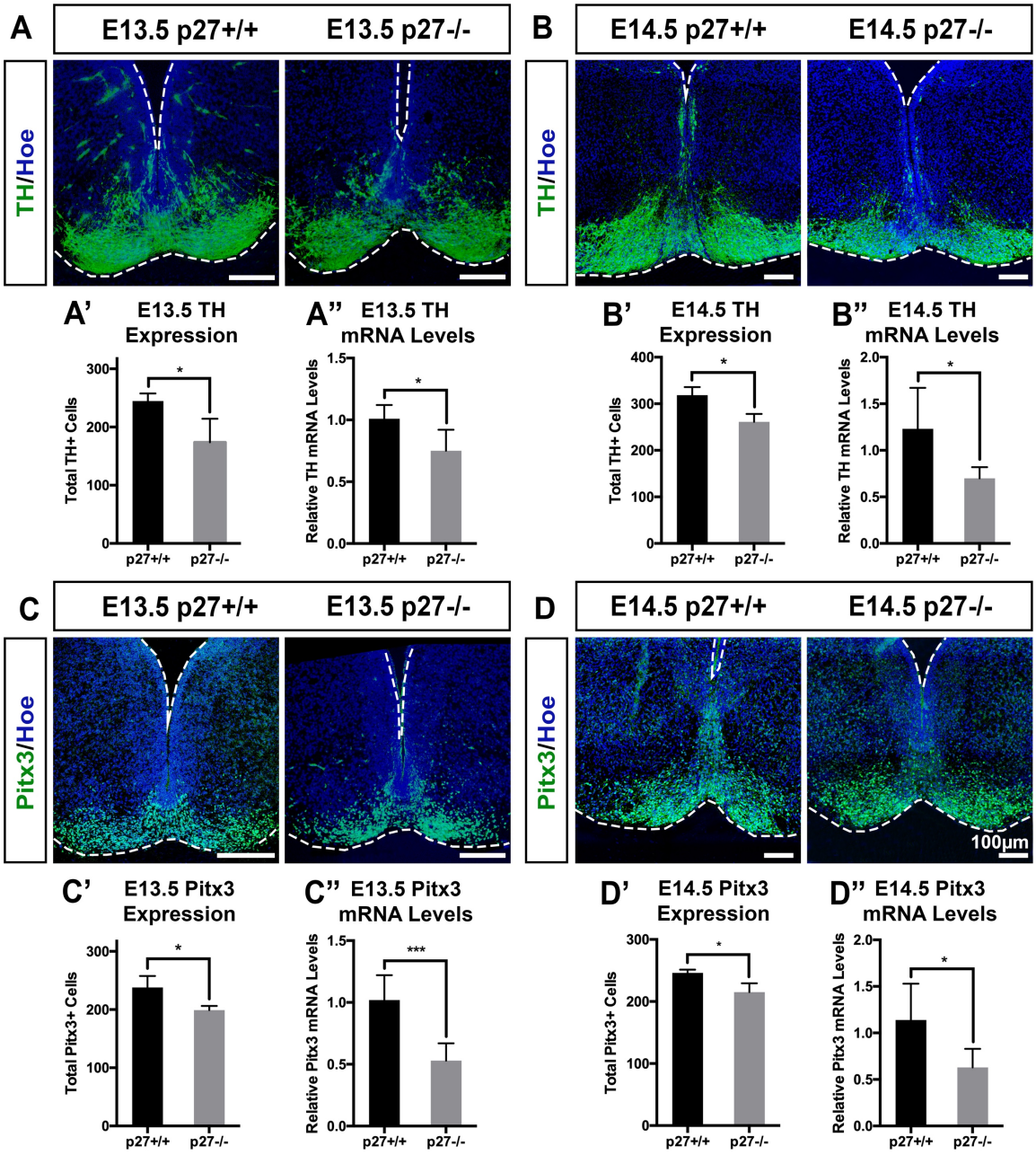

Figure 2.9: Effects of p27 deficiency are maintained at later developmental stages. A-A') Coronal sections of E13.5 VM showing decreased TH expression in p27 deficient mice as compared to control and A") decreased *TH* mRNA levels. B-B') Coronal sections of E14.5 VM showing decreased TH expression in p27 deficient mice as compared to control and B") decreased *TH* mRNA levels. C-C') Coronal sections of E13.5 VM showing decreased Pitx3 expression in p27 deficient mice as compared to control and C") decreased *Pitx3* mRNA levels. D-D') Coronal sections of E14.5 VM showing decreased Pitx3 expression in p27 deficient mice as compared to control and D") decreased *Pitx3* mRNA levels. Data represents mean ± S.E.M. (n=4-8 for each experiment). Statistical analysis was performed using Student's t-test between control and p27 deficient mice; $p<0.05$*; $p<0.001$***. Scale bars = 100µm.

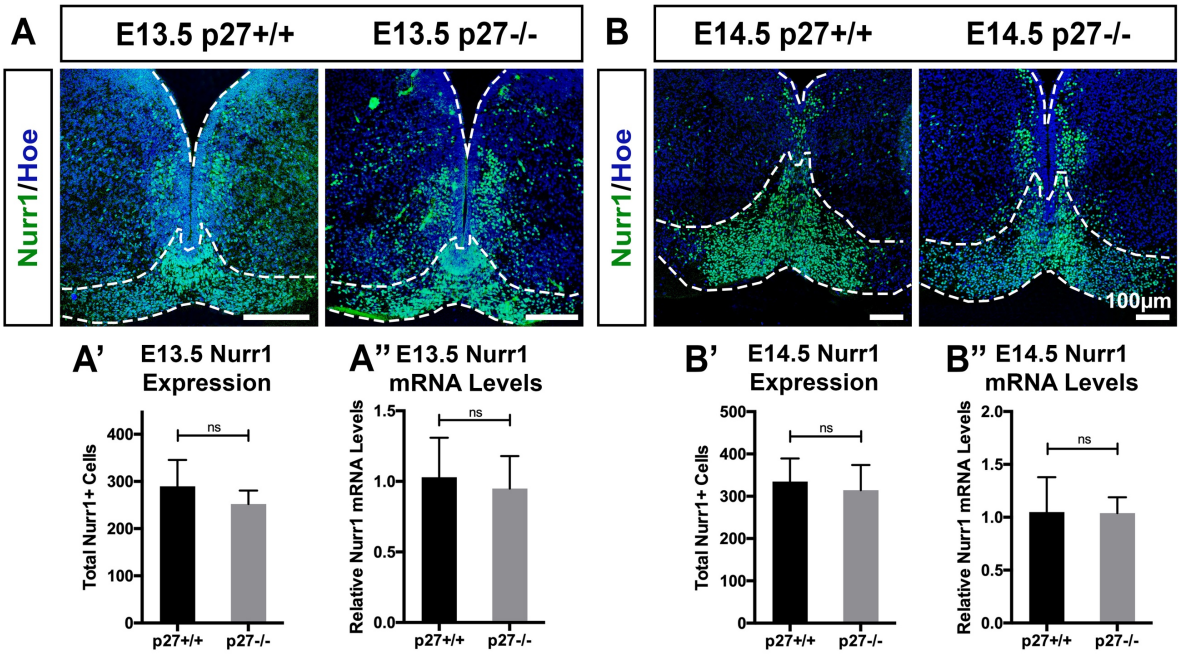

Figure 2.10: Effects of p27 deficiency begin to recover by later stages of development. A-A') Coronal sections of E13.5 VM showing recovered Nurr1 expression in p27 deficient mice as compared to control and A") recovered *Nurr1* mRNA levels. B-B') Coronal sections of E14.5 VM showing recovered Nurr1 expression in p27 deficient mice as compared to control and B") recovered *Nurr1* mRNA levels. Data represents mean ± S.E.M. (n=4-8 for each experiment). Statistical analysis was performed using Student's t-test between control and p27 deficient mice. Scale bars = 100µm.

2.11 p27 deficiency alters the progression of DA neuron development

Although we saw recovered Nurr1 levels by E13.5, we looked at the proper progression of DA neuron development by first investigating the number of Nurr1+ cells that had not yet acquired TH (Nurr1+TH- cells), which are DA-committed precursors residing in the IZ. We see an overall increase in total Nurr1+TH- precursors in p27 deficient mice (77.9 ± 15.4 Nurr1+TH- cells in p27-/- mice compared to 42.0 ± 12.0 Nurr1+TH- cells in controls; $p<0.01$**; Figure 2.11 A,A') and in the overall percentage of Nurr1+TH- cells in relation to total Nurr1+ cells (31.3% ± 7.7 Nurr1+TH-/Nurr1+ cells in p27-/- mice compared to 16.2% ± 4.3 in controls; $p<0.05$*; **; Figure 2.11 A,A"). Therefore, although Nurr1 expression begins to recover by E13.5, the majority of these Nurr1+ cells remain as precursors in the IZ. This is further supported by studying the overall number of mature DA neurons as measured by Pitx3+TH+ cells. In this case, we saw a significant decrease in the overall number of Pitx3+TH+ double cells in p27 deficient mice (154.0 ± 23.5 Pitx3+TH+ cells) as compared to controls (260.8 ± 4.7 Pitx3+TH+ cells; $p<0.01$**; Figure 2.11 B,B') and a significant decrease in the percentage of TH+ cells that were also Pitx3+ (69.9% ± 12.7 Pitx3+TH+/Total TH+ cells in p27-/- mice compared to 92.3% ± 4.7 in controls; $p<0.01$**; Figure 2.11 B,B"). These results support that

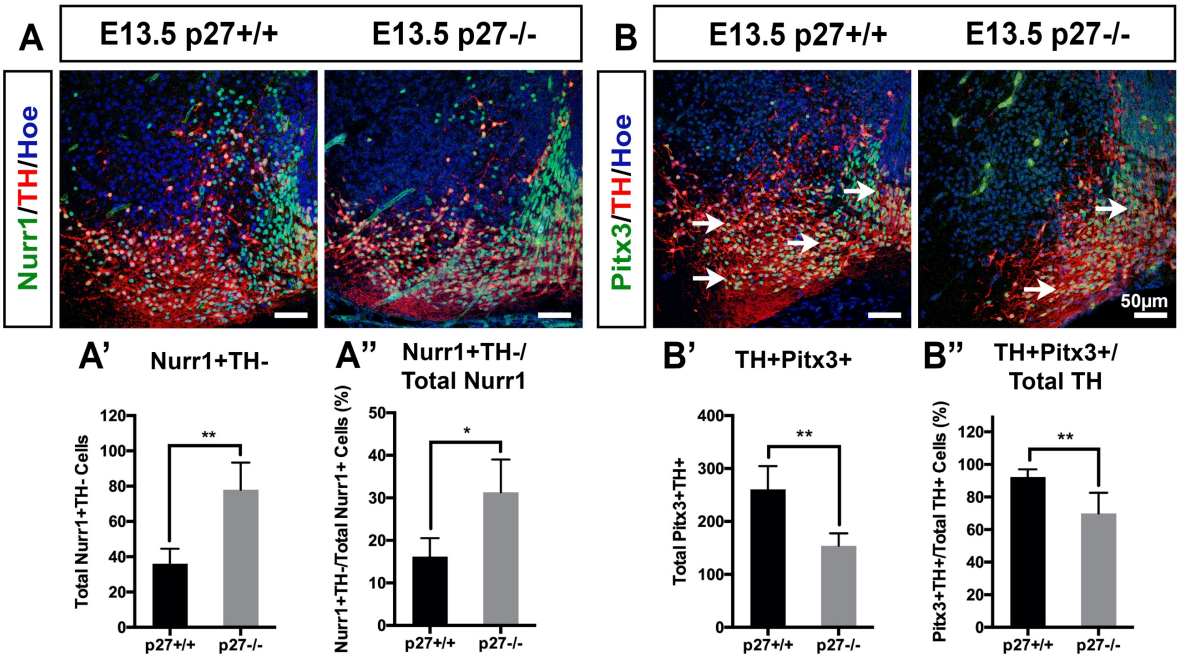

Figure 2.11: p27 deficiency alters the progression of DA neuron development. A-A'') Coronal sections of E13.5 VM showing increased expression of Nurr1+TH- cells in p27 deficient mice compared to controls. B-B'') Coronal sections of E13.5 VM showing decreased expression of Pitx3+TH+ double positive cells in p27 deficient mice compared to controls. Data represents mean ± S.E.M. (n=3 for each experiment). Statistical analysis was performed using Student's t-test between control and p27 deficient mice; $p<0.05$*; $p<0.01$**. Scale bars = 50µm.

p27 deficiency alters the progression of DA neuron development and may cause a developmental delay. Whether these neurons fully recover and develop into properly functioning DA neurons needs to be studied in more detail.

2.12 p27 deficiency maintains increased expression of cell cycle markers and neural precursors at later developmental stages

Since we saw that the effects of p27 deficiency were maintained at E13.5 and E14.5, we next studied the cell cycle marker Ki67 and the neural progenitor marker Sox2. We saw that Ki67 expression remained high at E13.5 (21.0% ± 5.1 expression in p27-/- mice compared to 9.9% ± 4.4 in controls; $p<0.05$* and 1.61 ± 0.43 relative *Ki67* E13.5 mRNA levels in p27-/- mice compared to 0.94 ± 0.26 in controls; $p<0.05$*; Figure 2.12 A-A") and E14.5 (11.7 ± 3.8 Ki67+ cells in p27-/- mice compared to 3.1 ± 2.0 in controls; $p<0.05$* and 1.42 ± 0.23 relative *Ki67* E14.5 mRNA levels in p27-/- mice compared to 1.07 ± 0.29 in controls; $p<0.05$*; Figure 2.12 B-B").

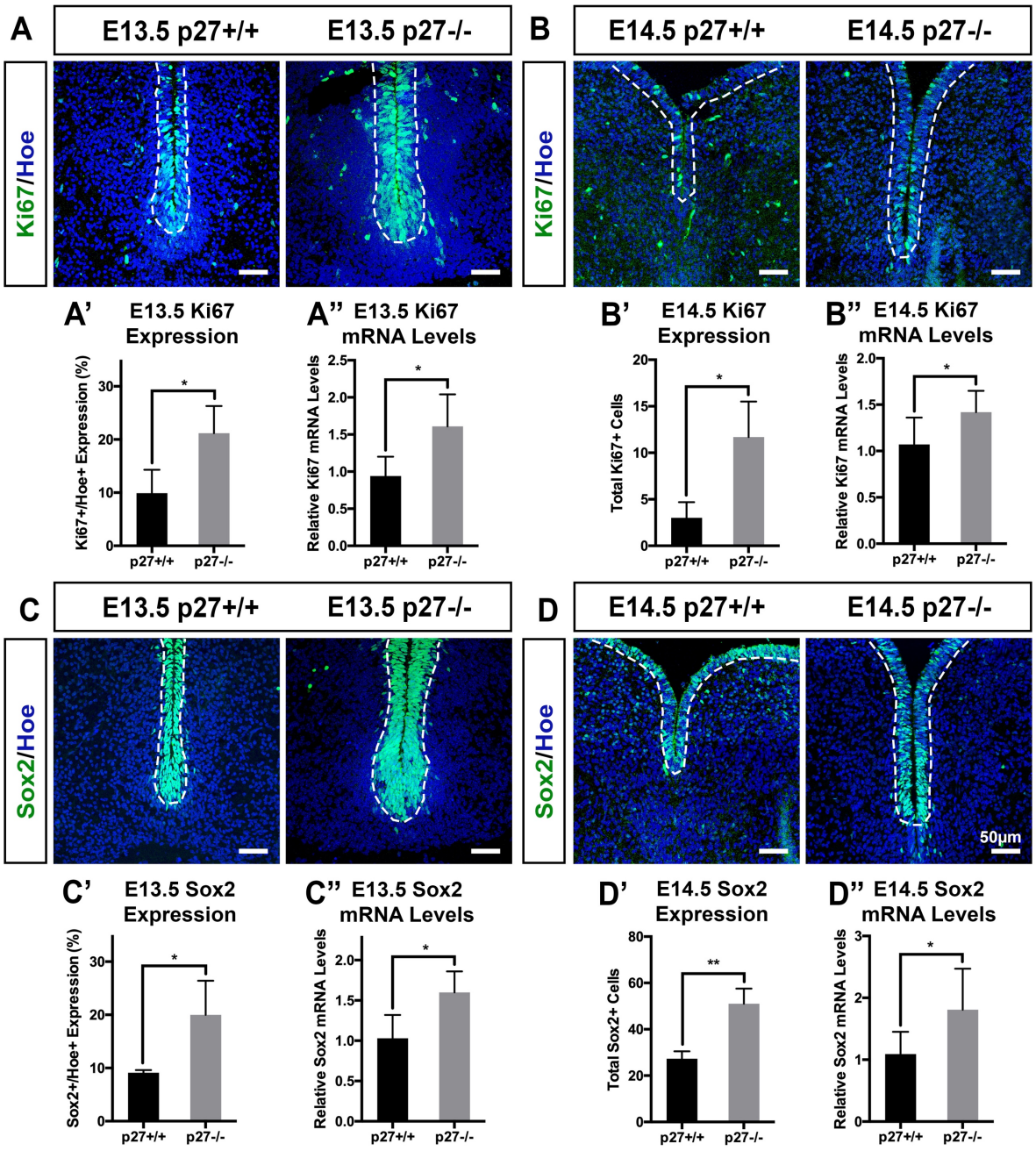

Figure 2.12: p27 deficiency maintains increased expression of cell cycle markers and neural precursors at later developmental stages. A-A') Coronal sections of E13.5 VM showing increased Ki67 expression in p27 deficient mice as compared to control and A") increased *Ki67* mRNA levels. B-B') Coronal sections of E14.5 VM showing increased Ki67 expression in p27 deficient mice as compared to control and B") increased *Ki67* mRNA levels. C-C') Coronal sections of E13.5 VM showing increased Sox2 expression in p27 deficient mice as compared to control and C") increased *Sox2* mRNA levels. D-D') Coronal sections of E14.5 VM showing increased Sox2 expression in p27 deficient mice as compared to control and D") increased *Sox2* mRNA levels. Data represents mean ± S.E.M. (n=4-8 for each experiment). Statistical analysis was performed using Student's t-test between control and p27 deficient mice; $p<0.05$*; $p<0.01$**. Scale bars = 50µm.

Similar results were obtained for Sox2, where we again observed increased expression at E13.5 (20.0% ± 6.1 Sox2 expression in p27-/- mice compared to 9.1% ± 0.5 in controls; p<0.01** and 1.6 ± 0.3 relative *Sox2* mRNA levels in p27-/- mice compared to 1.03 ± 0.29 in controls; p<0.05*; Figure 2.12 C-C") and E14.5 (51.0 ± 7.1 Sox2+ cells in p27-/- mice compared to 27.3 ± 3.2 in controls; p<0.05* and 1.81 ± 0.66 relative *Sox2* mRNA levels in p27-/- mice compared to 1.09 ± 0.36 in controls; p<0.05*; Figure 2.12 D-D").

Furthermore, knowing that Ki67 and Sox2 are co-expressed almost 100% with the proliferation markers BrdU and PCNA, these results are an indirect measure of increased proliferation at later developmental stages, allowing us to conclude that p27 deficiency increases the pool of proliferating precursors in the midbrain throughout development.

2.13 Effects of p27 deficiency on DA precursors are maintained at later developmental stages, but their distribution is recovered

When investigating the expression of Ngn2, we saw that at E13.5, the expression remained high (70.9 ± 8.1 Ngn2+ cells in p27-/- mice compared to 41.9 ± 2.2 in controls; p<0.0001**** and 1.23 ± 0.05 relative *Ngn2* mRNA levels in p27-/- mice compared to 1.01 ± 0.1 in controls; p<0.01**; Figure 2.13 A-A"). By E14.5, the expression of Ngn2 had disappeared in controls, whereas we observed some expression in p27 deficient mice (3.3 ± 1.5 Ngn2+ cells in E14.5 p27-/- mice compared to 0.1 ± 0.1 in controls; p<0.05* and 1.57 ± 0.35 relative *Ngn2* mRNA levels in E14.5 p27-/- mice compared to 1.12 ± 0.31 in controls; p<0.05*; Figure 2.13 B-B").

However, when looking at the distribution of DA neuron precursors, we saw that there was a trend indicating an increased level of Ngn2+Sox2+ double positive cells in E13.5 p27 deficient mice compared to controls (26.3 ± 5.9 Ngn2+Sox2+ cells in p27-/- mice compared to 15.3 ± 4 in controls; Figure 2.13 C,D), but this increase was not significant. Furthermore, we saw that the expression of Ngn2+Sox2+ cells in relation to total Sox2+ cells was recovered by E13.5 (14.5 ± 3 Ngn2+Sox2+/Total Sox2+ cells in p27-/- mice compared to 12.4 ± 3.1 in controls; Figure 2.13 D'). This led us to believe that perhaps the increased Ngn2+Sox2+ cells we saw at earlier stages had begun differentiating, and therefore, we initially expected to see a greater number of Ngn2+Sox2- cells in the IZ. However, like at earlier stages, we did not see an increase in the number of DA neuron precursors that had exited the cell cycle, making up the IZ (25.1 ± 11.0 Ngn2+Sox2- cells in p27-/- mice compared to 26.3 ± 8.5 in controls; Figure 2.13 D").

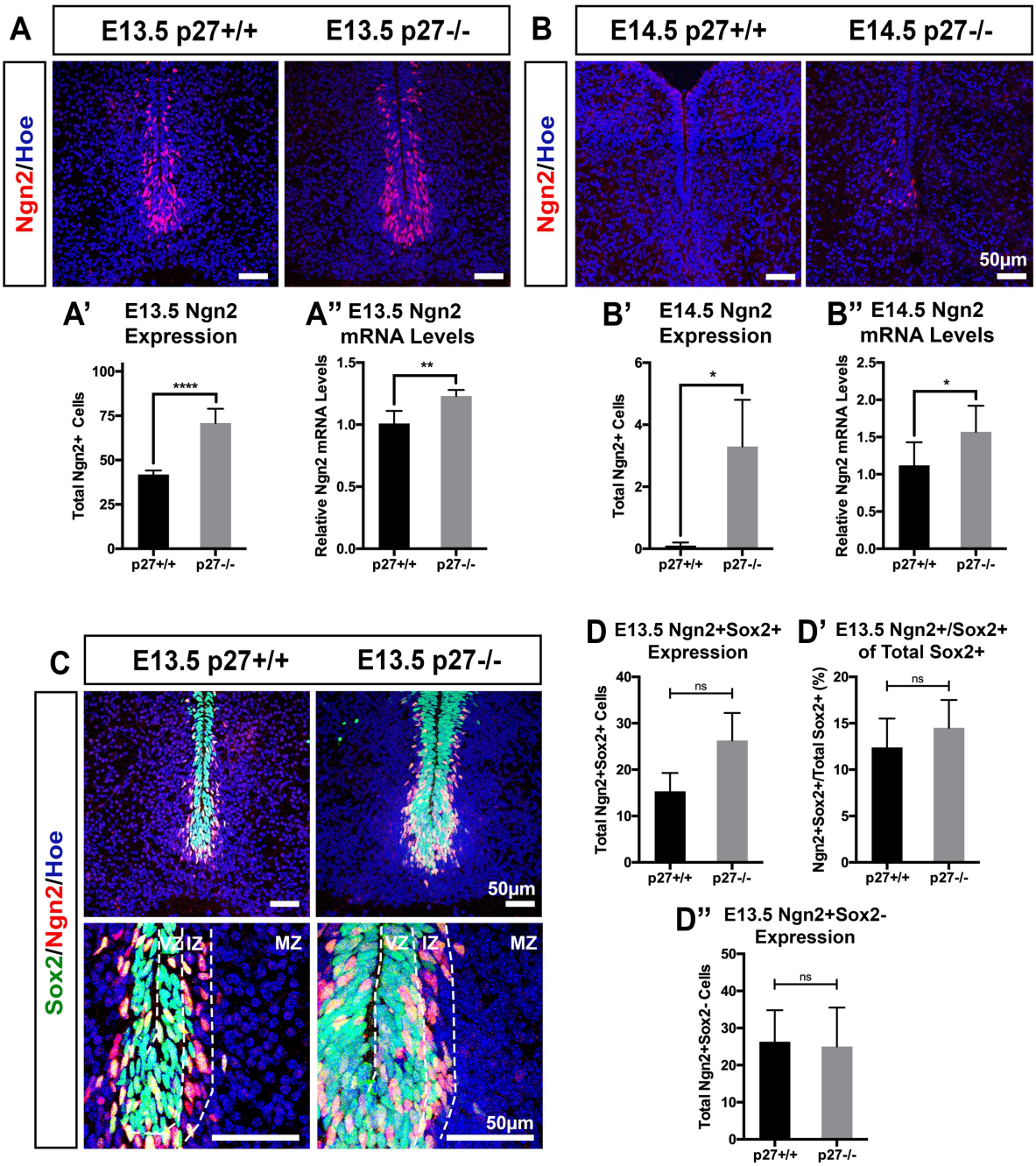

Figure 2.13: Effects of p27 deficiency on DA precursors are maintained at later developmental stages, but their distribution is recovered. A-A') Coronal sections of E13.5 VM showing increased Ngn2 expression in p27 deficient mice as compared to control and A") increased *Ngn2* mRNA levels. B-B') Coronal sections of E14.5 VM showing increased Ngn2 expression in p27 deficient mice as compared to control and B") increased *Ngn2* mRNA levels. C) Coronal sections of E13.5 VM showing co-expression of Ngn2 and Sox2. D-D") Quantification of Ngn2+Sox2+ double positive cells of the VZ and Ngn2+Sox2- cells of the IZ. Data represents mean ± S.E.M. (n=3 for each experiment). Statistical analysis was performed using Student's t-test between control and p27 deficient mice; $p<0.05$*; $p<0.01$**; $p<0.0001$****. Scale bars = 50µm.

In summary, we have seen that p27 deficiency decreases early DA neuron production, which is maintained at later stages of development, though markers such as Nurr1 begin to recover by E13.5. Furthermore, we observed that p27 deficiency caused an increase in cell proliferation at E12.5, as measured by BrdU and PCNA. This was further supported by an increase in the expression of the cell cycle marker Ki67 and the neural precursor marker Sox2 at all developmental stages examined. Our results also showed an increase in DA neuron-specific precursors (as measured by Ngn2+Sox2+ cells), although their distribution was altered at early developmental stages. These results, therefore, indicate an important function of p27 in the proper development of DA neurons *in vivo*.

SECTION III:

POSSIBLE MOLECULAR MECHANISMS OF P27 DEFICIENCY *IN VIVO*

After seeing the effects of p27 deficiency *in vivo* from embryonic ages E11.5-E14.5, we decided to look at possible molecular mechanisms to explain these effects. This included studying the effects of p27 on cell death, phenotype specification, cell cycle alterations and possible downstream effects of DA neuron progenitor differentiation.

3.1 p27 deficiency does not increase programmed cell death *in vivo*

To study the effects of p27 deficiency on cell death in the developing midbrain, we first studied the expression of pyknotic nuclei, which are fragmented nuclei indicative of cell death. We did not detect the presence of pyknotic nuclei, and thereby no significant differences in the expression between p27 deficient mice and controls (Figure 3.1 A-D, top panels). To confirm these results, we performed a similar study, staining for the apoptotic marker activated-Casp3, and again, did not detect the presence of this marker, and thereby no significant differences in p27 deficient mice as compared to controls (Figure 3.1 A-D, bottom panels). Therefore, increased cell death did not appear to be the cause of decreased DA neuron development in p27 deficient mice.

3.2 p27 deficiency does not alter phenotype specification in the developing VM

Since increased cell death did not appear to be present in p27 deficient brains, we thought perhaps p27 could be altering the phenotypic specification of DA neurons in the developing midbrain. We studied the expression of BIII-Tub as a neurogenesis marker and Gfap as a gliogenesis marker at E11.5 (early development) and E13.5 (late development). We saw no significant changes in the expression of BIII-Tub at E11.5 (64.1% ± 2.9 BIII-Tub expression in p27-/- mice as compared to 62.6% ± 5.2 BIII-Tub expression in controls) or at E13.5 (87.5% ± 3.6 BIII-Tub expression in p27-/- mice as compared to 89.6 ± 0.5 in controls) (Figure 3.2 A,B top panels; A',B'), indicating that p27 deficiency does not alter neurogenesis in the developing VM. When investigating the marker Gfap, we saw no expression and no significant differences at E11.5 or E13.5, indicating that p27 does not alter or accelerate gliogenesis (Figure 3.2 A,B bottom panels; A",B").

Seeing that the general processes of neurogenesis and gliogensis were not affected by p27 deficiency, we did a more in-depth analysis of the mRNA levels of specific neuronal phenotypes, both known to reside in the VM (such as GABA-ergic and glutamatergic neurons)

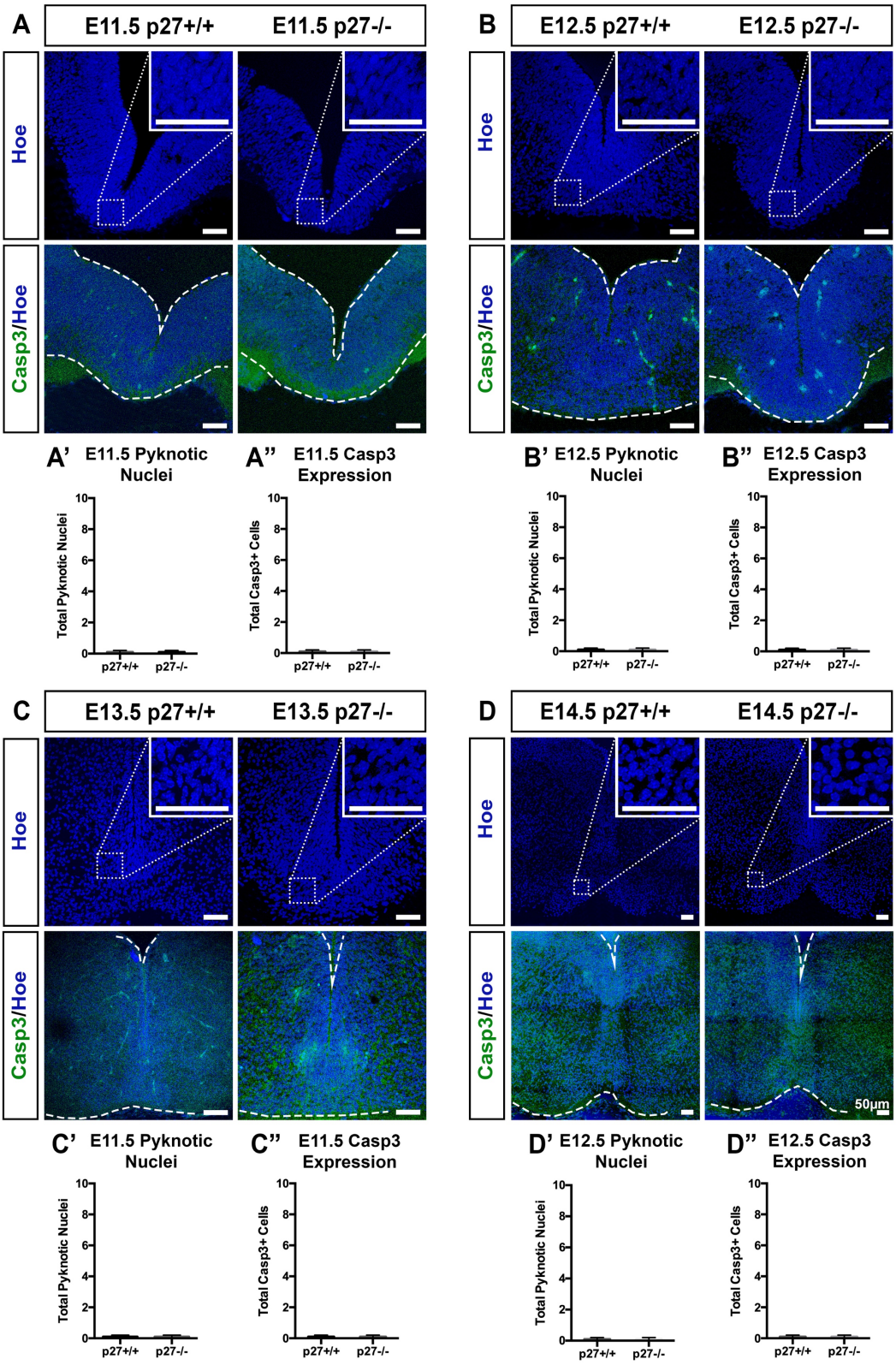

Figure 3.1: p27 deficiency does not increase programmed cell death *in vivo*. A-A") Coronal sections of E11.5 VM showing an apparent absence of pyknotic nuclei (top panels) and activated-Casp3 (bottom panels) in both p27 deficient mice and controls. Similar results were obtained at E12.5 (B-B"), E13.5 (C-C") and E14.5 (D-D"). Data represents mean ± S.E.M. (n=3 for each experiment). Statistical analysis was performed using Student's t-test between control and p27 deficient mice. Scale bars = 50µm.

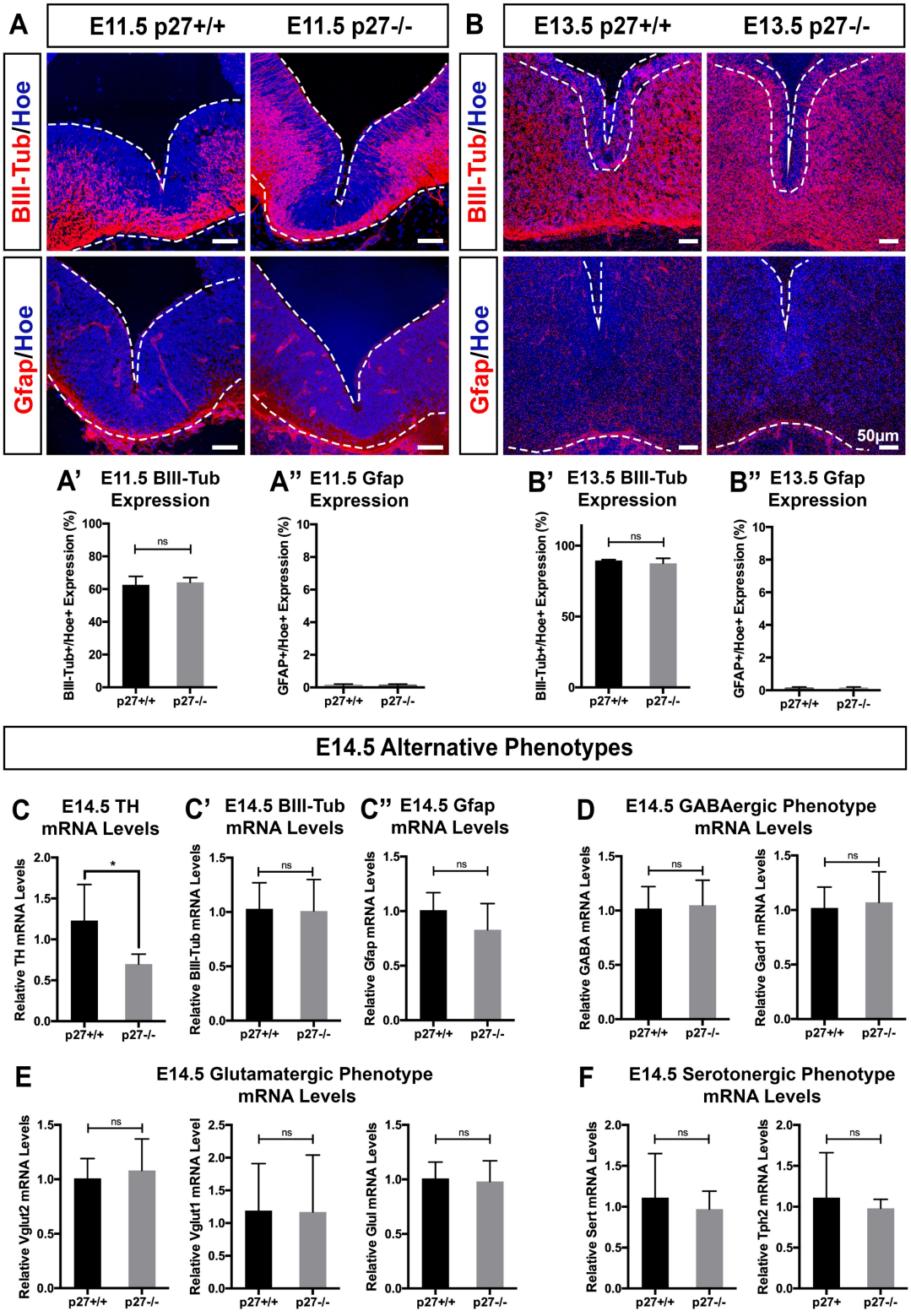

Figure 3.2: p27 deficiency does not alter cell fate specification. A-A") Coronal sections of E11.5 VM showing no differences in the expression of BIII-Tub (top panels) or Gfap (bottom panels) between p27 deficient mice and controls. Similar results were obtained at E13.5 (B-B"). RT-qPCR showing decreased *TH* mRNA levels (C) at E14.5 but no alterations in the mRNA levels of BIII-Tub (C') or Gfap (C"). RT-qPCR showing no alterations in the mRNA levels of GABAergic (D), Glutamatergic (E) or Serotonergic (F) markers at E14.5. Data represents mean ± S.E.M. (n=4-8 for each experiment). Statistical analysis was performed using Student's t-test between control and p27 deficient mice; $p<0.05$*. Scale bars = 50µm.

and outside the VM (serotonergic neurons). First, we confirmed that there were decreased *TH* mRNA levels in p27 deficient mice compared to controls at E13.5, as well as no changes in the mRNA levels of BIII-Tub or Gfap (Figure 3.2 C-C"). Then we studied the GABAergic markers GABA and Gad1 (Figure 3.2 D), the glutamatergic markers Vglut2, Vglut1 and Glul (Figure 3.2 E), and the serotonergic markers Sert1 and Tph2 (Figure 3.2 F), and saw no significant differences in the mRNA levels of either of these markers when comparing p27 deficient mice to controls. These results indicate that p27 deficiency does not alter cell fate specification and the effect appears to be specific to DA neurons.

3.3 Effects of p27 deficiency on G1 phase cyclins and CDKs

Since p27 is best known for its function in the cell cycle, we wanted to see how p27 deficiency affected different cyclins and CDKs. We first investigated the G1 phase cyclins D1, D2 and D3. *Cyclin D1* mRNA levels were decreased in p27 deficient mice at early developmental stages (Figure 3.3 A-A'''), whereas *Cyclin D2* mRNA levels were decreased at later developmental stages (Figure 3.3 B-B'''). *Cyclin D3* mRNA levels showed somewhat inconsistent results, with no clear pattern or effect of p27 deficiency (Figure 3.3 C-C'''). When studying the CDKs associated with these cyclins, we saw no significant effects of p27 deficiency on Cdk4 (Figure 3.3 D-D'''), but *Cdk6* mRNA levels were significantly decreased in p27 deficient mice, especially at later developmental stages (Figure 3.3 E-E''').

Since decreased Cyclin D levels are associated with longer cell cycles and the onset of differentiation (Bryja et al 2003), these results suggest that p27 deficiency decrease DA neuron development by shortening the cell cycle of these neurons despite decreased Cyclin D levels, most likely by affecting other parts of the cell cycle.

3.4 Effects of p27 deficiency on G1-S and G2-M phase cyclins and CDKs

The direct effect of p27 on promoting cell cycle exit lies in its function at the G1-S phase transition, where it inhibits Cyclin E/A-Cdk2 complexes. When studying the mRNA levels of Cyclin A, we saw significant increases in mRNA levels at all developmental stages studied Figure 3.4 A-A'''). We obtained similar results for Cyclin E, showing increased mRNA levels at all stages, with the exception of E14.5 (Figure 3.4 B-B'''). p27 deficiency caused a trend in slightly increasing *Cdk2* mRNA levels during development, but these differences were only significant at E14.5.

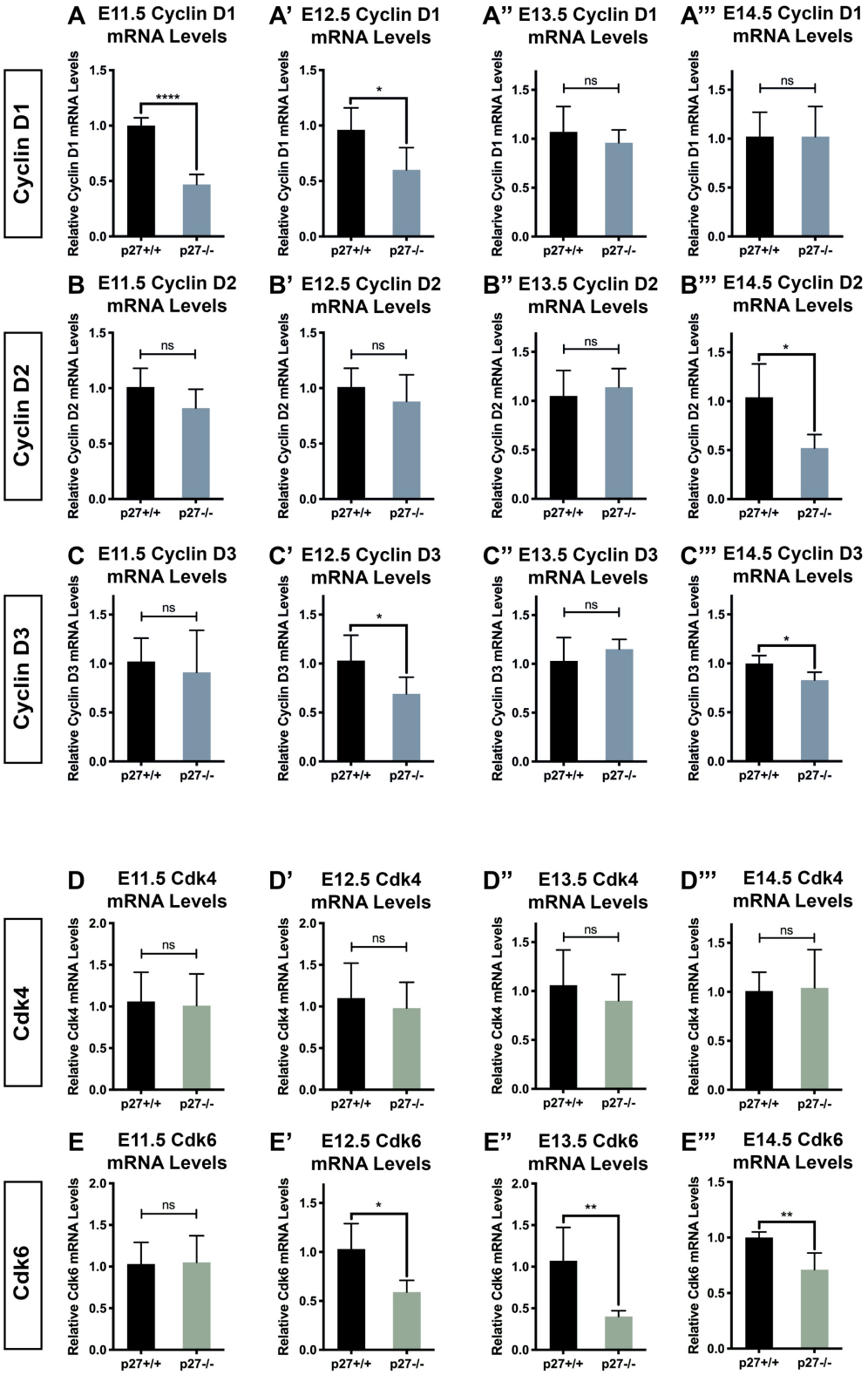

Figure 3.3: Effects of p27 deficiency on G1 phase cyclins and CDKs. A-A''') *Cyclin D1* mRNA levels from E11.5-E14.5. B-B''') *Cyclin D2* mRNA levels from E11.5-E14.5. C-C''') *Cyclin D3* mRNA levels from E11.5-E14.5. D-D''') *Cdk4* mRNA levels from E11.5-E14.5. E-E''') *Cdk6* mRNA levels from E11.5-E14.5. Data represents mean ± S.E.M. (n=8 for each experiment). Statistical analysis was performed using Student's t-test between control and p27 deficient mice; $p<0.05$*; $p<0.01$**; $p<0.0001$****.

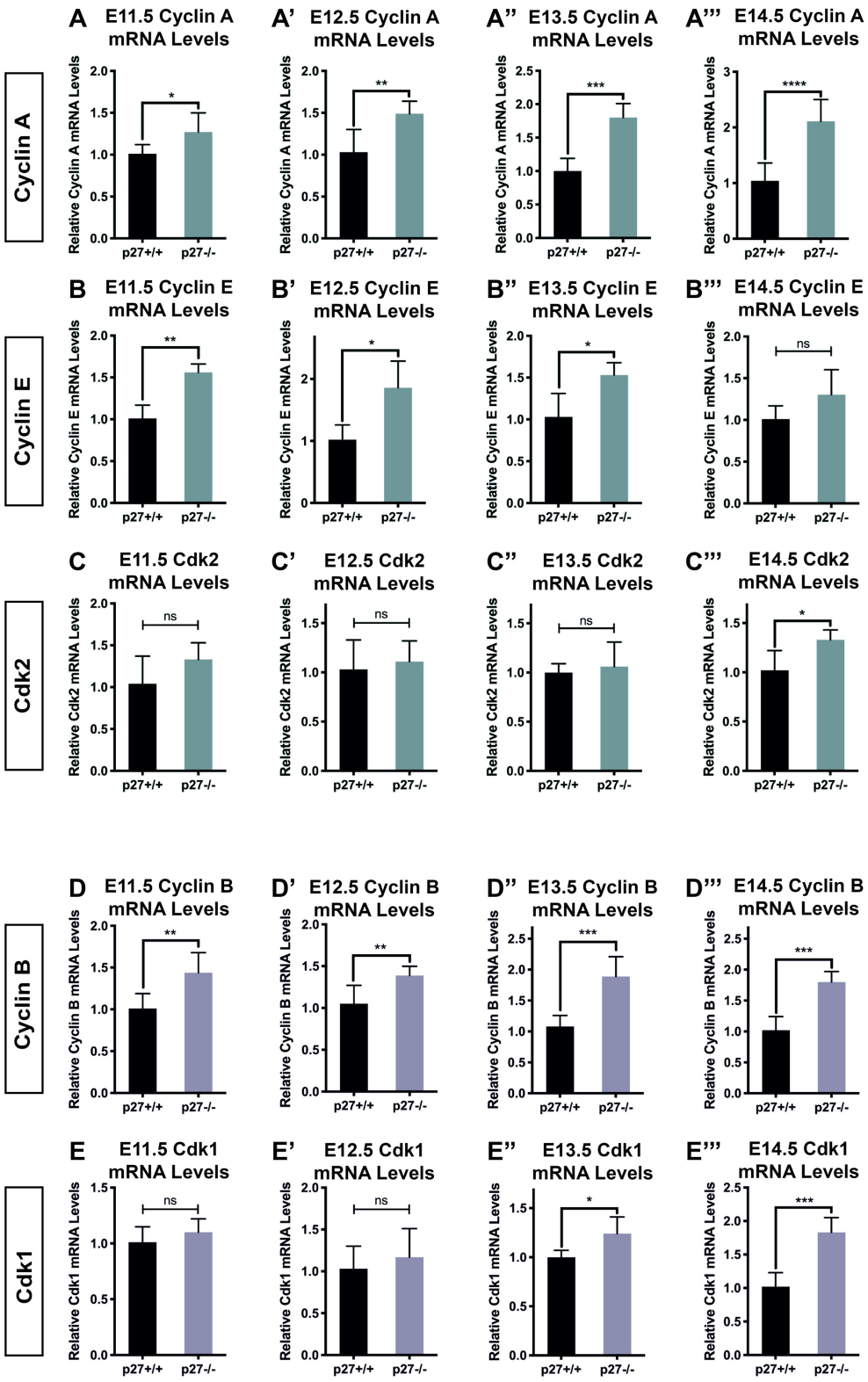

Figure 3.4: Effects of p27 deficiency on G1-S and G2-M phase cyclins and CDKs. A-A''') *Cyclin A* mRNA levels from E11.5-E14.5. B-B''') *Cyclin E* mRNA levels from E11.5-E14.5. C-C''') *Cdk2* mRNA levels from E11.5-E14.5. D-D''') *Cyclin B* mRNA levels from E11.5-E14.5. E-E''') *Cdk1* mRNA levels from E11.5-E14.5. Data represents mean ± S.E.M. (n=8 for each experiment). Statistical analysis was performed using Student's t-test between control and p27 deficient mice; *p<0.05; **p<0.01; ***p<0.001; ****p<0.0001.

Finally, studying the G2-M phase transition, we again saw significant increases in *Cyclin B* mRNA levels at all developmental stages studied (Figure 3.4 D-D'''). Again, when studying Cdk1, we see that p27 deficiency causes an increased trend during development, with significant differences at later developmental stages (Figure 3.4 E-E''').

3.5 Effects of p27 deficiency on CKI inhibitors in the developing VM

Since p27 is a member of the CKI family that also contains p57 and p21, we wanted to study how p27 deficiency affected the mRNA levels of these two CKIs. We saw a general pattern where p57 was significantly decreased in p27 deficient mice at early developmental stages but was recovered by E13.5 (Figure 3.5 A-A'''') and p21 was significantly increased in p27 deficient mice at early developmental stages, but, again, was recovered by E13.5 (Figure 3.5 B-B''').

3.6 Screen of possible novel targets of Ngn2 in the developing VM

Until now, we have seen that p27 deficiency significantly decreases DA neuron development but increases the production of DA neuron precursors. Furthermore, we have seen that these precursors are not undergoing cell death and they have not undergone altered phenotypic specification. The altered distribution of DA precursors (as measured by Ngn2+Sox2+)

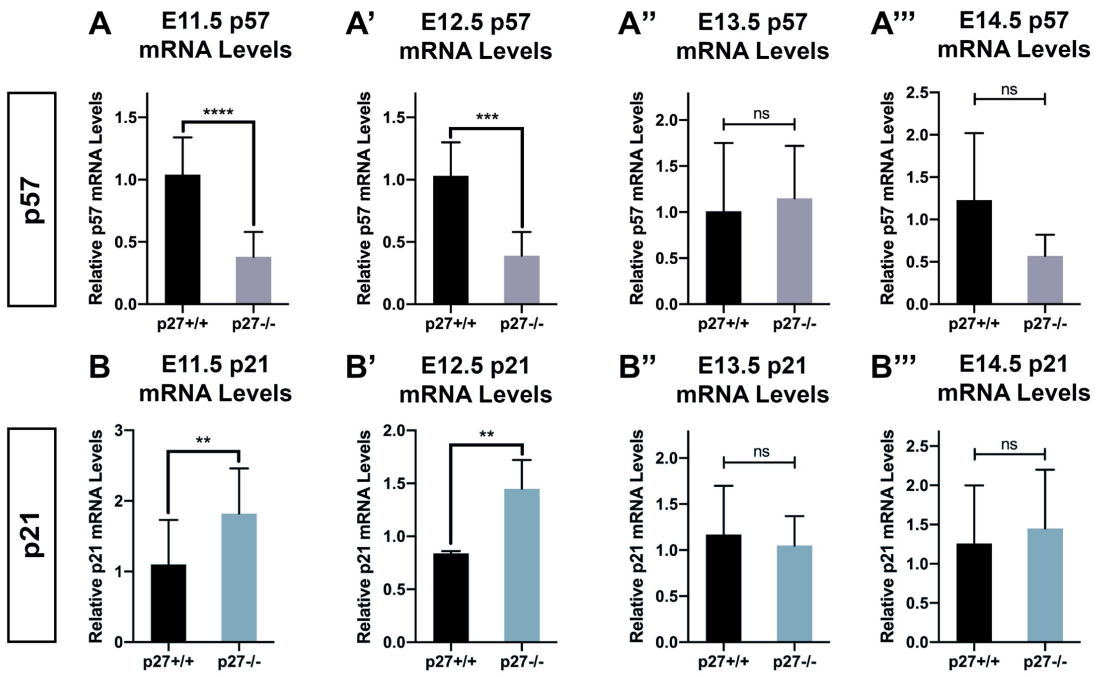

Figure 3.5: Effects of p27 deficiency on CKI inhibitors in the developing VM. A-A''') *p57* mRNA levels from E11.5-E14.5. B-B''') *p21* mRNA levels from E11.5-E14.5. Data represents mean ± S.E.M. (n=8 for each experiment). Statistical analysis was performed using Student's t-test between control and p27 deficient mice; p<0.01**; p<0.001***.

suggests that p27 deficiency halts the differentiation of these double positive cells in a precursors state. We therefore did a screening of Ngn2-related factors, including known direct-downstream targets. The first screen included Mash1, which has been known to cooperate with Ngn2 during DA neuron development (Kele et al 2006), and we saw a significant increase in mRNA levels at E12.5 in p27 deficient mice (1.35 ± 0.19 *Mash1* mRNA levels) compared to controls (1.03 ± 0.26 *Mash1* mRNA levels; $p<0.05$*; Figure 3.6 A). Next, we studied the expression of the progenitor maintenance markers Hes1, Hes5 and Dll1, thinking that p27 deficiency halted DA neuron development by promoting a progenitor state. However, we saw no significant differences in the expression of any of these markers at E12.5 (Figure 3.6 B-D). Pax5, another important factor in DA neuron development, also appeared unaffected by p27 deficiency (Figure 3.6 E).

Knowing that p27 deficiency did not appear to promote a progenitor state, we did a screen of NeuroD proteins, known downstream targets of Ngn2, that have been shown to promote neurogenesis in the retina (Cherry et al 2011) and inner ear (Boutin et al 2010). Interestingly, we saw a significant decrease in *NeuroD1* mRNA levels at E12.5 in p27 deficient mice compared to controls (0.78 ± 0.12 *NeuroD1* mRNA levels in p27-/- mice compared to

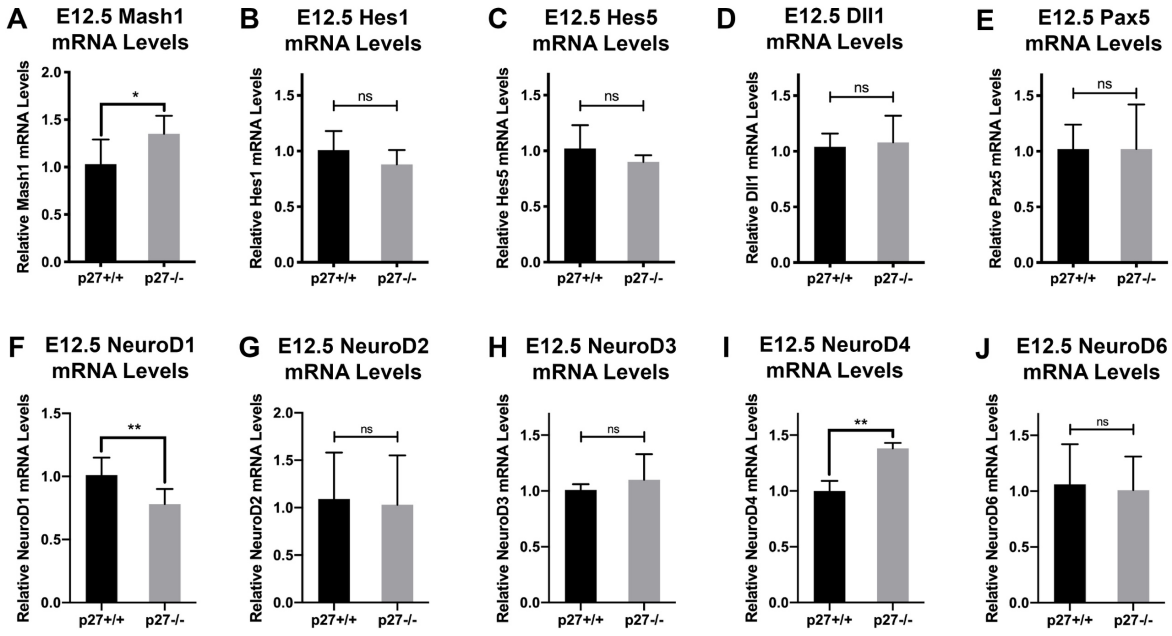

Figure 3.6: Screen of possible novel targets of Ngn2 in the developing VM. RT-qPCR results from E12.5 showing A) increased *Mash1* mRNA levels and unaltered *Hes1* (B), *Hes5* (C), *Dll1* (D) and *Pax5* (E) mRNA levels in p27 deficient mice compared to control. F-J) Screen of NeuroD1 proteins in the VM, of which NeuroD1 is of special interest, showing decreased mRNA levels in p27 deficient mice compared to controls (F). Data represents mean ± S.E.M. (n=8 for each experiment). Statistical analysis was performed using Student's t-test between control and p27 deficient mice; $p<0.05$*; $p<0.01$**.

1.01 ± 0.14 in controls; p<0.01**; Figure 3.6 F), while the majority of other NeuroD proteins appeared unaffected (Figure 3.6 G-J). There was a significant increase in *NeuroD4* mRNA levels (Figure 3.6 I), which should be studied in more detail, however due to previous work describing the role of NeuroD1 in neural tissue, and its relevance in neuronal differentiation, we did a deeper investigation of the possible role of NeuroD1 in DA neuron development.

3.7 p27 deficiency decreases NeuroD1 in the developing VM

We first studied the mRNA levels of Mash1 at all developmental stages, and saw significant increases at E11.5 to E13.5, but these increases recovered to control levels by 14.5. These results suggest a possible compensatory mechanism for p27 deficiency. Next, based on the results we obtained from our screen of downstream-Ngn2 targets, we did a deeper investigation of NeuroD1 expression in the developing midbrain. We saw that *NeuroD1* mRNA levels were decreased at E11.5 (0.71 ± 0.15 relative *NeuroD1* mRNA levels in p27-/- mice compared to 1.01 ± 0.14 in controls; p<0.05*; Figure 3.7 B), at E12.5 (mentioned above, Figure 3.7 B'), at E13.5 (0.79 ± 0.13 relative *NeuroD1* mRNA levels in p27-/- mice compared to 1.01 ± 0.17 in controls; p<0.05*; Figure 3.7 B"), and these differences recovered by E14.5 (0.93 ± 0.19 relative *NeuroD1* mRNA levels in p27-/- mice compared to 1.03 ± 0.14 in controls; Figure 3.7 B'''). These results were confirmed in brain sections at early developmental stages, where we again saw a significant decrease in NeuroD1 expression at E11.5 in p27 deficient mice (9.3 ± 4.5 NeuroD1+ cells in p27-/- mice compared to 57.0 ± 2.0 in controls; p<0.0001****; Figure 3.7 C) and E12.5 (19.7 ± 8.5 NeuroD1+ cells in p27-/- mice compared to 52.7 ± 11.9 in controls; p<0.05*; Figure 3.7 D). We also observed that the decreased expression of NeuroD1 was almost completely absent from the ventral most part of the IZ in the VM, with an expression pattern in p27 deficient mice restricted to a more lateral position (Figure 3.7 B). Furthermore, since NeuroD1 has not yet been described in the context of the developing VM, we investigated if NeuroD1 was co-expressed with TH. We saw no NeuroD1+TH+ double positive cells in p27 deficient or control mice (Figure 3.7 C,D bottom panels), indicating that the function of NeuroD1 is most likely upstream of TH.

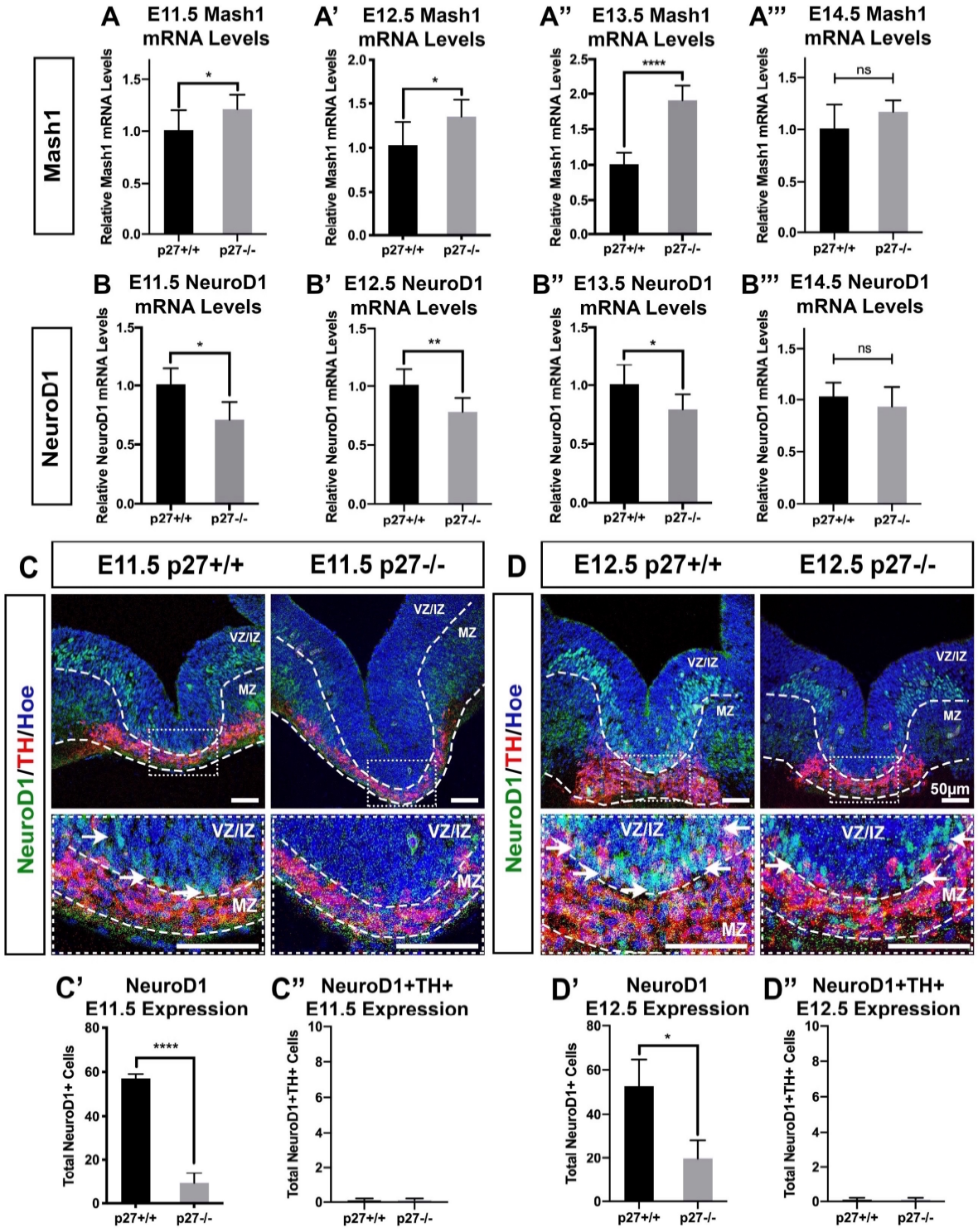

Figure 3.7: p27 deficiency decreases NeuroD1 in the developing VM. A-A''') RT-qPCR results showing increased *Mash1* mRNA levels from E11.5-E14.5. B-B''') RT-qPCR results showing decreased *NeuroD1* mRNA levels from E11.5-E14.5. C,C') Coronal sections of E11.5 VM showing decreased NeuroD1 and C") no co-expression with TH. D,D') Coronal sections of E12.5 VM showing decreased NeuroD1 and D") no co-expression with TH in p27 deficient mice compared to controls. Data represents mean ± S.E.M. (n=4-8 for each experiment). Statistical analysis was performed using Student's t-test between control and p27 deficient mice; $p<0.05$*; $p<0.01$**; $p<0.0001$****. Scale bars = 50µm.

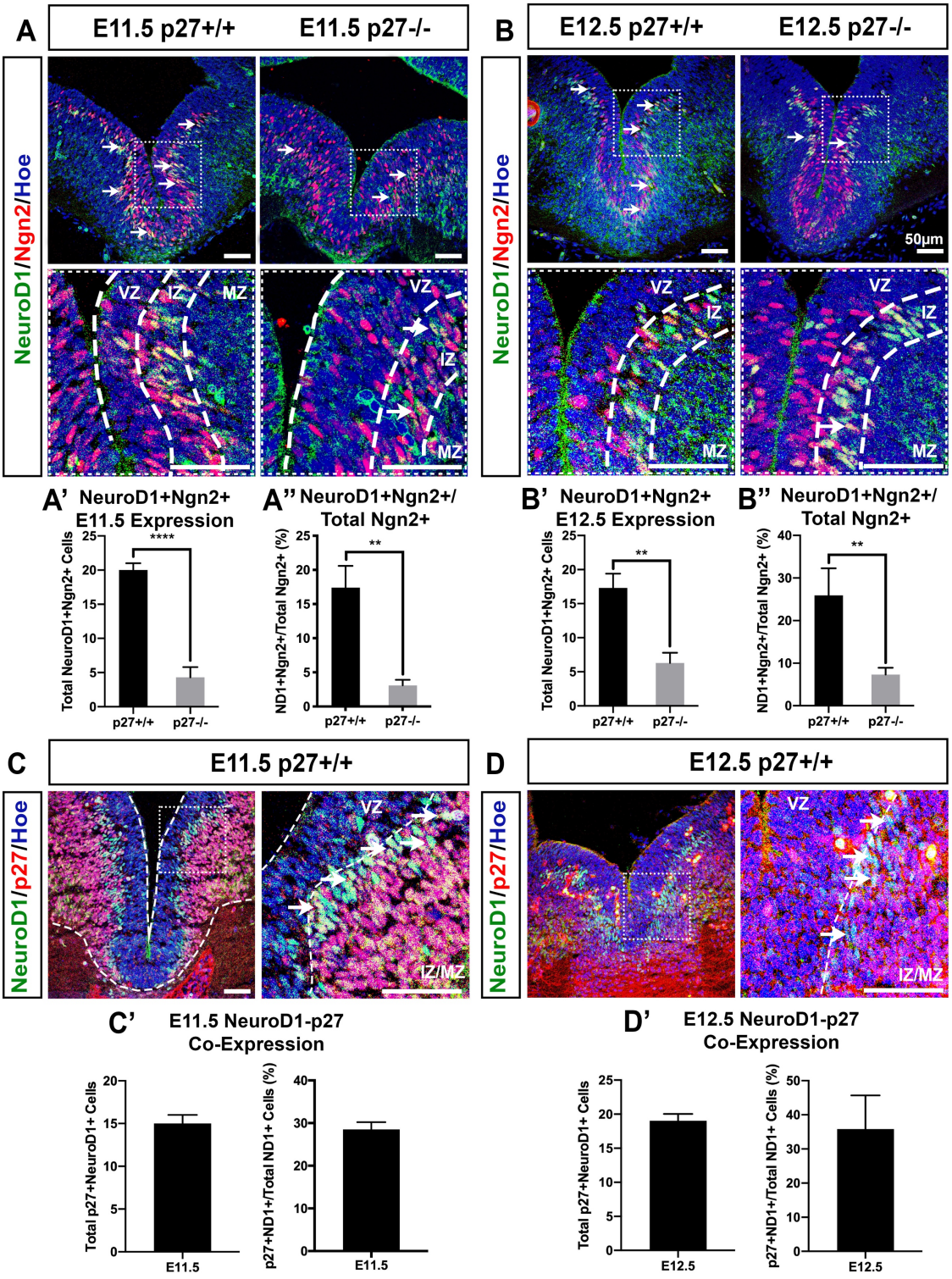

Figure 3.8: Description of possible importance of NeuroD1 in the developing VM. A-A'') Coronal sections of E11.5 VM showing decreased expression of NeuroD1+/Ngn2+ double positive cells in p27 deficient mice compared to controls. B-B'') Coronal sections of E12.5 VM showing decreased expression of NeuroD1+/Ngn2+ double positive cells in p27 deficient mice compared to controls. C-C'') Coronal sections of E11.5 VM showing expression pattern of NeuroD1 and p27 in control mice. D-D'') Coronal sections of E12.5 VM showing expression pattern of NeuroD1 and p27 in control mice. Data represents mean ± S.E.M. (n=3 for each experiment). Statistical analysis was performed using Student's t-test between control and p27 deficient mice; $p<0.01$**; $p<0.001$***; $p<0.0001$****. Scale bars = 50µm.

3.8 Description of possible importance of NeuroD1 in the developing VM

Although we saw no co-expression of NeuroD1 with TH, we studied the expression of NeuroD1 with upstream factor Ngn2 and saw some co-expression of these two factors in controls at E11.5 (20.1 ± 1.0 NeuroD1+Ngn2+ cells), which was significantly decreased in p27 deficient mice (4.3 ± 1.5 NeuroD1+Ngn2+ cells; p<0.0001****; Figure 3.8 A-A'). These results were confirmed at E12.5 (6.3 ± 1.5 NeuroD1+Ngn2+ cells in p27-/- mice compared to 17.3 ± 2.1 in controls; p<0.01**; Figure 3.8 B-B'). When studying NeuroD1+Ngn2+ cells in relation to the total Ngn2+ cells, we also see that the majority of NeuroD1+ cells are in the IZ, which is diminished in p27-/- mice (3.1 ± 0.8 NeuroD1+Ngn2+/Total Ngn2+ cells in p27-/- mice compared to 17.4 ± 3.2 in controls at E11.5; p<0.01**; Figure 3.8 A" and 7.3 ± 1.6 NeuroD1+Ngn2+/Total Ngn2+ cells in p27-/- mice compared to 25.9 ± 6.4 in controls at E12.5; p<0.01**; Figure 3.8 B"). Seeing the distribution of NeuroD1 in the IZ, we did a study of the expression pattern of NeuroD1 with p27, and saw a similar pattern as seen with Ngn2 earlier. However, in the case of NeuroD1, about 30% of NeuroD1+ cells were p27+NeuroD1+ double positive at E11.5, which raised to about 35% at E12.5 (Figure 3.8 C,D). These results strongly suggest an important function of NeuroD1 in the cascade of proper signaling to generate mature DA neurons, which could describe a novel factor linking Ngn2 and TH.

In summary, we have shown that p27 deficiency does not decrease DA neuron development by increasing cell death or altering phenotypic specification *in vivo.* Furthermore, we have seen a general effect of p27 deficiency on the cell cycle, showing increased mRNA levels of Cyclin A, Cyclin E and Cdk2, consistent with the effects observed for increased proliferation. Finally, in an attempt to explain how we see more proliferation and a greater number of DA neuron precursors, but an overall decrease in DA neuron development, we studied direct downstream targets of Ngn2. We saw a significant decrease in the expression of NeuroD1, a novel factor in the context of the VM, which could explain a cell-cycle independent function of p27, where the absence of p27 may hinder the proper progression of DA neuron development by affecting the ability of Ngn2 to activate downstream targets necessary to promote neurogenesis.

SECTION IV:

EFFECTS OF P27 DEFICENCY ON VM PRIMARY CULTURES

Although p27 has previously been associated with increased cell death (Bryja et al 2004, Bryja et al 2005), we did not observe such effects in tissue sections from the VM. Therefore, we decided to dissect the VM of E13.5 embryos, manually dissociate and seed the cells to see if p27 deficiency had an effect on the differentiation of VM primary cultures.

4.1 p27 deficiency decreases DA neurons in VM primary cultures

We first studied the effects of p27 deficiency on TH expression, and saw that in p27 deficient cultures there was a significant decrease (2.13% ± 0.73 TH+ cells/Hoe) compared to controls (7.31% ± 1.44 TH+ cells/Hoe; $p<0.01$*; Figure 4.1 B,C). These results were supported by decreased Nurr1 expression in p27 deficient cultures (3.18% ± 1.08 Nurr1+ cells/Hoe) compared to controls (12.03% ± 0.28 Nurr1+ cells/Hoe; $p<0.001$***; Figure D,E). These results confirm our previous results that p27 deficiency decreases DA neuron production.

4.2 p27 deficiency increases mitotic precursors in VM primary cultures

We next studied the effects of p27 on the cell cycle marker Ki67 and the neural precursor marker Sox2. In line with our previous results, we saw a significant increase in both Ki67 (46.1% ± 7.0 Ki67+ cells/Hoe in p27-/- cultures compared to 20.0% ± 5.1 in controls; $p<0.01$**; Figure 4.2 A-A') and Sox2 (23.6% ± 5.6 Sox2+ cells/Hoe in p27-/- cultures compared to 11.8% ± 3.0 in controls; $p<0.05$*; Figure B-B').

4.3 p27 deficiency increases cell proliferation in VM primary culture

To study the effects of p27 deficiency on proliferation in primary cultures, we treated the cells with BrdU for 4 hours before fixing the cells in 4% PFA. We saw that p27 deficient cultures had a significant increase in BrdU expression (47.4% ± 7.9 BrdU+ cells/Hoe) compared to controls (11.9% ± 4.5 BrdU+ cells/Hoe; $p<0.01$**; Figure 4.3). These results support our previous findings that p27 deficiency increases cell proliferation.

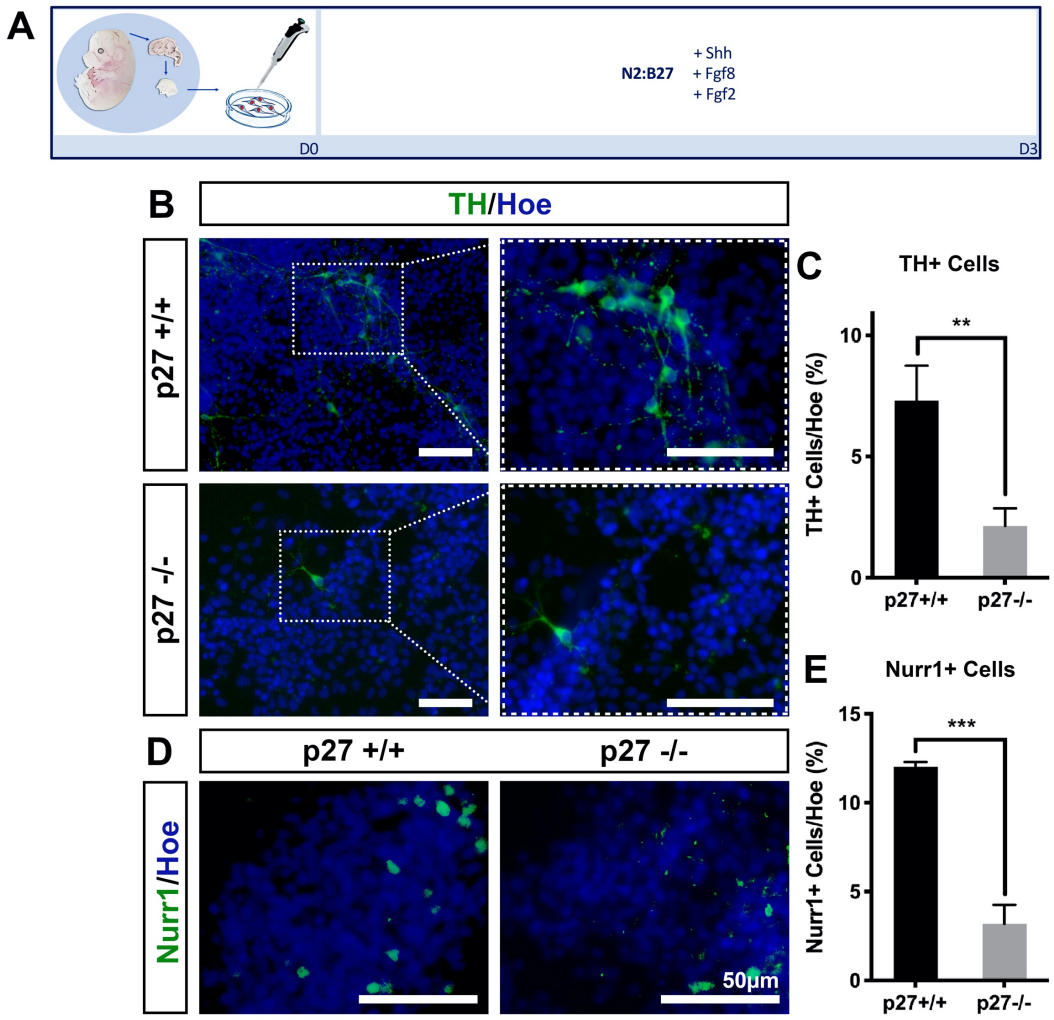

Figure 4.1: p27 deficiency decreases DA neurons in VM primary cultures. A) Diagram of differentiation protocol followed. B,C) ICC showing decreased TH+ neurons in p27 deficient primary cultures compared to control. D,E) ICC showing decreased Nurr1+ neurons in p27 deficient primary cultures compared to control. Data represents mean ± S.E.M. (n=3 for each experiment). Statistical analysis was performed using Student's t-test between control and p27 deficient cultures; $p<0.01$**; $p<0.001$***. Scale bars = 50µm.

4.4 DA neurons appear immature in p27 deficient VM primary cultures

One effect that became apparent in primary cultures was that the aspect of TH+ DA neurons appeared much more immature than control cells. To quantify this, we counted the total number of dendrites on at least 50 TH+ DA neurons per group, and the average length of those dendrites. We saw that in p27 deficient cultures, the average number of dendrites per TH+ neuron was 1.5 ± 0.12 compared to 2.2 ± 0.16 in controls ($p<0.0001$****; Figure A,B). The average length of dendrites in p27 deficient cultures was 21.6µm ± 0.1 compared to 77.5µm ± 3.4 in controls ($p<0.0001$****; Figure A,C). These results suggest that although TH+ cells are present in p27 deficient cultures, these neurons appear more immature.

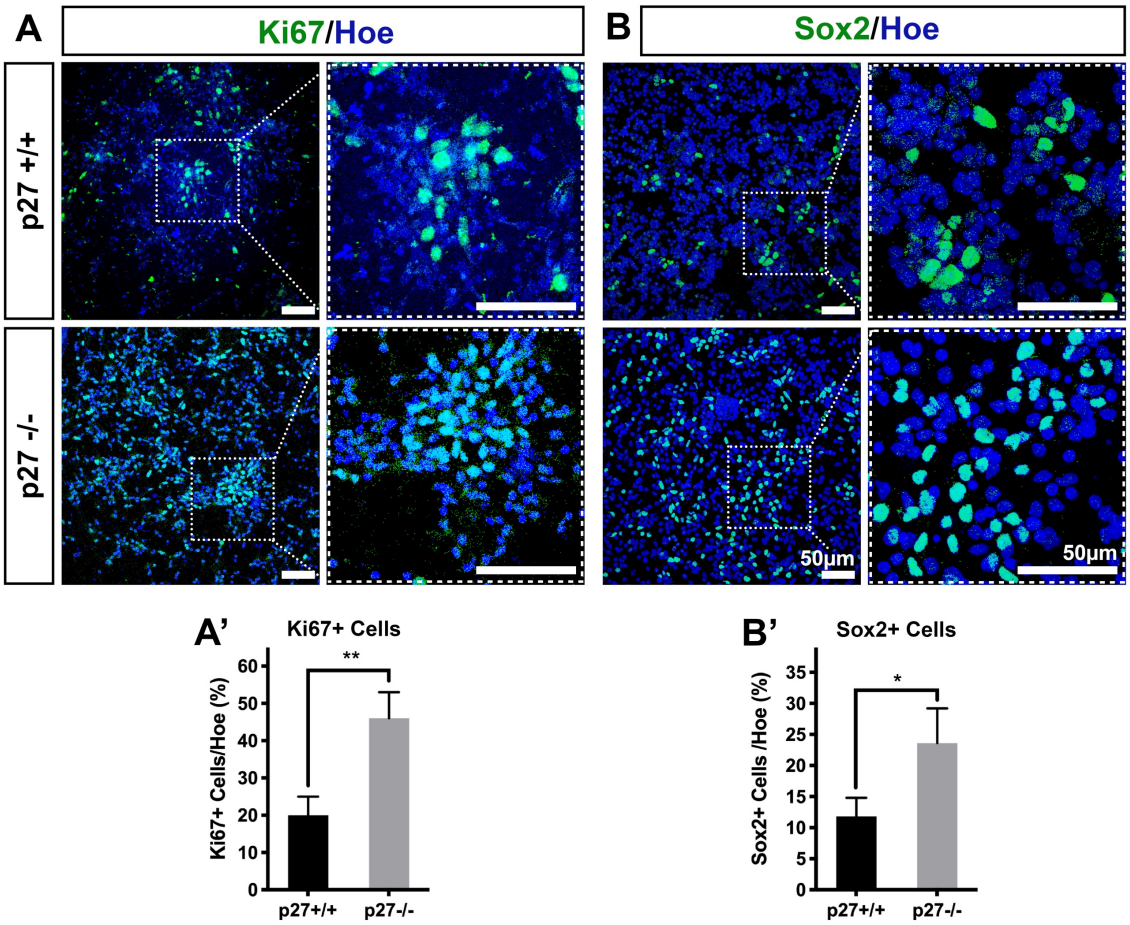

Figure 4.2: p27 deficiency increases mitotic precursors in VM primary cultures. A,A') ICC showing increased Ki67+ cells in p27 deficient primary cultures compared to control. B,B') ICC showing increased Sox2+ cells in p27 deficient primary cultures compared to control. Data represents mean ± S.E.M. (n=3 for each experiment). Statistical analysis was performed using Student's t-test between control and p27 deficient cultures; $p<0.05$*; $p<0.01$**. Scale bars = 50µm.

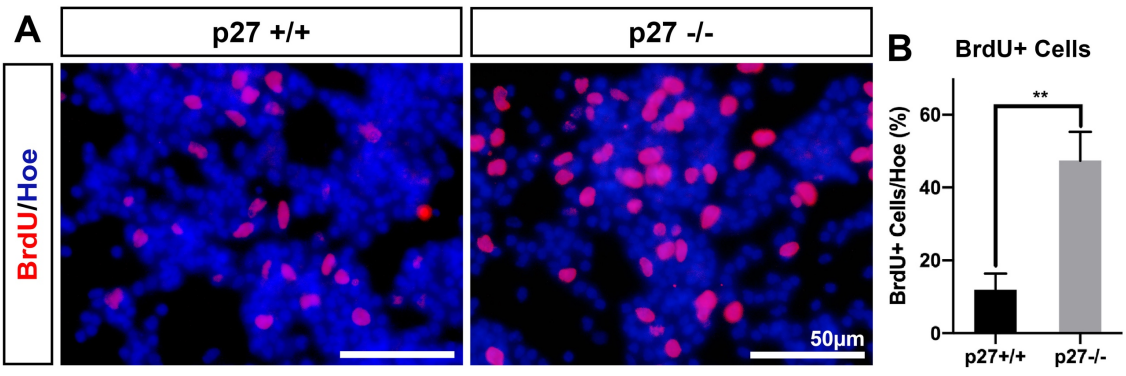

Figure 4.3: p27 deficiency increases cell proliferation in VM primary cultures. A,B) ICC showing increased BrdU+ cells in p27 deficient primary cultures compared to control. Data represents mean ± S.E.M. (n=3 for each experiment). Statistical analysis was performed using Student's t-test between control and p27 deficient cultures; $p<0.01$**. Scale bars = 50µm.

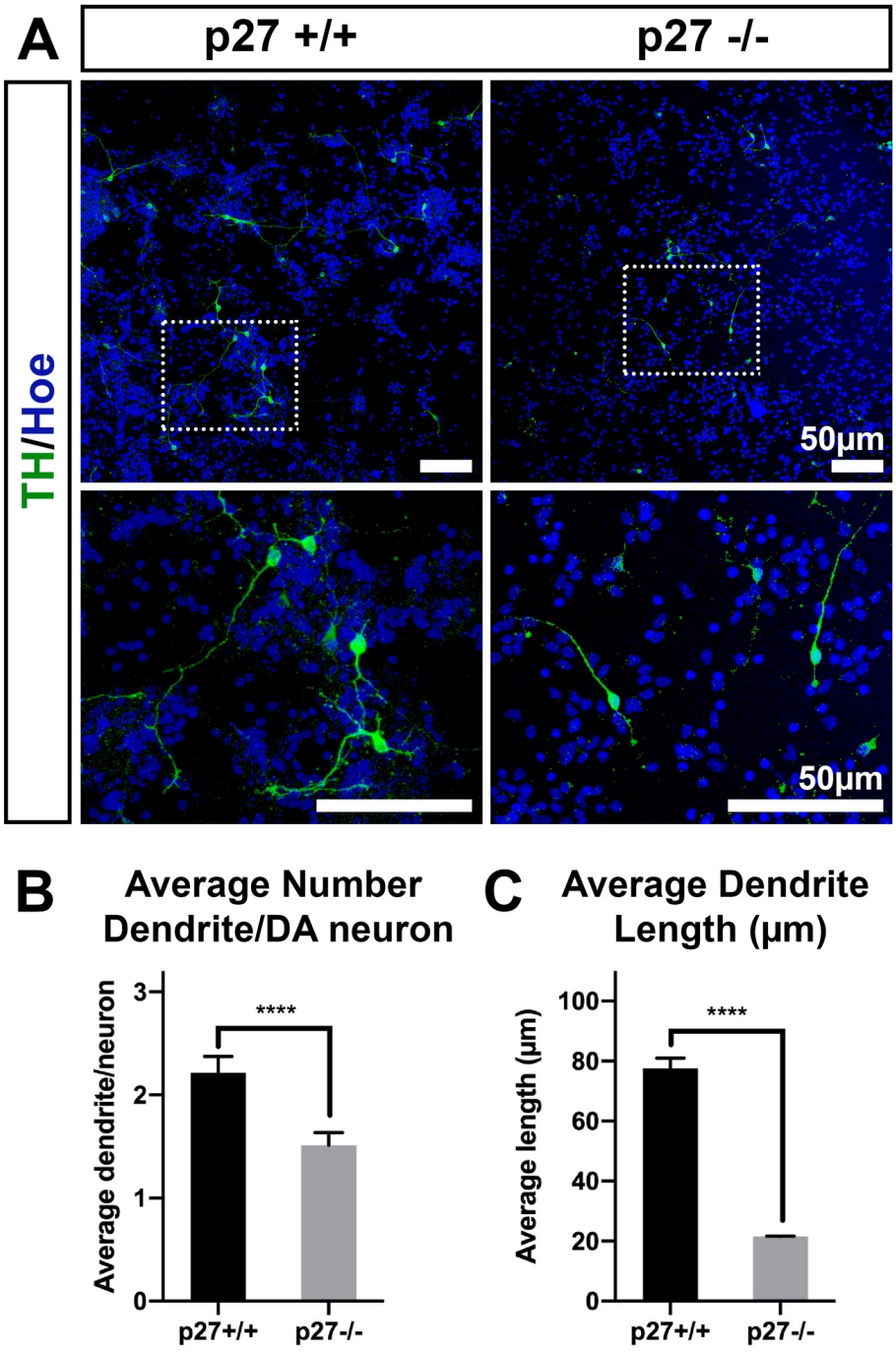

Figure 4.4: DA neurons appear immature in p27 deficient VM primary cultures. A) ICC showing general aspect of TH+ neurons. B) Quantification of average dendrite length in p27 deficient cultures compared to control. C) Quantification of average number of dendrites per TH+ neuron. Data represents mean ± S.E.M. (n=3 for each experiment, and at least 50 neurons were counted per n). Statistical analysis was performed using Student's t-test between control and p27 deficient cultures; $p<0.0001$****. Scale bars = 50µm.

In summary, we saw that p27 deficient primary cultures had decreased TH+ and Nurr1+ DA neurons, and these neurons appeared more immature (quantified by dendrite number and length). p27 deficient primary cultures also showed an increased pool of proliferating precursors. These results support our previous result *in vivo,* showing that p27 has an important function in the proper development of DA neurons.

SECTION V:

EFFECTS OF P27 ON DA NEURON DEVELOPMENT *IN VITRO*

To study the effects of p27 on DA neuron development *in vitro*, we generated several different cell lines, that we later used to manipulate p27 expression levels, which allowed us to study the effects of p27 deficiency, p27 recovery and p27 overexpression. Based on the results we obtained for NeuroD1, we also generated a cell line where we ectopically expressed NeuroD1 in p27 deficient cells in order to see if any effect could be recovered.

5.1 Generation and characterization of p27-deficient mouse iPSCs

5.1.1 Generation of p27-deficient mouse iPSCs

To generate p27-deficient miPSCs, we nucleofected MEFs extracted from E13.5 embryos with the CoMIP plasmid containing the four pluripotency genes *Sox2, Oct4, Klf4* and *c-Myc* as described in materials and methods, and according to the schematic in Figure 5.1.1 A. The efficiency of this nucleofection was confirmed by co-nucleofecting the CoMIP plasmid with GFP to quantify the green cells, indicative of successful nucleofection. We saw a nucleofection efficiency of approximately 30-40% in both control and p27-/- MEFs (Figure 5.1.1 B-C). MEFs

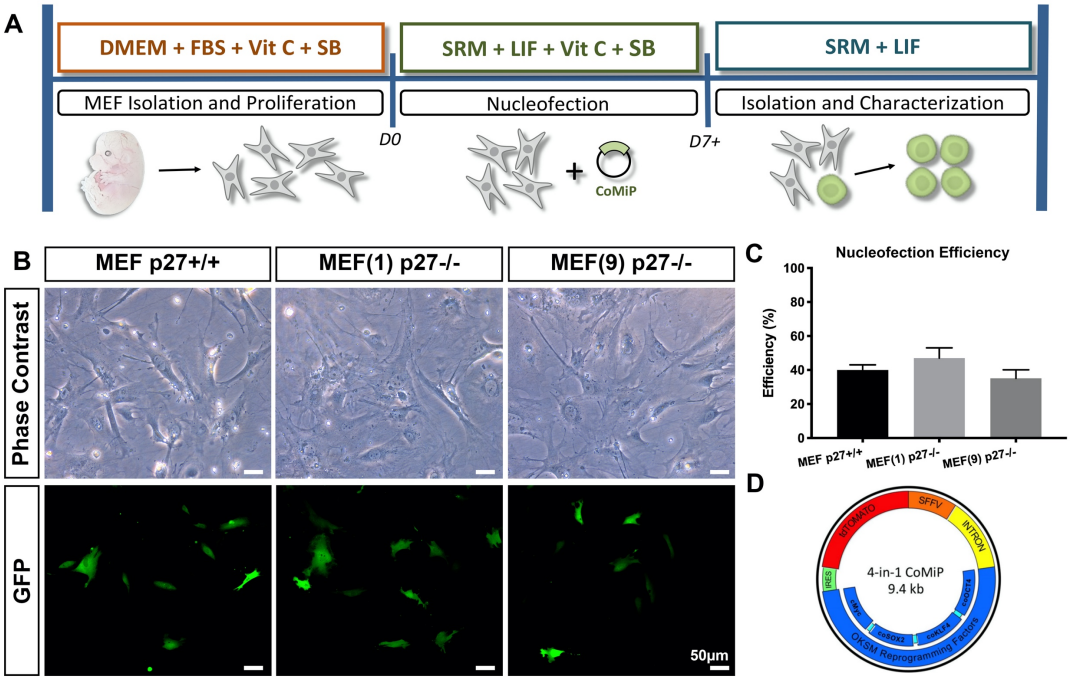

Figure 5.1.1 Generation of p27-deficient mouse iPSCs A) Diagram of reprogramming protocol. B) Phase contrast images of MEFs after nucleofection (top panels) and cells that have incorporated the reprogramming plasmid as indicated by co-transfection with GFP (bottom panels). C) Nucleofection efficiency. D) CoMIP plasmid structure (Diecke et al 2015). Scale bars = 50µm.

from p27-/- embryos E13.5(1) and E13.5(9) were reprogrammed to become miPSC p27KO(1) and miPSC p27KO(9), respectively. MEFs from p27+/+ embryos were reprogrammed to become miPSC WT controls.

5.1.2 Characterization of miPSCs in proliferation

When reprogramming adult somatic cells such as MEFs to a pluripotent state, it is essential to confirm the pluripotency of these cells. We first confirmed that the morphology of our proliferating miPSC WT, p27KO(1) and p27KO(9) cells were identical to R1 mESC control cells (Figure 5.1.2 A). Next, we studied the basal expression of the pluripotency markers Sox2,

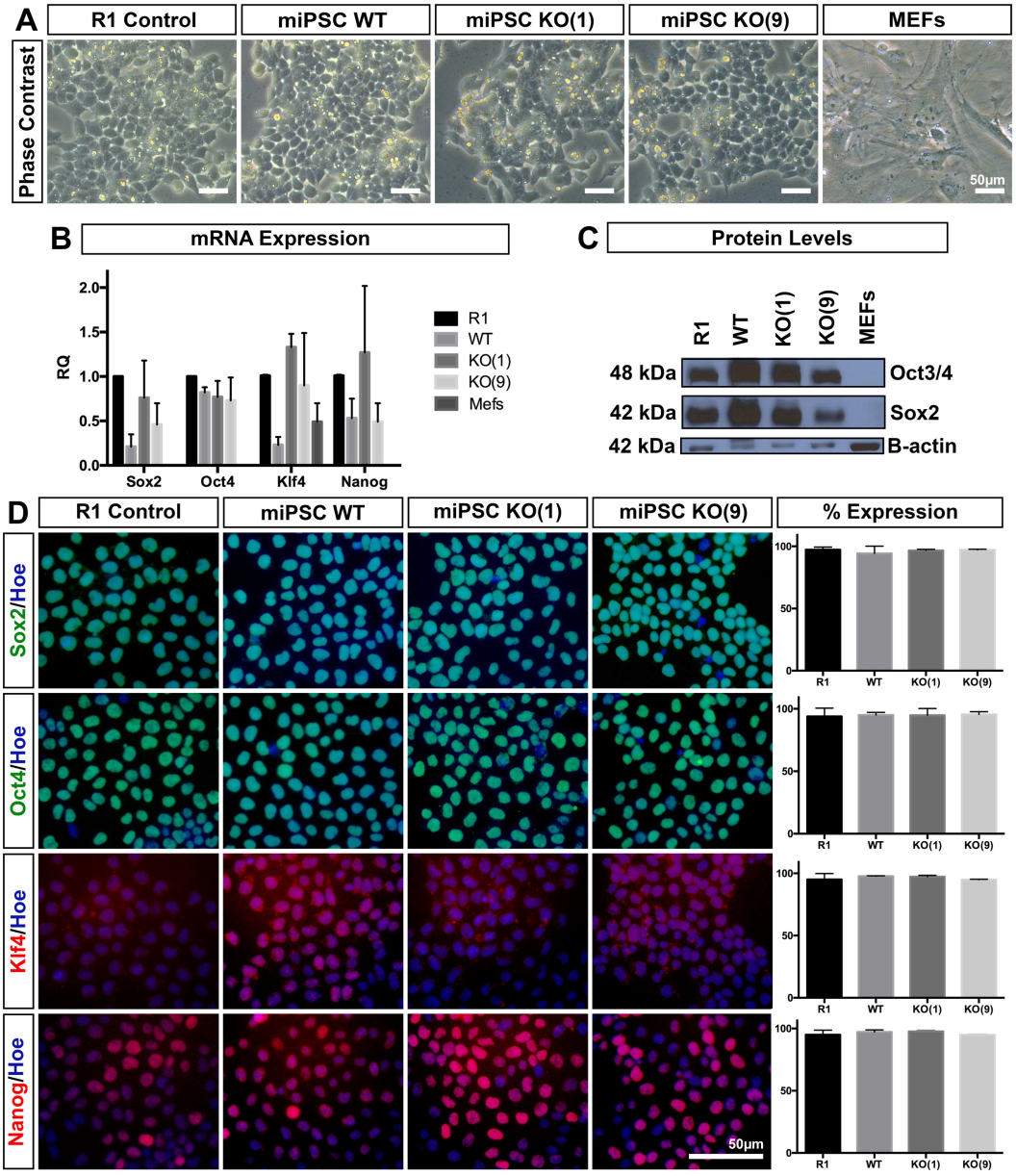

Figure 5.1.2 Characterization of miPSCs in proliferation A) Phase contrast images comparing morphology of reprogrammed cells to R1 control cells and MEFs as negative control. B) RT-qPCR showing mRNA levels of the pluripotency genes *Sox2, Oct4, Klf4* and *Nanog.* C) WB showing protein expression of Sox2 and Oct4. D) ICC showing expression of pluripotency genes. Scale bars = 50µm.

Oct4 and Klf4 (all from the original plasmid) and Nanog (not present in the reprogramming plasmid). We confirmed mRNA expression via RT-qPCR experiments and protein expression via WB and ICC experiments (Figure 5.1.2 B-D).

5.1.3 Characterization of miPSCs in differentiation

Another important characteristic of pluripotent stem cells is their ability to differentiate to the three germ layers (endoderm, mesoderm and ectoderm). We therefore seeded embryoid bodies and left these cells in a non-specified differentiation medium to allow the cells to differentiate spontaneously, and later stained for Afp (endoderm), α-actin (mesoderm) and BIII-

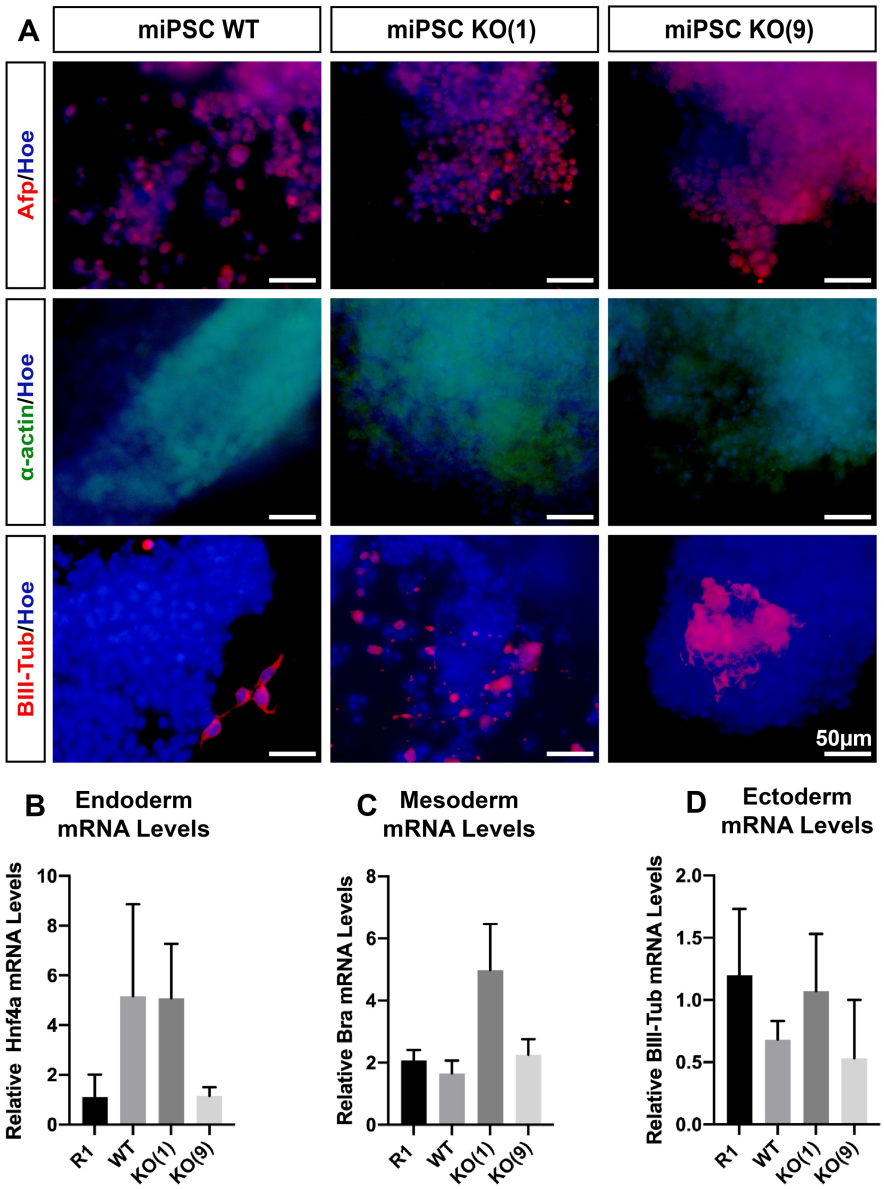

Figure 5.1.3 Characterization of miPSCs in differentation A) ICC showing expression of all three germ layers after spontaneous differentiation of EBs. RT-qPCR showing mRNA levels of endoderm markers (B), mesoderm markers (C) and ectoderm markers (D). Scale bars = 50µm.

Tub (ectoderm) to ensure the differentiation potential of these cells (Figure 5.1.3 A). We confirmed these results by RT-qPCR experiments (Figure 5.1.3 B-D).

5.2 p27 deficiency decreases directed differentiation of DA neurons *in vitro*

Once we established that our MEFs had been properly reprogrammed and that they presented the necessary traits of pluripotency, we wanted to see if there were specific effects of p27 deficiency on the directed differentiation of these miPSCs towards a DA phenotype, following the protocol described in Figure 5.2 A. We first studied the expression of BIII-Tub, and saw no significant differences between WT control and p27KO cultures (Figure 5.2 B,C). Next, we studied the expression of TH+ colonies, where we counted the total number of colonies expressing at least 100 TH+ cells, compared to total number of colonies (measured by Hoescht). We saw a significant decrease in TH+ colonies in p27 deficient cultures compared to control (87.9% ± 3.9 TH+ colonies in WT cultures compared to 25.1% ± 25.0 TH+ colonies in p27KO(1) cultures, $p<0.01$**; and 34.1% ± 7.21 TH+ colonies in p27KO(9) cultures, $p<0.0001$****; Figure 5.2 B,C). Furthermore, when counting TH+ cells per area, we observed significant decreases in p27KO(1) and p27KO(9) cultures compared to control (Figure 5.2 B,C). We confirmed these results with RT-qPCR studies, with a clear trend consistent with our *in vivo* results, showing decreased TH, Nurr1 and Pitx3 levels and increased Ki67, Sox2 and Ngn2 levels, and these differences reached significant levels in p27KO(1) cultures (Figure 5.2 D). It is important to note that NeuroD1 levels were also significantly decreased in p27KO(1) cultures, which supports our earlier claim that it may be a novel factor important for proper DA neuron development.

5.3 Generation of p27KO$^{p27\ recovery}$ mouse iPSCs

After seeing the effects of p27 deficiency *in vitro* (which corroborated our *in vivo* results), we wanted to see if we could recover some of these effects by re-introducing p27 into the deficient cells (Figure 5.3). We did this by nucleofecting the plasmid pBabep27 into p27KO(1) and p27KO(9) cells, using the empty pBabe vector as a control. KO(1) cells show a lower nucleofection efficiency of around 20%, while KO(9) cells had an efficiency of around 40% (Figure 5.3 B,C). After two weeks of puromycin selection, the cells were subjected to a limiting dilution protocol to isolate individual cells, thereby forming homogenous clones. p27KO(1)$^{p27\ recovery}$ Clones 4 and 5, as well as p27KO(9)$^{p27\ recovery}$ Clones 2 and 5 were selected for further experiments based on p27 expression detected by WB (Figure 5.3 D,E).

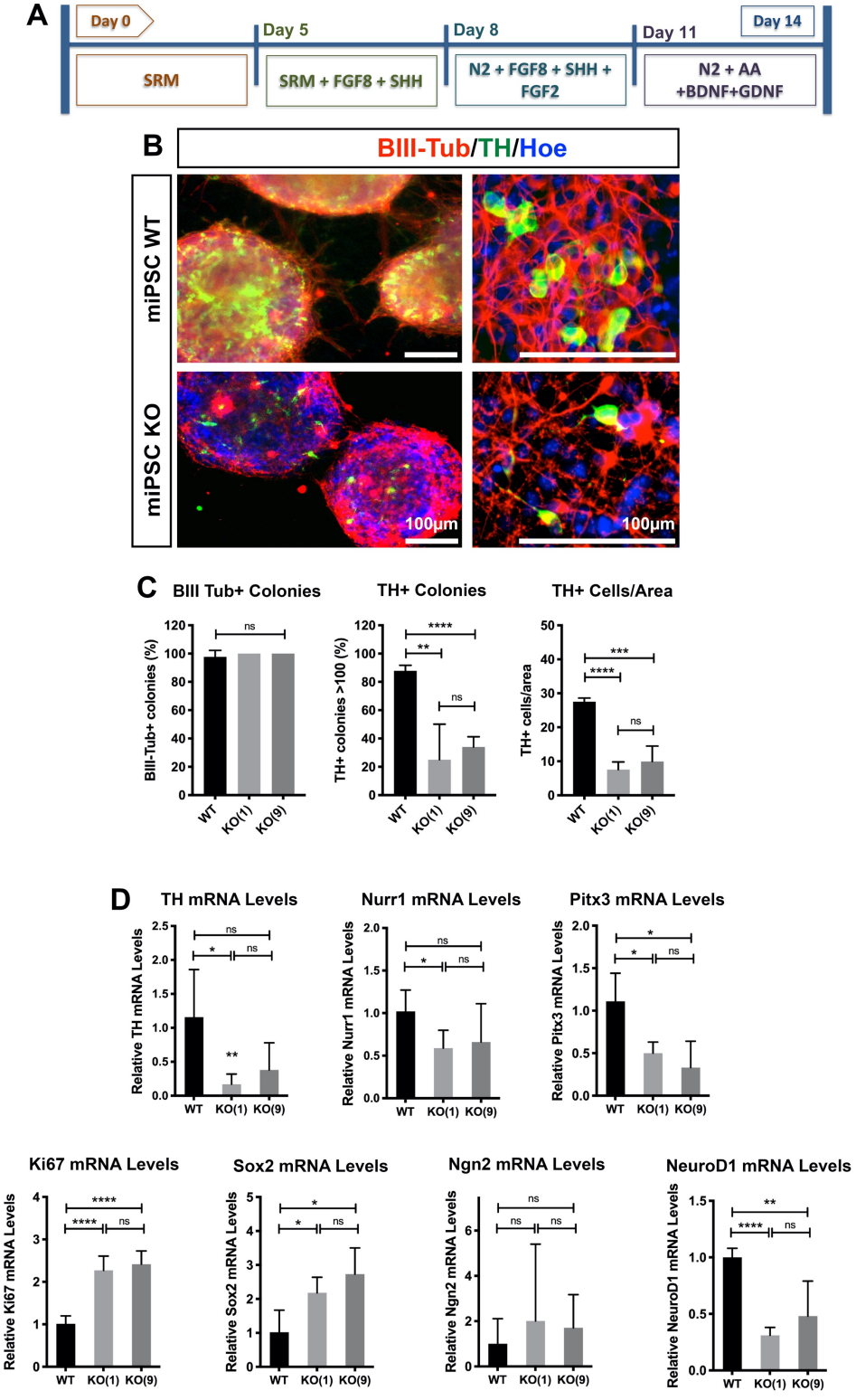

Figure 5.2: p27 deficiency decreases directed differentiation of DA neurons *in vitro.* A) Differentiation protocol followed. B) ICC showing decreased TH+ colonies and TH+ cells/area in p27KO miPSCs compared to controls C) Quantification of ICC. D) RT-qPCR results comparing the mRNA levels of *TH, Nurr1, Pitx3, Ki67, Sox2, Ngn2* and *NeuroD1* in p27KO miPSCs to controls. Data represents mean ± S.E.M. (n=3 for each experiment, and at least 3 wells were quantified per n). Statistical analysis was performed using ANOVA between WT, p27KO(1) and p27KO(9) cell lines; $p<0.05$*; $p<0.01$**; $p<0.001$***; $p<0.0001$****. Scale bars = 100µm.

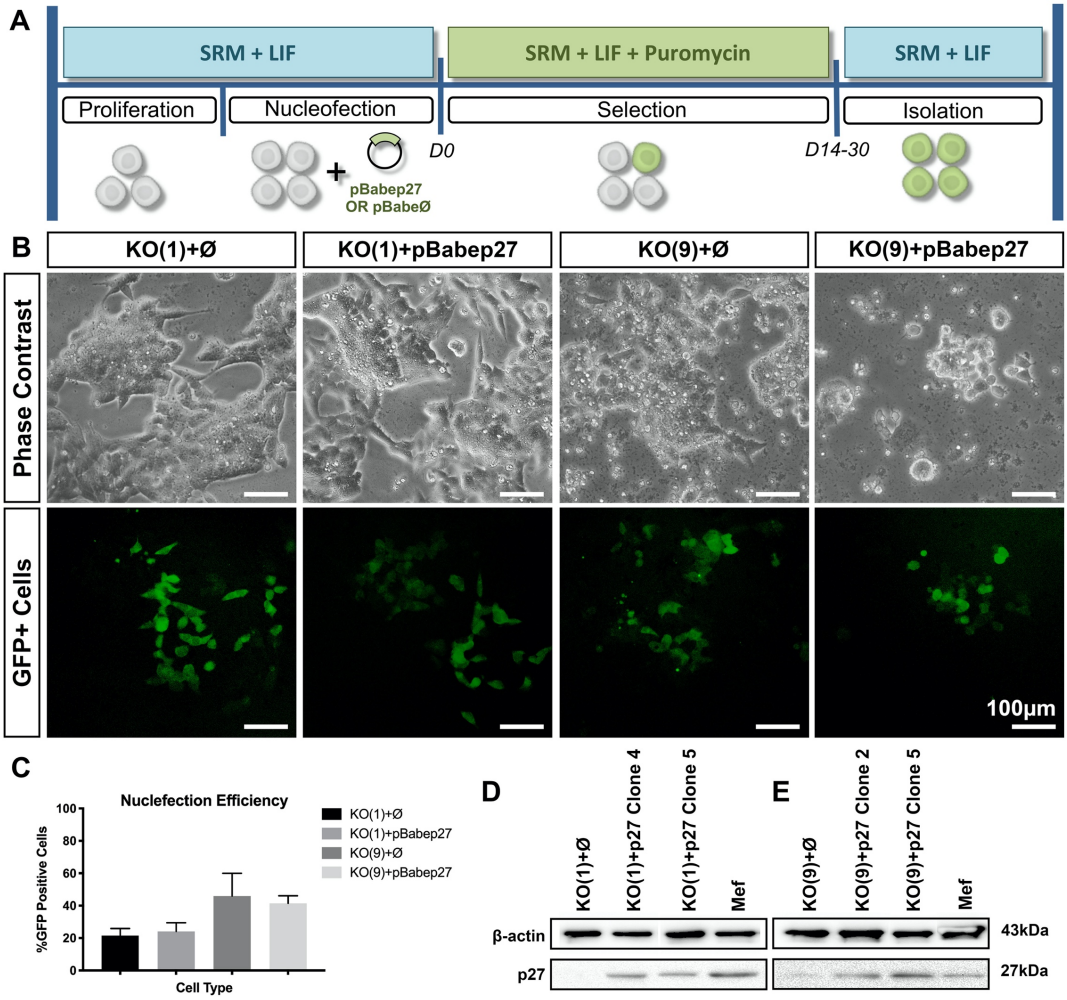

Figure 5.3 Generation of p27KO$^{p27\ recovery}$ miPSCs A) Diagram of reprogramming protocol. B) Phase contrast images of miPSCs after nucleofection (top panels) and cells that have incorporated the reprogramming plasmid as indicated by co-transfection with GFP (bottom panels). C) Nucleofection efficiency. D) WB confirming p27 expression and p27KO(1)$^{p27\ recovery}$ clones selected. D) WB confirming p27 expression and p27KO(9)$^{p27\ recovery}$ clones selected. Scale bars = 100µm.

5.4 p27 recovery improves directed differentiation of DA neurons *in vitro*

We next wanted to see the effects of p27 recovery on the directed differentiation of our p27KO miPSCs towards a DA phenotype, following the protocol described in Figure 5.4 A. We first studied the expression of BIII-Tub+ colonies in relation to Hoescht+ colonies, and to our surprise, saw a significant decrease in the total number of BIII-Tub colonies in p27 recovery cells compared to p27 deficient controls (Figure 5.4 B-D). However, this result should be investigated in more detail by, for example, studying total number of BIII-Tub/area or quantifying the aspect of these positive colonies. Next, we studied the expression of TH+ colonies, where we counted the total number of colonies expressing at least 100 TH+ cells compared to total number of colonies (measured by Hoescht). We saw a partial recovery, and

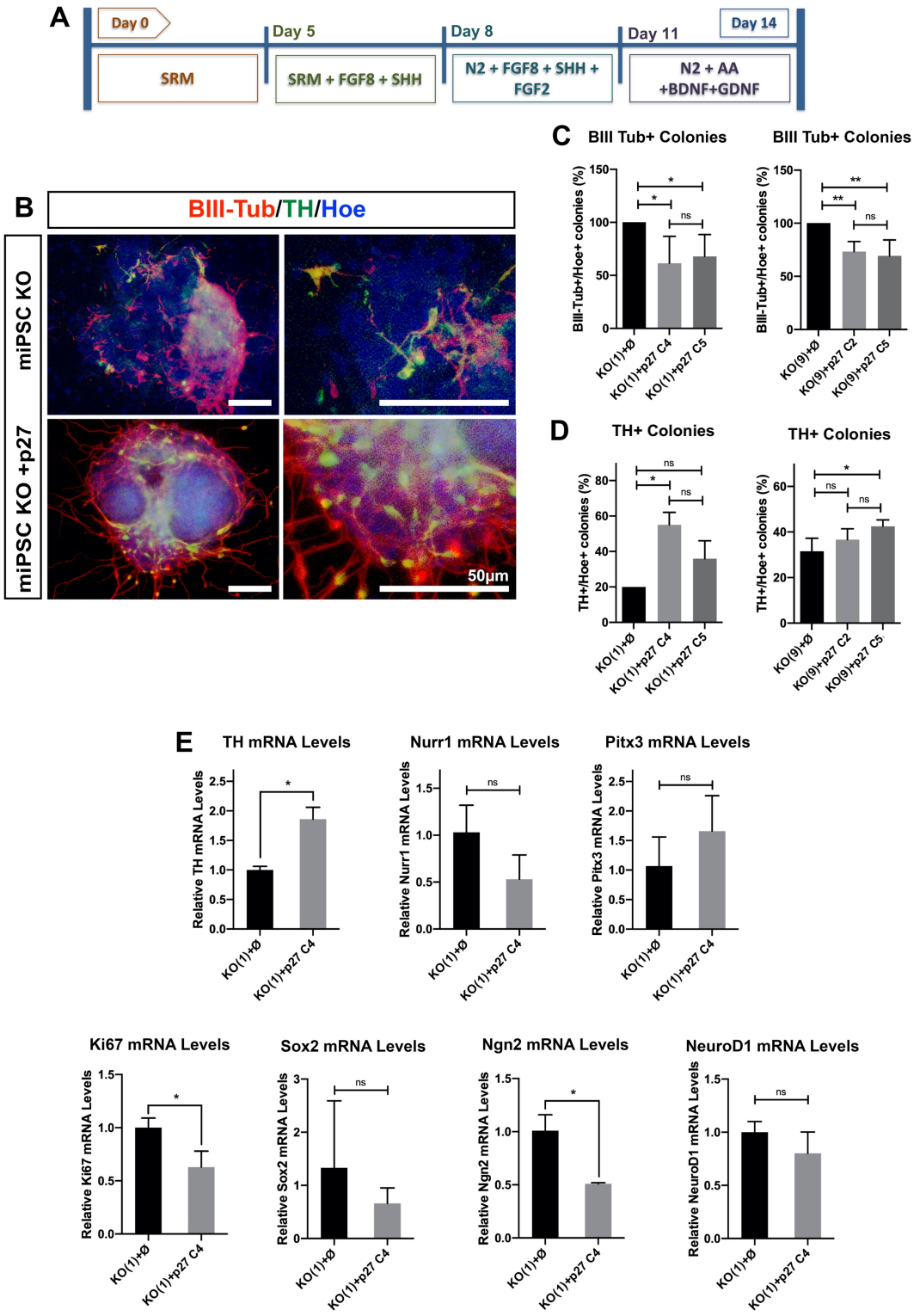

Figure 5.4: p27 recovery improves directed differentiation of DA neurons A) Differentiation protocol followed. B) ICC showing increased TH+ colonies in p27KO$^{p27\ recovery}$ miPSCs compared to p27KO controls. C-D) Quantification of ICC. E) RT-qPCR results comparing the mRNA levels of *TH, Nurr1, Pitx3, Ki67, Sox2, Ngn2* and *NeuroD1* in p27KO$^{p27\ recovery}$ miPSCs to p27KO controls. Data represents mean ± S.E.M. (n=3 for each experiment, and at least 3 wells were quantified per n). Statistical analysis was performed using ANOVA between p27KO control and p27KO$^{p27\ recovery}$ clones for ICC analysis or Student's t-test between p27KO(1) control and p27KO(1)$^{p27\ recovery}$ Clone 4 for RT-qPCR analysis; $p<0.05$*; $p<0.01$**. Scale bars = 50µm.

there was a clear trend indicating increased TH+ colonies in p27KO$^{p27\ recovery}$ cultures compared to p27KO control, where p27KO(1)$^{p27\ recovery}$ Clone 4 and p27KO(9)$^{p27\ recovery}$ Clone 5 showed significant increases (55.0% ± 7.1 TH+ colonies in p27KO(1)$^{27\ recovery}$ Clone 4 compared to 20.1% ± 0.1 in p27KO(1) control; $p<0.05$* and 42.5% ± 2.7 TH+ colonies in KO(9)$^{p27\ recovery}$ Clone 5 compared to 31.5% ± 5.7 in p27KO(9) control; $p<0.01$**; Figure 5.4 B-D). No significant differences were observed between p27KO$^{p27\ recovery}$ clones, supporting the trend of increased TH+ colonies (Figure 5.4 C,D). These results were supported by RT-qPCR experiments, where p27KO(1)$^{p27\ recovery}$ Clone 4 showed a partial recovery of DA neuron markers when compared to p27KO(1) control cultures (Figure 5.4 E).

5.5 Generation of p27 overexpressing mouse PSCs

After seeing the effects of p27 recovery *in vitro*, we wanted to see the effects of directly overexpressing p27 into R1 mESC and miPSC WT control cells. We did this by nucleofecting the plasmid pBabep27 into R1 and WT cells, using the empty pBabe vector as a control. R1 mESCs showed a lower nucleofection efficiency of around 25%, while miPSC WT had an efficiency between 40-45% (Figure 5.5). After two weeks of puromycin selection, the cells were subjected to a limiting dilution protocol to isolate individual cells, thereby forming homogenous clones. R1 mESC$^{p27\ overexpression}$ Clones 1 and 4, while miPSC WT$^{p27\ overexpression}$ Clones 5 and 6 were selected for further experiments based on p27 expression detected by WB (Figure 5.5 D,E).

5.6 p27 overexpression increases directed differentiation of DA neurons

We next wanted to see the effects of p27 overexpression on the directed differentiation of these cells towards a DA phenotype, following the protocol described in Figure 5.6 A. We first studied the expression of BIII-Tub, and saw no significant differences in the total number of BIII-Tub colonies in R1 mESC$^{p27\ overexpression}$ cells compared to R1 mESC controls (Figure 5.6 B,C). Next, we studied the expression of TH+ colonies, where we counted the total number of colonies expressing at least 100 TH+ cells compared to total number of colonies (measured by Hoescht). Interestingly, we saw a significant increase in the number of TH+ colonies in R1 mESC$^{p27\ overexpression}$ cultures (51.6% ± 7.7 TH+ colonies in R1 mESC control cultures compared to 82.7% ± 6.38 in R1 mESC$^{p27\ overexpression}$ Clone 1; $p \leq 0.01$** and 84.2% ± 2.11 R1 mESC$^{p27\ overexpression}$ Clone 4; $p \leq 0.01$**; Figure 5.6 B,C). RT-qPCR studies confirmed this increase in TH expression, while also indicating an increase in both *Ngn2* and *NeuroD1* mRNA levels, supporting our previous results (Figure 5.6 D).

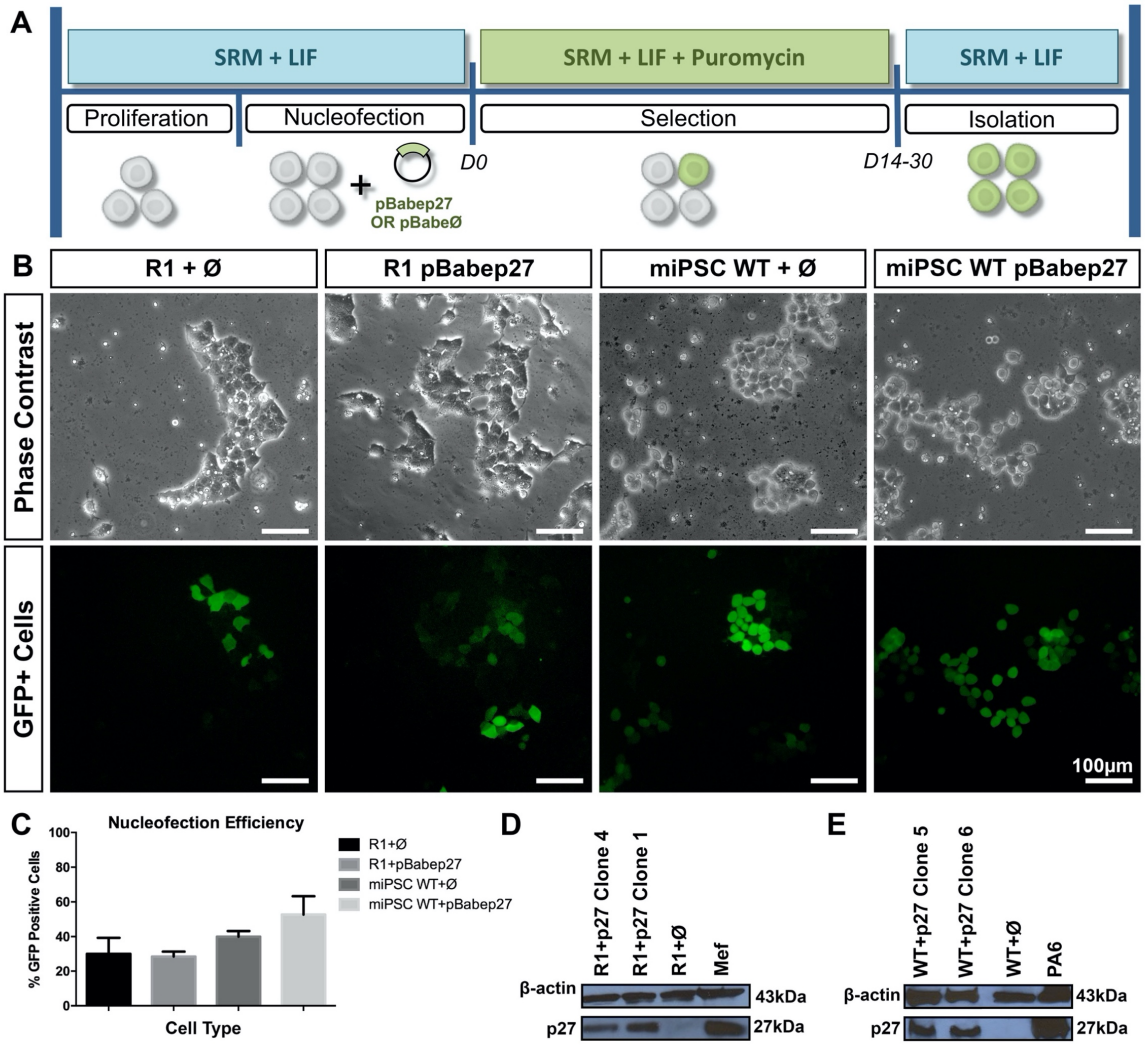

Figure 5.5 Generation of p27-overexpressing mPSCs A) Diagram of reprogramming protocol. B) Phase contrast images of mPSCs after nucleofection (top panels) and cells that have incorporated the reprogramming plasmid as indicated by co-transfection with GFP (bottom panels). C) Nucleofection efficiency. D) WB confirming p27 expression and R1 mESC$^{p27\ overexpression}$ clones selected. D) WB confirming p27 expression and miPSC WT$^{p27\ overexpression}$ clones selected. Scale bars = 100µm.

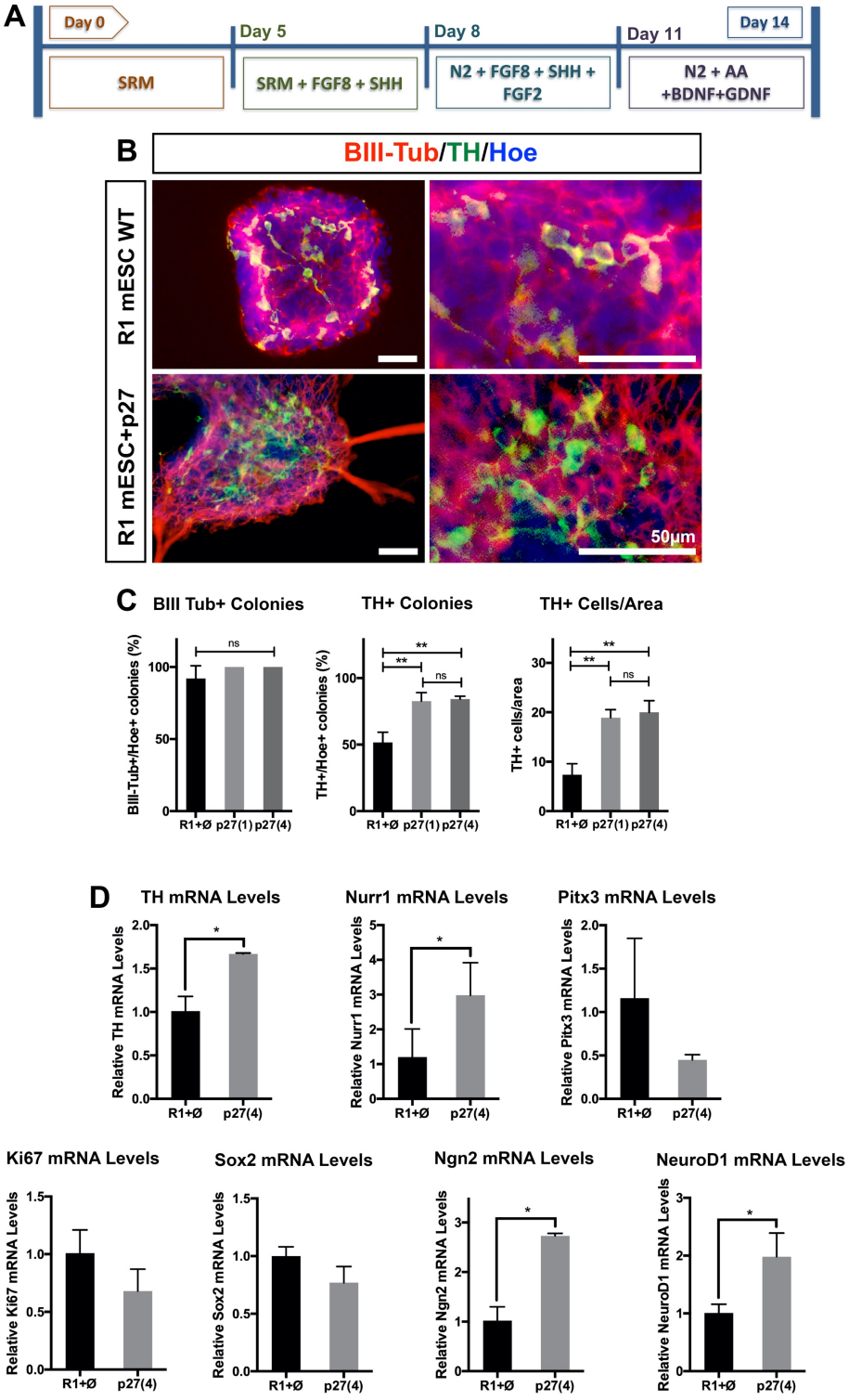

Figure 5.6: p27 overexpression increases the directed differentiation of DA neurons. A) Differentiation protocol followed. B) ICC showing increased TH+ colonies and TH+ cells/area in p27 overexpressing cells compared to control. C) Quantification of ICC. D) RT-qPCR results comparing the mRNA levels of *TH, Nurr1, Pitx3, Ki67, Sox2, Ngn2* and *NeuroD1* in R1 mESC$^{p27\ overexpression}$ cells to controls. Data represents mean ± S.E.M. (n=3 for each experiment, and at least 3 wells were quantified per n). Statistical analysis was performed using ANOVA between R1 mESC control and R1 mESC$^{p27\ overexpression}$ Clones 1 and 4 for ICC analysis or Student's t-test between R1 mESC control and R1 mESC$^{p27\ overexpression}$ Clone 4 for RT-qPCR analysis; $p<0.05$*; $p<0.01$**. Scale bars = 50µm.

5.7 Generation of p27KO^{NeuroD1} mouse iPSCs

Based on the results of NeuroD1 observed *in vivo*, we wanted to see if we could directly recover the effects of p27 deficiency by expressing NeuroD1 in p27 deficient cells. We did this by nucleofecting the plasmid pCX-NeuroD1 into p27KO(1) cells, using the empty pCX vector as a control. These cells showed a nucleofection efficiency of around 80% (Figure 5.7 B,C). After two weeks of neomycin selection, the cells were subjected to a limiting dilution protocol to isolate individual cells, thereby forming homogenous clones. p27KO(1)^{NeuroD1} Clones 7 and 9 were selected for further experiments based on NeuroD1 expression detected by WB (Figure 5.7 B,C).

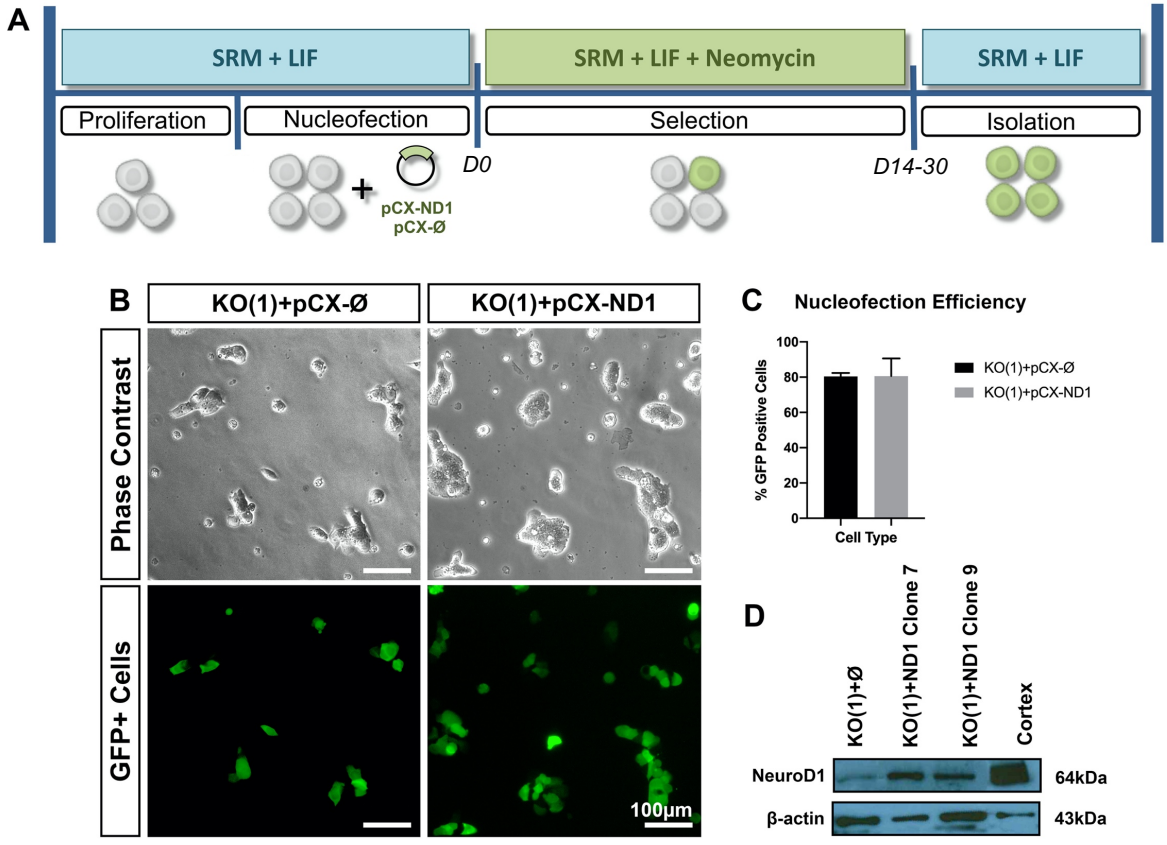

Figure 5.7 Generation of p27KO^{NeuroD1} miPSCs A) Diagram of reprogramming protocol. B) Phase contrast images of miPSCs after nucleofection (top panels) and cells that have incorporated the reprogramming plasmid as indicated by co-transfection with GFP (bottom panels). C) Nucleofection efficiency. D) WB confirming NeuroD1 expression and p27KO^{NeuroD1} clones selected. Scale bars = 100µm.

5.8 Effects of NeuroD1 expression in p27 deficient miPSCs on DA neuron development

We performed the same experiment as before, differentiating the cells according to the diagram in Figure 5.8 A. When investigating the effects of NeuroD1 expression in p27 deficient cells on BIII-Tub expression, we saw no significant differences in BIII-Tub+ colonies in relation to Hoescht between p27KO^{NeuroD1} cultures and p27KO controls (Figure 5.8 B,C). However, when investigating the effects of NeuroD1 expression in p27 deficient cells on TH production, we saw a significant increase in TH+ colonies in relation to Hoescht, in both clones selected (36.6% ± 4.7 TH+ colonies in p27KO control cultures compared to 71.3% ± 6.6 in p27KO^{NeuroD1} Clone 7; $p<0.05$* and 65.7% ± 5 p27KO^{NeuroD1} Clone 9; $p<0.05$*; Figure 5.8 B,C). These results strongly support our previous results and suggest that p27 deficiency decreases DA neuron development by affecting NeuroD1. However, these results are preliminary, and more experiments are needed to confirm interactions between p27 and NeuroD1 as well as NeuroD1 with TH.

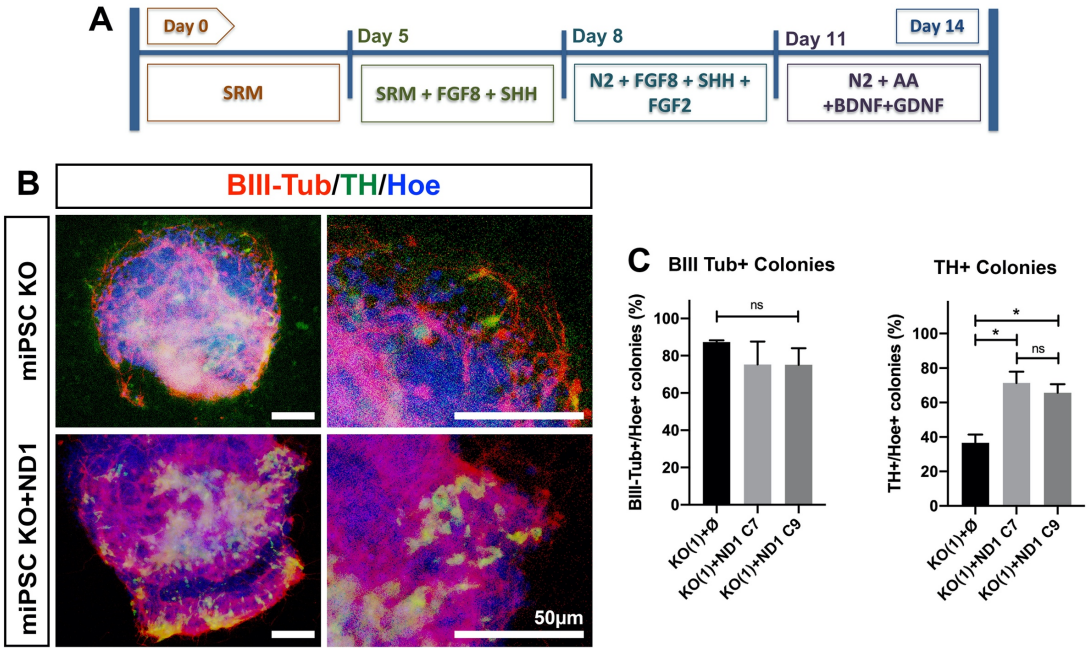

Figure 5.8: Effects of NeuroD1 expression in p27KO miPSCs on DA neuron development. A) Differentiation protocol followed. B) ICC showing unaltered BIII-Tub expression and increased TH+ colonies in p27KO^{NeuroD1} miPSCs compared to p27KO controls. C) Quantification of ICC. Data represents mean ± S.E.M. (n=2 for each experiment, and at least 3 wells were quantified per n). Statistical analysis was performed using ANOVA between p27KO control cells and p27KO^{NeuroD1} Clones 7 and 9 for ICC analysis. $p<0.05$*. Scale bars = 50µm.

In summary, we have shown a link between p27 expression and DA development, indicating an important function of p27 in this process. We have shown that p27 deficient cells produce less TH+ colonies and less TH+ cells/area as compared to control cells, indicating that p27 deficiency decreases DA neuron development *in vitro*. This effect was supported by re-introducing p27 into p27 deficient cells, which showed a partial recovery in the differentiation of DA neurons. Since we saw a partial recovery, we decided to investigate the effect of p27 overexpression in control cells, and, interestingly, saw increased DA neuron development as quantified by increased TH+ colonies and TH+ cells/area in these cells. Finally, our preliminary results of NeuroD1 expression in p27 deficient cells also suggest a mechanism whereby p27 affects DA neuron development by interacting with NeuroD1.

DISCUSSION

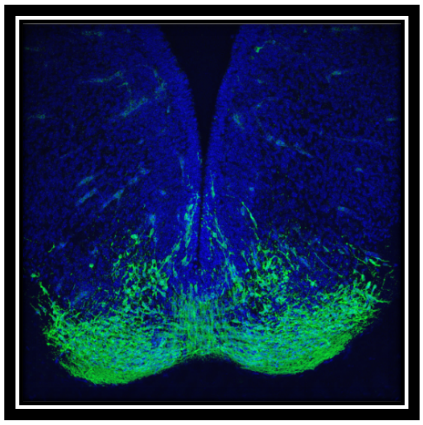

Parkinson's Disease is the second most common neurodegenerative disease affecting a steadily increasing number of people, which could reach 9.3 million cases worldwide by 2030 (Dorsey et al 2007). Treatment options have been developed that can be highly effective in treating primary motor symptoms in certain patients (Fox et al 2018). However, despite decades of excellent research, there is still no cure for this disease. Therefore, PD has become an intense area of research in an attempt to find new, alternative treatment options that can lessen, halt or even reverse the pathological progression of this disease.

The primary objective of this thesis has been to study the complex process of DA neuron development, in an attempt to find new and novel markers that could be useful in the development of alternative treatment options, such as stem cell replacement therapies. This process is tightly coordinated and based on the time-sensitive expression of several factors in specific contexts, making it an exceptionally complicated process to replicate *in vitro*. Our results provide novel evidence for the importance of p27 in the development of DA neurons, which in the context of the VM was seen to increase the pool of neural progenitors and affected the expression of Ngn2, where both p27 and Ngn2 are important and necessary for proper cell cycle exit followed by the onset of neurogenesis (Ohnuma and Harris 2003, Guillemot 2007, Kaldis and Richardson 2012). In an attempt to find the mechanistic action of p27, we saw interesting results for NeuroD1, where our preliminary results suggest an important novel function in the context of DA neuron development. Below we discuss our findings and suggest the importance of p27 via Ngn2 and NeuroD1, as possible key factors in the context of the VM that could help improve the development of DA neurons *in vitro*, and its potential application in PD.

p27 Expression Pattern in the Developing VM

Before studying the effects of p27, we first determined if p27 was present in the midbrain, and next established its expression pattern in the developing VM. Previous work had originally shown that p27 was not present in the midbrain (Joseph et al 2003). However, these results were initially contradicted by a study showing that p27 gain of function promoted VM neurosphere differentiation (Sacchetti et al 2009), supported by another study showing that p27 directly promoted neurogenesis in the cortex via Ngn2 (Nguyen et al 2006).

We therefore investigated the expression of p27 by RT-qPCR and WB experiments, and saw in both cases, that p27 was expressed as early as E11.5, and this expression increased with the development of the brain. These results are expected, since p27 is exclusively expressed in post-mitotic cells. We see a direct relationship between the number of proliferating precursors

(early development) with low p27 expression, as well as a direct relationship between the number of post-mitotic precursors and mature neurons (late development) with high p27 expression.

We next performed IHC studies to see how p27 was distributed in the developing VM. We know DA neuron development begins in the floor plate of the VM (Arenas et al 2015), a region making up the VZ, consisting mainly of proliferating precursors (Ono et al 2007, La Manno et al 2016). As development progresses, these precursors begin to migrate and become post-mitotic, making up the IZ (Wallén et al 1999). These cells continue to migrate as they gradually begin losing progenitor identity while simultaneously gaining mature DA neuron identity, and are considered fully mature upon reaching the MZ (Ang 2006). Therefore, our results confirm that p27 expression corresponds to the expression of post-mitotic precursors in the IZ and mature neurons in the MZ and is absent from the VZ made up of mitotic precursors.

Due to the complexity of DA neuron development, we simplified the process by looking at five main stages, as defined by key markers important in these specific processes: TH, Nurr1 and Pitx3 to study DA neuron identity, Foxa2 to study regionalization, Lmx1a to study specification, Ngn2 to study DA neurogenesis and the markers Ki67 (cell cycle) and Sox2 (neural precursors) to study p27-related effects (Figure D.1).

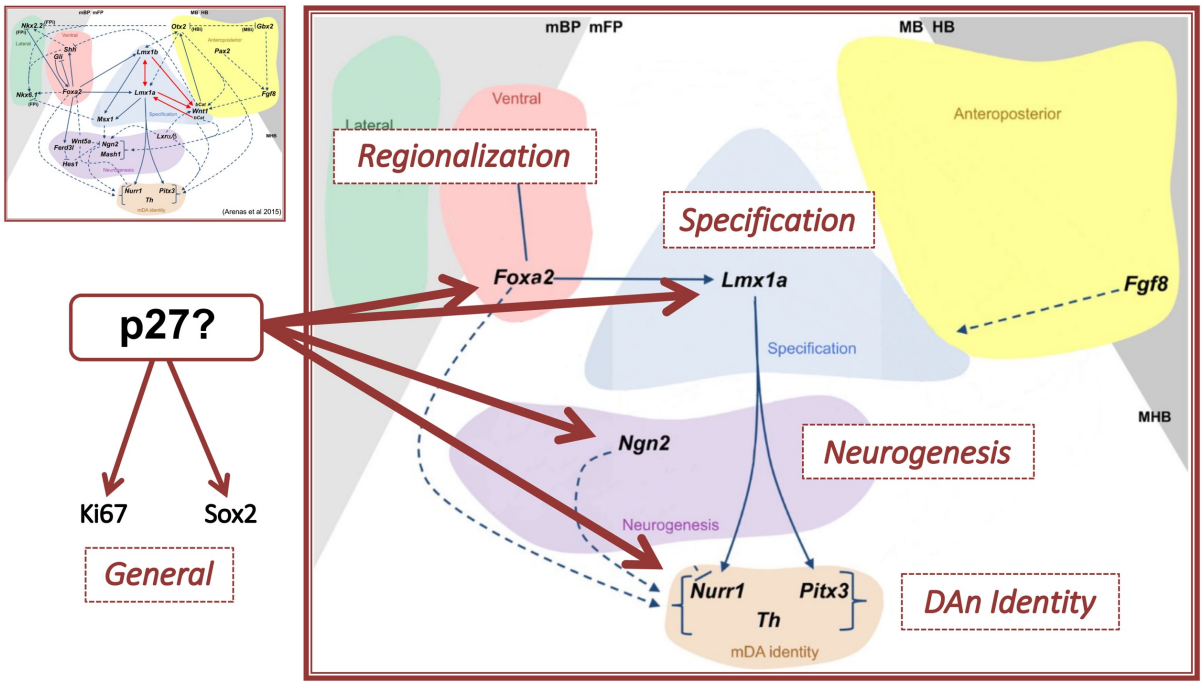

Figure D.1: Simplified diagram of DA neuron development. In order to perform a comprehensive study of the effects of p27 deficiency on DA neuron development, we simplified the process by studying markers representative of five main stages: DA neuron identity, regionalization, specification, general p27-related markers and DA neurogenesis (adapted from Arenas et al 2015).

We first studied p27 expression with DA neuron identity markers. Nurr1 is the first post-mitotic DA neuron marker and is expressed in the IZ and MZ (Zetterström et al 1997, Wallén et al 1999, Kadkhodaei et al 2009), whereas TH and Pitx3 are markers of mature DA neurons, present mainly in the MZ (Smidt et al 2000, Smidt et al 2004, Ang 2009, Li et al 2009). These markers were almost exclusively co-expressed with p27, supporting our previous conclusion that p27 is expressed in the IZ and MZ, and further suggests a possible function of p27 in the development of these neurons.

We next studied the expression of p27 with the regionalization marker Foxa2 and the specification marker Lmx1a, as representative markers of these two early developmental processes. However, it should not be forgotten that both factors coordinate the expression of several more genes (Prakash and Wurst 2006, Ang 2009, Arenas et al 2015), all important for DA neuron development. We detected both Foxa2 and Lmx1a expression in the VZ, and these markers were also co-expressed with p27 in the IZ and MZ, effectively demonstrating an expression pattern spanning all three developmental zones.

We studied the expression of p27 with more general markers related to the cell cycle (Ki67, Sun and Kaufman 2018) and the expression of neural precursors (Sox2, Graham et al 2003). We saw that both of these markers were restricted to the region lining the ventricle and was entirely complementary to p27 expression. These results are expected, as the expression of Ki67 or Sox2 with p27 would be mutually exclusive based on their expression profiles. Since Ki67 and Sox2 show the expression pattern of mitotic precursors, it becomes a way to measure the area of the VZ as development progresses and our study shows a steady decrease in the size of the VZ at later developmental stages. Whether p27 is responsible for inhibiting the expression of these markers, or if the downregulation of these markers by other mechanisms allows for the expression of p27 needs to be investigated in further detail, though it has been shown that p27 can repress the expression of Sox2 in differentiating ESCs (Li et al 2012).

Finally, the importance of Ngn2 in the onset of neurogenesis of DA neurons has been previously described (Andersson et al 2006a, Kele et al 2006). Therefore, we studied the expression of Ngn2 with p27, and saw that the majority of Ngn2+ cells was mainly distributed throughout the VZ. A few Ngn2+ cells were found outside the VZ, interspersed, but not co-expressed with, p27+ cells, which defines the region of the IZ. This suggests a regulatory role of p27 in the expression of Ngn2, but the exact interaction between p27 and Ngn2 in the VM needs to be studied in further detail.

In summary, we have defined an expression pattern for p27 in the developing midbrain, and along with markers representative of important stages of differentiating DA neurons, have

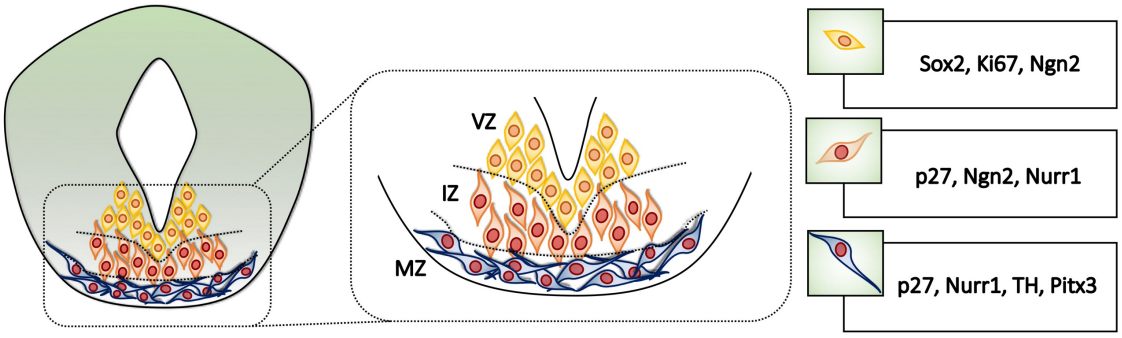

Figure D.2: Layered zones of DA neuron development. DA neurons are born in the VZ (yellow cells) where they express Ki67, Sox2 and Ngn2 and are considered mitotic precursors. As these cells mature, the migrate through the IZ (orange cells), where some cells are Ngn2+ and the rest begin expressing p27 and Nurr1. These cell continue to migrate, losing progenitor identity and become mature DA neurons upon reaching the MZ (blue cells) where they express p27, Nurr1, TH and Pitx3.

been able to define and study the three developmental zones in relation to p27 expression under normal conditions (Figure D.2).

Effects of p27 on DA neuron development

We saw a dramatic decrease in the early production of TH+, Nurr1+ and Pitx3+ neurons in p27 deficient mice as compared to controls. These results were supported by *in vitro* experiments, where p27 deficient primary cultures and p27 deficient miPSCs produced fewer TH+ colonies and fewer TH+ cells/area as compared to controls under the same differentiation conditions. These results therefore indicate an important function of p27 in the initial production of DA neurons and confirm our main hypothesis, that p27 deficiency significantly decreases DA neuron production, *in vivo* and *in vitro*.

Following a similar process as described above, we did an initial study of the effect of p27 deficiency on regionalization (Foxa2), specification (Lmx1a), p27-related effects (Ki67 and Sox2) and neurogenesis (Ngn2). We saw that p27 did not affect the expression of Foxa2 or Lmx1a, suggesting that p27 may decrease DA neuron development by affecting the developmental process after the establishment of early regionalization (Ferri et al 2007, Kittappa et al 2007, Arenas 2008, Chung et al 2009) and specification (Andersson et al 2006b, Chung et al 2009, Yan et al 2011). This was contrary to what we originally expected, since we believed the co-expression observed between p27 and Foxa2 or Lmx1a to be indicative of an interaction between p27 and these two markers. However, the fact that Foxa2 and Lmx1a were expressed in both p27+ and p27- cells in WT controls, and that their expression pattern extended from the VZ to the MZ, showed that early regionalization and specification are p27-independent pathways, undisturbed by the absence of p27.

We next studied the effects of p27 on the cell cycle, by studying the marker Ki67. At early stages of development, we saw a significant increase in the expression of Ki67 in p27 deficient mice, which we can expect to see in the absence of p27 (whose primary function is inhabiting the cell cycle; Sherr and Roberts 1999, Besson et al 2008, Abbastabar et al 2018), and these results were confirmed *in vitro*. Similar results were obtained for the neural precursor marker Sox2, where we saw significant increases in the absence of p27, both *in vivo* and *in vitro.* These results therefore allow us to conclude that p27 deficiency increases the pool of mitotic precursors.

To study the effect of p27 on proliferation, we injected pregnant mice at E11.5 with BrdU (a thymidine analog with the ability to incorporate into newly synthesized DNA of actively dividing cells; Wojtowicz and Kee 2006) which were sacrificed 24 hours later at E12.5. We saw significant increases in BrdU expression in p27 deficient mice, confirming that p27 deficiency increases proliferation. These results were supported by studies in primary cultures, showing the same result. Furthermore, we performed co-expression experiments with BrdU and Ki67 or Sox2, and saw that the overall number of BrdU+Ki67+ and BrdU+Sox2+ double positive cells also increased significantly in p27 deficient mice. Interestingly, when comparing the overall number of BrdU+Ki67+ and BrdU+Sox2+ double positive cells with the total expression of either Ki67 or Sox2 respectively, we saw that Ki67 and Sox2 were co-expressed almost 100% with BrdU, making these two markers an indirect measure of proliferation in the developing VM. To confirm this, we double stained Ki67 or Sox2 with PCNA, another marker of proliferation (Moldovan et al 2007). Again, we saw near 100% co-expression in all cases, further supporting Ki67 and Sox2 as indirect markers of proliferation and confirming that p27 deficiency increases the pool of proliferating precursors.

Knowing that Sox2 is expressed in the VZ, we can use the area of Sox2 expression as a measure of the size of the VZ in p27 deficient mice and controls. Thereby, we see a significant increase in the VZ in p27 deficient mice, leading to a change in the organization of the developmental zones in the VM, and a consequent decrease in the IZ and MZ. Furthermore, we have seen that the expression of p27 is exclusively complementary to the expression of Sox2, which suggests that p27 may have a regulatory role in the expression of Sox2 during DA neuron development. Previous work has shown that Sox2 expression was downregulated in proliferating progenitors in their final cell cycle, which was done by studying mitosis and Sox2 expression with markers of post-mitotic neurons, but levels of cell cycle inhibitors were not investigated (Graham et al 2003). However, a direct relationship between p27 and Sox2 was shown in a later study, demonstrating that p27 directly represses Sox2 during embryonic stem

cell differentiation (Li et al 2012). Specifically, p27 has been shown to associate with the p130-E2F4-SIN3A complex at the promoter of target genes to directly repress their transcription (Pippa et al 2012), including the Sox2-SSR2 regulatory element responsible for Sox2 expression (Sikorska et al 2008).

Sox2 is an established marker of all neural precursors, which make up a pool of precursors that can give rise to neurons, glia and oligodendrocytes (Ellis et al 2003). In the absence of p27, we have observed that this general pool of neural precursors is significantly increased. Therefore, we next investigated the neurogenesis marker Ngn2, a specific marker of DA neuron precursors in the context of the VM (Thompson et al 2006).

Ngn2 is a highly conserved basic-helix-loop helix (bHLH) pro-neural transcription factor, which regulates neurogenesis (Martynoga et al 2012) by promoting progenitor cell cycle exit, initiating the development of neuronal lineages and promoting the generation of progenitors committed to differentiation (Ma et al 1999, Guillemot 1999, Farah et al 2000, Bertrand et al 2002). For example, Ngn2 has been shown to promote primary neurogenesis in the cortex (Nguyen et al 2006) and has been associated with neuronal subtype specification (Ma et al 1999, Bertrand et al 2002). Furthermore, Ngn2 has been defined as a context-dependent precursor in the VM and is necessary for proper DA neuron differentiation (Andersson et al 2006a, Kele et al 2006). Based on previous results showing a direct relationship between p27 and Ngn2 (Nguyen et al 2006) in combination with our own results (seeing an increase in general precursors as defined by Sox2 but an overall decrease in the generation of DA neurons in the absence of p27), we expected to see a decrease in the expression of Ngn2. However, in p27 deficient mice, we saw a significant increase in Ngn2 expression, which maintained its spatiotemporal expression pattern but was much more expanded, consistent with an increased VZ.

These results strongly suggest an important interplay between p27, Sox2 and Ngn2 in the transition from mitotic precursors to the onset of DA neuron differentiation. In order to study this in more detail, we investigated Ngn2 expression with Sox2. Ngn2+Sox2+ double positive cells indicate the specific population of precursors destined to become DA neurons. In p27 deficient mice, we saw a significant increase in the total number of Ngn2+Sox2+ cells, which is consistent with our previous observations of these two markers individually. However, by examining the number of Ngn2+Sox2+ cells in relation to the total number of Sox2+ cells, we can study the total number of precursors that are DA neuron specific. Interestingly, we saw a significant increase in the percentage of Ngn2+Sox2+ cells in relation to total Sox2+ cells, indicating that p27 deficiency specifically increases the expression of DA neuron precursors,

and most of these cells remain in the VZ as mitotic precursors, without affecting the organization of the IZ.

We know that Sox2 is expressed in the general population of neural precursors, and that Ngn2 is expressed at the onset of neurogenesis, but the direct interaction between these markers is unknown. The absence of p27 leads to decreased inhibition of the Sox2-SRR2 promotor (Li et al 2012, Pippa et al 2012), thereby upregulating Sox2 expression. Since Ngn2 has been shown to inhibit Sox2, which later allows the up-regulation of post-mitotic neuronal markers (Bylund et al 2003), a similar mechanism could be occurring in the developing midbrain, where increased expression of Sox2 leads to a physiological response of increased Ngn2 expression to compensate for increased precursor levels.

Based on our results showing increased Ngn2 expression in the absence of p27, if we assume a direct relationship between p27 and Ngn2, we can therefore expect to see decreased Ngn2 when overexpressing p27. However, we saw increased Ngn2 levels upon differentiating our p27-overexpressing cells, indicating that p27 overexpression increases neurogenesis, supported by the increased number of TH+ colonies observed in these cells. For this reason, it remains unclear whether p27, Sox2 and Ngn2 all function as parts of the same mechanism, or if p27 interacts with both Sox2 and Ngn2 in independent mechanisms that occur simultaneously.

Taken together, our results show that p27 deficiency increases DA neuron-specific precursors but causes an overall decrease in DA neuron development. Having increased precursors at early stages of development could indicate that these cells eventually differentiate at later stages, with the effect of p27 deficiency being a developmental delay, causing an early increase in proliferation and a delayed onset of neurogenesis. Therefore, we studied later developmental stages, but saw that the effects observed at early stages were maintained as late as E14.5, with significant decreases detected for the markers TH and Pitx3, and increased expression observed for the markers Sox2, Ki67 and Ngn2. However, it does appear that the effects of p27 deficiency begin to improve by E13.5, as Nurr1 expression in p27 deficient mice was recovered to control levels. Despite the effects of p27 beginning to recover by later stages of development, as indicated by the recovery of Nurr1 expression at E13.5, we still see an effect on the normal progression of DA neuron development, where the majority of these cells at E13.5 remain Nurr1+TH- precursors. Whether this delay affects the integrity of the DA neurons that eventually develop needs to be investigated in more detail.

Possible Mechanism of p27 in the VM

To explain the dilemma presented by our results, we investigated whether p27 deficiency was preventing Ngn2+Sox2+ precursors from developing to DA neurons due to increased cell death. We studied both the presence of pyknotic nuclei and the expression of activated Casp3. Pyknotic nuclei area a morphological hallmark of apoptosis, where nuclei appear brighter and more fragmented. Casp3 is a protease enzyme that plays an essential role in programmed cell death, including apoptotic chromatin condensation and DNA fragmentation (Porter and Jänicke 1999). However, we did not see any differences or indication that loss of p27 was causing increased cell death in our embryonic mouse brain sections.

Seeing an increase in Sox2, which indicates an increase in all neural precursors, we did a study to see if the phenotypic specification of these precursors was being altered in the absence of p27. We first studied the expression of BIII-Tub (as a marker of neurogenesis) and Gfap (as a marker of gliogenesis) and saw no significant changes in their expression. Furthermore, Gfap usually appears at later developmental stages (Miller and Gauthier 2007), and our results show that p27 deficiency does not alter or accelerate gliogenesis. We next studied the mRNA levels of specific neuronal phenotypes, such as *GABA* and *Gad1* (GABAergic phenotype; Waite et al 2011), *Vglut1*, *Vglut2* and *Glul* (Glutamatergic phenotype; Morales and Root 2014, Root et al 2016) and finally *Sert* and *Tph2* (Serotonergic phenotype; Alenina et al 2006). No changes were observed for the mRNA levels of these markers, indicating that p27 does not alter the phenotypic specification of cells in the VM and the effect of p27 deficiency appears specific to DA neurons.

Since p27 is best known for its function in the cell cycle (Sherr and Roberts 2004, Lim and Kaldis 2013), we cannot ignore the effects p27 deficiency may have on altering normal cell cycle biology, and how this may affect the transition from proliferating precursors to the onset of neurogenesis and DA neuron development.

We first studied the effects of p27 deficiency on G_1 phase cyclins. G_1 is the first gap phase of the cell cycle, where the cell is preparing for DNA synthesis in the following S phase (Schafer 1998). The expression of D-type cyclins is induced in response to mitogenic signals (Sherr and Roberts 1999) and depends on CKIs for proper activation (LaBaer et al 1997, Cheng et al 1999). Of the effects observed for p27 deficiency on D-type cyclins, we saw a general trend indicating decreases mRNA levels, but this was not observed at all embryonic stages for all D-type cyclins and CDKs. However, the trend is expected and is supported by previous work showing a similar p27-dependent decrease in G_1 phase cyclins (Hampl et al 2000, Geng et al 2001, Bryja et al 2003). Interestingly, decreased Cyclin D levels are consistent with a longer

cycle and favors neurogenesis (Kaldis and Richardson 2012). However, despite decreased *Cyclin D* mRNA levels, we see increased proliferation (consistent with a shorter cycle) and less neurogenesis in the absence of p27. This indicates that p27 deficiency most likely increases proliferation by affecting a different part of the cell cycle.

Therefore, we studied the effects of p27 deficiency on cyclins and CDKs involved in the G_1/S transition. In simple terms, when the cell is ready to exit the cycle, decreased mitogenic stimuli cause D-type cyclins to release p27, which binds to and inhibits Cyclin E/A-Cdk2 complexes, preventing their ability to phosphorylate Rb proteins (Besson et al 2008, Ludlow et al 1990). Hypophosphorylated Rb remains associated to E2F complexes, inhibiting their transcriptional abilities (Ludlow et al 1990, Sherr and Roberts 1999). In the absence of p27, we saw an increase in *Cyclin E/A-Cdk2* mRNA levels, consistent with increased proliferation. Similar results were obtained for G_2/M phase *Cyclin B* and *Cdk1* mRNA levels and these results were also expected.

The results for Cyclin A and B, although expected, provide another possible explanation for why increased Ngn2 expression does not lead to increased DA neuron development. It has previously been shown that increasing cyclin-CDK activity inhibits neurogenesis (Richard-Parpaillon et al 2004, Lange and Calegari 2010). A mechanism for this was suggested when Cyclin A-Cdk2 overexpression inhibited primary neurogenesis in xenopus embryos (Ali et al 2011), specifically due to the direct phosphorylation of Ngn2 on multiple sites by both Cyclin A and B dependent kinases, indicating a post-translational control of Ngn2 that hinders the induction of neuronal differentiation (Ali et al 2011). Furthermore, these post-translational modifications were shown to have different effects on the transcription of direct downstream targets of Ngn2, including Delta and NeuroD1(Hindley et al 2012).

Delta (Dll1, a notch ligand) and NeuroD1 are important downstream targets of Ngn2 (Sommer et al 1996, Seo et al 2007) that are involved in the process of lateral inhibition, where Ngn2 restricts its own activity to single progenitor cells, inhibiting its own expression in adjacent cells to control neuronal differentiation. In addition to Dll1, Hes1 and Hes5 are also important downstream targets of Ngn2 (Ohtsuka et al 1999), all three of them involved in Notch signaling and known to promote progenitor maintenance (Ohtsuka et al 1999). The study by Hindley et al., showed that the Dll1 promoter was not sensitive to increased phosphorylation of Ngn2 (Hindley et al 2012), leading us to believe that increased Ngn2 expression in the VM could perhaps be increasing the expression of genes responsible for promoting progenitor maintenance, despite increased expression of Cyclin A and B. However, our results at E12.5 did not indicate alterations in the mRNA levels of Dll1, Hes1 or Hes5 in p27 deficient mice.

Therefore, we did a screen of NeuroD proteins, which are best known for their function in promoting neurogenesis by inhibiting progenitor maintenance (Seo et al 2007) and include NeuroD1, NeuroD2, NeuroD3 (also known as Ngn1), NeuroD4 and NeuroD6. Of these genes, only NeuroD1 was significantly decreased.

NeuroD1 in the developing VM

The ability of NeuroD1 (also NeuroD, Beta2) to convert ectodermal tissue to neurons was first described in 1995 (Lee et al 1995). NeuroD1 is highly expressed in the developing nervous system, with peak expression during development in areas such as the cortex (Chae et al 2004). Previous work supports the role of NeuroD1 in promoting neurogenesis as a direct downstream target of Ngn2 in olfactory tissue (Boutin et al 2010) and in proper development of the retina (Cherry et al 2011). Its expression pattern has been seen restricted mainly to post-mitotic cells (D'Amico et al 2013) and in certain brain regions, including the cerebellum and hippocampus, NeuroD1 expression has been detected in fully differentiated structures, indicating it may also have maintenance functions in these tissues (Miyata et al 1999).

The expression of pro-neural genes is transient, and cells exit the proliferative zone (or VZ) and begin to differentiate after pro-neural genes are downregulated (Bertrand et al 2002). The involvement of NeuroD1 in this process can be supported by its expression pattern in the VM. When double staining NeuroD1 with p27, we see a scattered expression with NeuroD1+ cells interspersed, but rarely co-expressed with p27 in the IZ. Their location outside of the VZ indicates their commitment to differentiation, and in the context of the VM, a likely commitment to a DA neuron fate.

The decreased expression observed for NeuroD1 in our initial screening led us to investigate the expression of this marker at early developmental stages and saw significant decreases in NeuroD1 expression in p27 deficient mice compared to controls. Its distribution was mainly restricted to the IZ, as seen by IHC studies, double stained with either Ngn2 or p27 (described above). Therefore, although we did not see altered Ngn2 expression in the IZ, we do see decreased NeuroD1, further suggesting that Ngn2 is in some way inhibited from activating NeuroD1 to promote neurogenesis.

Since NeuroD1 has not yet been described in the context of the VM or in DA neuron development, we performed an experiment where we nucleofeted the NeuroD1 plasmid into our p27 deficient miPSCs, to see if we could recover the effect of p27 deficiency on Ngn2, and its ability to promote DA neuron differentiation (via NeuroD1). Our initial results show a significant increase in DA neuron production (quantified as TH+ colonies) in our p27KO^{NeuroD1}

cells as compared to p27KO controls. These results strongly support NeuroD1 as an important downstream factor of Ngn2, necessary to promote DA neuron development. However, these results are somewhat preliminary and need to be studied in further detail.

Taken together, these results suggest both direct and indirect functions of p27 in the developing VM. We thereby suggest a cascade where p27 is a master regulator of proper cell cycle exit and onset of neurogenesis driven by Ngn2, and where p27 deficiency could have a direct effect on increasing Sox2 expression, which may, in turn, lead to increased Ngn2 expression. Additionally, in the absence of p27, increased Cyclin A and B levels could directly phosphorylate Ngn2, decreasing its ability to activate downstream targets like NeuroD1, important to initiate neuronal differentiation. Therefore, we suggest a cascade where multiple mechanisms could be interacting simultaneously to ultimately decrease the differentiation of DA neurons in the VM (Figure D.3).

Possible compensation for loss of p27

We earlier saw that p27 deficiency began to recover by later stages of development, and that Nurr1 was recovered by E13.5. Therefore, we studied the expression of p57 and p21 to see if altered levels in their expression could help explain, at least in part, some of this compensation.

As mentioned before, the Cip/Kip family of CKIs include the three family members p27, p21 and p57. These proteins share a conserved N-terminal domain which interacts with cyclins and CDKs to exert their inhibitory functions on the cell cycle, but they differ in the remainder of their sequence indicating that they may have individual functions outside the cycle (Besson et al 2008)

Some evidence suggests overlapping functions for CKIs due to their inherently disordered nature and the fact that they take shape upon binding to substrates (Besson et al 2008, Bachs et al 2018). Furthermore, a knock-in model of p57 deficient mice expressing p27 showed that most of the functions performed by p57 could also be performed by p27 (Susaki et al 2009). We therefore wanted to see if the opposite could also be true. Our simple studies of *p57* mRNA levels show decreased p57 levels at early developmental stages in p27 deficient mice, supported by previous studies linking decreased p57 expression to decreased expression of the DA neuron marker Nurr1 (Joseph et al 2003). Therefore, in the context of DA neuron development, the partial compensation observed is unlikely due to p57 expression. We next investigated p21, and interestingly, saw increased mRNA levels during early developmental stages. Again, structural similarities between p21 and p27 suggest that they could have

overlapping functions (Bachs et al 2018). This is supported by an observed collaboration between p21 and p27, where they cooperate in the recruitment of cyclin-CDK complexes to the promotor of target genes to regulate transcription (Orlando et al 2015). Furthermore, embryonic fibroblasts that lack p27 were found to have increased p21 expression, due to an inhibitory effect of p27 on p21 (Gallastegui et al 2017). These recent findings support the possibility that p21 could be compensating, at least in part for the loss of p27 in the developing midbrain (Figure D.3)

Another important factor that we have not studied in much detail is Mash1. We chose to focus on Ngn2 expression, because although both Mash1 and Ngn2 have been implicated in DA neuron development, only Ngn2 was shown to be necessary for DA neuron differentiation (Kele et al 2006, Arenas et al 2015). Mash1 has previously been implicated in the specification of certain neuronal types (Hirsch et al 1998, Casarosa et al 1999, Pattyn et al 2004, Helms et al 2005) and it has the ability to re-specify neuronal lineages when expressed in Ngn2 deficient mice (Fode et al 2000, Parras et al 2002; Bertrand et al 2002). In the context of the VM,

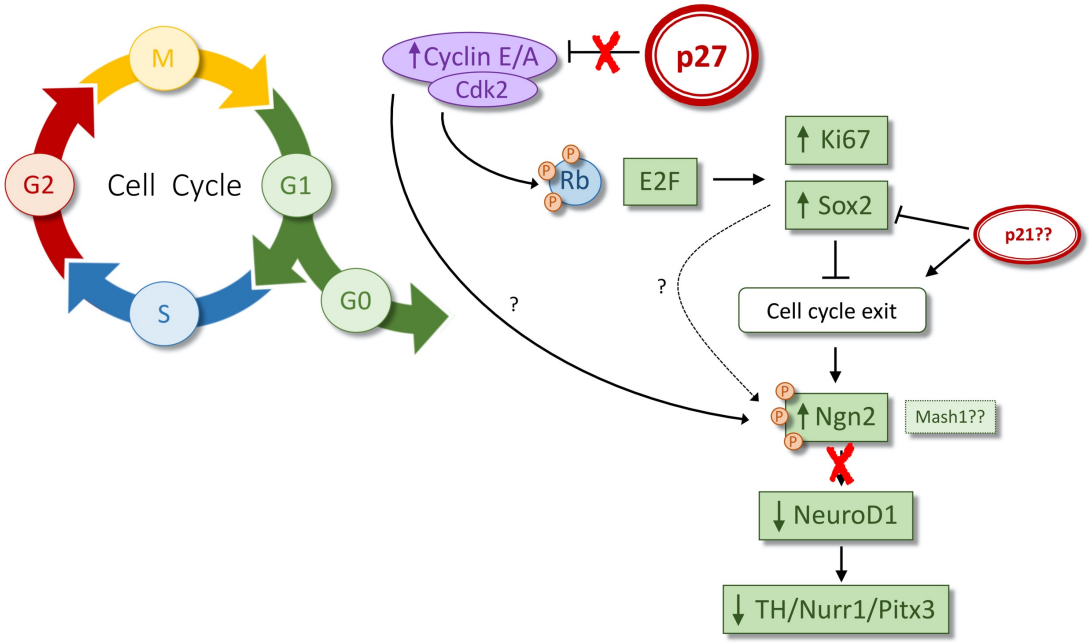

Figure D.3: Possible mechanism of p27 deficiency in DA development. In the absence of p27, we have increased Cyclin E/A-Cdk2 activity, which hyperphosphorylates Rb proteins, causing their dissociation from the E2F complex, leading to cell cycle progression. This leads to increased proliferation and expression of the cell cycle marker Ki67 and the neural precursor marker Sox2. This alters the organization of the developing VM, leading to increased Ngn2 expression in the VZ, but decreased cell cycle exit and decreased neurogenesis. This can be caused by direct interactions between p27-Sox2-Ngn2 and/or indirect interactions due to increased Cyclin A dependent kinase activity known to phosphorylate and inactivate Ngn2. Decreased Ngn2 activity leads to decreased induction of neuronal differentiation as measured by decreased NeuroD1 and, decreased expression of DA neuron markers such as TH, Nurr1 and Pitx3. Some of these effects may be partially compensated for by p21 and Mash1 expression.

however, Mash1 does not re-specify DA neuron progenitors and has been shown to compensate for the loss of Ngn2 (Kele et al 2006). Due to the similar functions observed for Ngn2 and Mash1, we investigated the effects of p27 deficiency on Mash1 mRNA levels and saw significant increases in Mash1 expression throughout development. These results suggest another compensatory mechanism that could protect DA neuron development from p27 deficiency.

Future Perspectives

The current study has provided significant new information about p27 as a novel factor important for proper DA neuron development. However, these discoveries are initial studies that need to be investigated in much more detail in order to understand the full effect of p27 on the differentiation of DA neurons and the precise molecular mechanisms involved.

Although our experiments have provided valuable information about the effects of p27 *in vivo*, this thesis has been limited to the study of embryonic development, and the effects of p27 in post-natal or adult brains has not been studied. Although we have seen that DA neuron development begins to recover by E14.5 in p27 deficient mice, we have yet to determine if this deficiency ever fully recovers by later embryonic or post-natal stages. Furthermore, it must be determined if the apparent developmental delay caused by p27 deficiency affects the overall functionality and stability of the neurons that do eventually develop. This information is vital for the future applicability of p27 in new protocols for the directed differentiation of DA neurons *in vitro*.

Furthermore, we have seen effects that appear to be general to p27 as a cell cycle inhibitor, such as increased proliferation (BrdU) and increased Ki67. However, some results may also be specific to p27 in the context of the VM, independent of its function as a cell cycle inhibitor, such as the effects observed for Sox2, Ngn2 and NeuroD1. Therefore, in order to distinguish the effect of p27 in the VM from its function in the cell cycle, we would need to perform similar studies in mice carrying mutated versions of p27 (Kiyokawa et al 1996, Besson et al 2006) that do not allow p27 to bind to cyclins and CDKs. In the case of cell cycle independent functions of p27, direct interactions between p27 and Ngn2, Sox2 and NeuroD1 should also be established.

Despite the limitations presented by this thesis, there is currently enough evidence of the effects of p27 on DA neuron development to warrant experiments using human stem cell systems, including human embryonic stem cells. In order to obtain p27 deficient embryonic stem cells, the CRISPR-Cas9 system (Doudna and Charpentier 2014) could be used,

specifically designing guide RNA for genomic editing to eliminate p27 from these cells. Overexpression can easily be studied following a similar nucleofection protocol and subsequent selection as performed in our murine stem cell models. Since we have seen that the re-introduction of p27 was able to partially recover the effects of p27 deficiency, it would be of interest to use inducible vectors, in order to manipulate the expression of p27 at different stages of development. Furthermore, with an inducible vector, the effects of cyclins and CDKs on this process could be studied in more detail and provide valuable information about their effects on DA neuron development. In the event that these cyclin and CDK complexes are really phosphorylating and inhibiting Ngn2 in the absence of p27 (as hypothesized above), upon the administration of an analogous inhibitor, we could expect to see increased neurogenesis in response to increased, unphosphorylated Ngn2.

With evidence from human stem cell trials, we would also be able to begin testing new protocols to improve the differentiation of human stem cells towards DA neuron phenotypes. Several effective protocols currently exist (Chambers et al 2009, Kriks et al 2011, Kirkeby et al 2012, Grealish et al 2014), but none have been utilized for large scale application. Based on our results, we could suggest a protocol that relies on inhibiting p27 at early stages of development to promote the production of mitotic DA-specific precursors, and the addition of p27 at later stages to promote the differentiation of these precursors to fully mature DA neurons. Such a protocol would be a huge advancement in the field of stem cell therapy for PD.

CONCLUSIONS

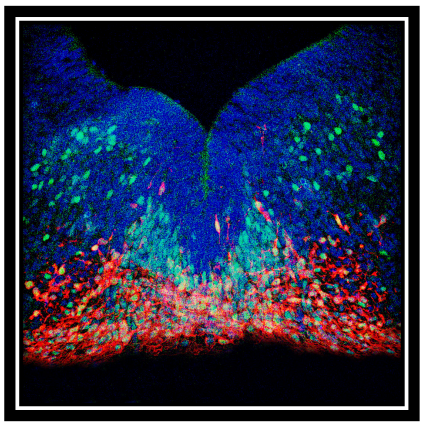

CONCLUSIONS

The results from this work allow us to conclude the following:

1.) p27 is expressed in the developing VM and this expression increases as development progresses.
2.) p27 is co-expressed with DA neuron markers in the IZ and MZ, whereas its expression is absent from the VZ and complementary to proliferation markers, cell cycle markers and precursor markers.
3.) p27 deficiency causes a significant decrease in DA neuron development, indicated by significant decreases in the markers TH, Pitx3 and Nurr1. These results were confirmed *in vivo*, in primary cultures and upon the directed differentiation of miPSC cell models.
4.) p27 deficiency significantly increases proliferation and the pool of mitotic precursors, indicated by significant increases in the markers BrdU, Ki67 and Sox2. These results were confirmed *in vivo* and in primary cultures.
5.) p27 deficiency significantly increases DA neuron specific precursors as measured by Ngn2 and alters the distribution of these precursors by increasing the size of the VZ.
6.) The effects observed in p27 deficient cultures can be, at least in part, recovered by the re-introduction of p27.
7.) The overexpression of p27 increases the differentiation of DA neurons *in vitro*.
8.) NeuroD1 could be a novel factor in DA neuron development affected by p27 expression. Although we see increased numbers of Ngn2+ precursors, p27 could be affecting the progression of these DA-specific precursors by decreasing downstream NeuroD1 levels. This is supported by a partial recovery of DA neurons in p27 deficient cultures over-expressing NeuroD1.

In summary, we demonstrate important implications of p27 in the proper development of DA neurons and we believe this information will be useful for future application in the differentiation of DA neurons *in vitro* for possible new therapies to treat PD.

CONCLUSIONES

Los resultados de esta tesis nos permiten concluir lo siguiente:

1.) p27 se expresa en el MV y su expresión aumenta según el desarrollo.
2.) p27 se co-expresa con marcadores de ND en la zona intermedia (IZ) y en la zona del manto (MZ), pero su expresión es ausente de la zona ventricular (VZ) y complementaria a marcadores de proliferación, ciclo celular y precursores.
3.) La deficiencia de p27 impide el desarrollo de ND, indicado por una disminución significativa en los marcadores TH, Pitx3 y Nurr1. Estos resultados se confirman *in vivo,* en cultivos primarios y en la diferenciación dirigida de células miPSC.
4.) La deficiencia de p27 favorece la proliferación y el numero de precursores mitóticos, indicado por un aumento significativo en los marcadores BrdU, Ki67 y Sox2. Estos resultados se confirman *in vivo* y en cultivos primarios.
5.) La deficiencia de p27 aumenta el número de precursores específicos de ND, indicado por un incremento significativo en el marcador Ngn2, y altera la distribución de esos precursores, aumentando el área de la VZ.
6.) Se puede recuperar, por lo menos en parte, los efectos observados en los cultivos deficientes de p27, al re-expresar p27 en esos cultivos.
7.) La sobreexpresión de p27 aumenta la diferenciación de ND *in vitro.*
8.) NeuroD1 podría ser un factor nuevo en el desarrollo de ND, afectado por la expresión de p27. Aunque vemos un aumento en el número de precursores Ngn2+, p27 podría estar afectando a esos precursores disminuyendo los niveles de NeuroD1, un factor importante pro-neurogénico.

En resumen, hemos demostrado que p27 tiene un papel importante en el desarrollo de las ND y creemos que esa información podría ser útil para futuras aplicaciones en la diferenciación de las ND, así como para posibles terapias de la EP.

B I B L I O G R A P H Y

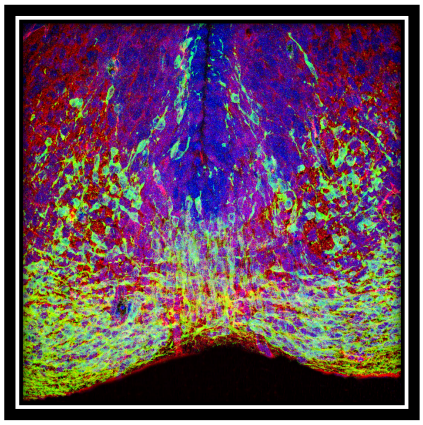

BIBLIOGRAPHY

- Abbastabar M, Kheyrollah M, Azizian K, Bagherlou N, Tehrani SS, Maniati M and Karimian A (2018). Multiple functions of p27 in cell cycle, apoptosis, epigenetic modifications and transcriptional regulation for the control of cell growth: a double ended sword protein. DNA Repair 69: 63-72

- Alenina N, Bashammakh S and Bader M (2006). Specification and differentiation of serotonergic neurons. Stem Cell Rev 2: 2-5

- Ali F, Hindley C, McDowell G, Deibler R, Jones A, Kirschner M, Guillemot F and Philpott A (2011). Cell cycle-regulated multi-site phosphorylation of Neurogenin2 coordinates cell cycling with differentiation during neurogenesis. Development 138: 4267-4277

- Andersson E, Jensen J, Parmar M, Guillemot F and Björklund A (2006a). Development of the mesencephalic dopaminergic neuron system is compromised in the absence of neurogenin 2. Development 133: 507-516

- Andersson E, Saltó C, Villaescusa C, Cajanek L, Yang S, Bryjova L, Nagy I, Vainio S, Ramierz C, Bryja V and Arenas E (2013). Wnt5a cooperates with canonical Wnts to generate midbrain dopaminergic neuros in vivo and in stem cells. Proc Natl Acad Sci USA. 110(7): E602-E610

- Andersson E, Tryggvason U, Deng Q, Friling S, Alekseenko Z, Robert B, Perlmann T and Ericson J (2006b). Identification of intrinsic determinants of midbrain dopamine neurons. Cell 124: 393-405

- Ang SL (2006). Transcriptional control of midbrain dopaminergic neuron development. Development 133: 3499-3506

- Ang SL (2009). Foxa1 and Foxa2 transcription factors regulate differentiation of midbrain dopaminergic neurons. Advances in Experimental Medicine and Biology, Springer 651: 58-61

- Ang SL and Rossant J (1994). Hnf-3ß is essential for node and notochord formation in mouse development. Cell 78: 561-571

- Arenas E (2008). Foxa2: the rise and fall of dopamine neurons. Cell Stem Cell 2: 110-112

- Arenas E, Denham M and Villaescusa C (2015). How to make a dopaminergic neuron. Development 142: 1918-1936

- Ascherio A and Schwarzschild M (2016). The epidemiology of Parkinson's disease: risk factors and prevention. Lancet Neruol 15: 1257-1272

- Bachs O, Gallastegui E, Orlando S, Bigas A, Morante-Redolat JM, Serratosa J, Fariñas I, Aligué R and Pujol MJ (2018). Role of p21Kip1 as a transcriptional regulator. Oncotarget 9(40): 26259-26278

- Barberi T, Klivenyi P, Calingasan N, Lee H, Kawamata H, Loonam K, Perrier A, Bruses J, Rubio M, Topf N, Tabar V, Harrison N, Beal M, Moore M and Studer L (2003). Neural subtype specification of fertilization and nuclear transfer embryonic stem cells and application in parkinsonian mice. Nat Biotechnol 21(10): 1200-1207

- Barker A (2014). Developing stem cell therapies for Parkinson's disease: waiting until the time is right. Cell Stem Cell 15: 539-542

- Barker R, Barett J, Mason S and Björklund A (2013). Fetal dopaminergic transplantation trials and the future of neural grafting in Parkinson's disease. Lancet Neurol 12: 84-91

- Bertrand N, Castro D and Guillemot F (2002). Proneural genes and the specification of neural cell types. Nat Rev 3: 517-530

- Besson A, Gurian-West M, Chen X, Kelly-Spratt KS, Kemp CJ and Roberts JM. 2006. A pathway in quiescent cells that controls p27Kip1 stability, subcellular localization, and tumor suppression. Genes Dev 20: 47–64

- Besson A, Dowdy S and Roberts J (2008). CDK inhibitors: cell cycle regulators and beyond. Dev Cell 14: 159-169

- Biçer A, Orlando S, Islam A, Gallastegui E, Besson A, Aligué R, Bachs O and Pujol MJ (2017). ChIP-Seq analysis identifies p27(Kip1)-target genes involved in cell adhesion and cell signaling in mouse embryonic fibroblasts. PLoS One 12 (11): e0187891

- Bilodeau S, Roussel-Gervais A and Drouin J (2009). Distinct developmental roles of cell cycle inhibitors p57Kip2 and p27Kip1 distinguish pituitary progenitor cell cycle exit from cell cycle reentry of differentiated cells. Mol Cel Biol 29(7): 1895-1908

- Björklund A and Dunnett B (2007). Dopamine neuron system in the brain: an update. Trends Neurosci 30(5): 194-202

- Björklund A and Lindvall O (2017). Replacing dopamine neurons in Parkinson's disease: how did it happen? J Parkinson Dis 7: S21-S31

- Blesa J and Przedborski S (2014). Parkinson's disease: animla models and dopamine cell vulnerability. Front Neuroanat 8(155): 1-12

- Boutin C, Hardt O, Chevigny A, Coré N, Goebbles S, Seidenfaden R, Bosio A and Cremer H (2010). NeuroD1 induces terminal neuronal differentiation in olfactory neurogenesis. Proc Natl Acad Sci USA 107(3): 1201-1206

- Braak H, Tredici K, Rüb U, de Vos R, Jansen Steur E and Braak E (2003). Staging of brain pathology to sporadic Parkinson's disease. Neurobiol Aging 24: 197-211

- Brichta L, Greengard P and Fajolet M (2013). Advances in the pharmacological treatment of Parkinson's disease: targeting neurotransmitter systems. Trends Neurosci 36(9): 543-554

- Bryja V, Pachernik J, Faldikova L, Krejci P, Pogue R, Nevriva I, Dvorak P and Hampl A (2003). The role of p27Kip1 in maintaining levels of D-type cyclins in vivo. Biochim Biophys Acta 1691: 105-116

- Bryja V, Pachernik J, Soucek K, Horvath V, Dvorak P and Hampl A (2004). Increased apoptosis in differentiating p27-deficient mouse embryonic stem cells. Cell Mol Life Sci 61: 1384-1400

- Bryja V, Cajanek L, Pachernik J, Hall A, Horvath V, Dvorak P and Hampl A (2005). Abnormal development of mouse embryoid bodies lacking p27Kip1 cell cycle regulator. Stem Cells 23: 965-974

- Bylund M, Andersson E, Novitch B and Muhr J (2003). Vertebrate neurogenesis is counteracted by Sox1-3 activity. Nat Neurosci 6(11): 1161-1168

- Casarosa S, Fode C and Guillemot F (1999). Mash1 regulates neurogenesis in the ventral telencephalon. Development 126: 525-534

- Chae J, Stein G and Lee J (2004). NeuroD: The predicted and the surprising. Mol Cell 18(3): 271-288

- Chambers S, Fasano C, Papapetrou E, Tomishima M, Sadelain M and Studer L (2009). Highly efficient neural conversion of human ES and iPS cells by dual inhibition of SMAD signaling. Nat Biochem 27(3): 275-280

- Chaudhuri K and Schapira A (2009). Non-motor symptoms of Parkinson's disease: dopaminergic pathophysiology and treatment. Lancet Neruol 8: 464-474

- Cheng M, Olivier P, Diehl J, Fero M, Roussel M, Roberts J and Sherr C (1999). The p21Cip1 and p27Kip1 CDK 'inhibitors' are essential activators of cyclin-D-dependent kinases in murine fibroblasts. EMBO 18(6): 1571-1583

- Cherry T, Wang S, Bormuth I, Schwab M, Olson J, Cepko C (2011). NeuroD factors regulate cell fate and neurite stratification in the developing retina. J Neurosci 31(20): 7365-7379

- Chu I, Hengst L and Slingerland J (2008). The cdk inhibitor p27 in human cancer: prognostic potential and relevance to anticancer therapy. Nat Rev 8: 253-267

- Chu I, Sun J, Arnaout A, Kahn H, Hanna W, Narod S, Sun P, Tan CK, Hengst L and Slingerland J (2007). p27 phosphorylation by Src regulates inhibition of Cyclin E-Cdk2 and p27 proteolysis. Cell 128(2): 281-294

- Chung S, Leung A, Han BS, Chang MY, Moon JI, Kim CH, Hong S, Pruszak J, Isacson O and Kim KS (2009). Wnt1-lmx1a forms a novel autoregulatory loop and controls midbrain dopaminergic differentiation synergistically with Shh-Foxa2 pathway. Cell Stem Cell 5: 646-658

- Courtois E, Castillo C, Seiz E, Ramos M, Bueno C, Liste I and Martínez-Serrano A (2010). In vitro and in vivo enhanced generation of human A9 dopamine neurons from neural stem cells by Bcl-XL. J Biol Chem 285(13): 9881-9897

- D'Amico L, Boujard D and Coumailleau P (2013). The neurogenic factor NeuroD1 is expressed in post-mitotic cells during juvenile and adult xenopus neurogenesis and not in progenitor or radial glial cells

- De Almeida M, Pérez-Sayáns M, Súarez-Peñaranda JM, Somoza-Martín JM and García-García A (2015). p27Kip1 expression as a prognostic marker for squamous cell carcinoma of the head and neck. Oncol Lett 10: 2675-2682

- Diecke S, Lu J, Lee J, Termglinchan V, Kooreman N, Burridge P, Ebert A, Churko J, Sharma A, Kay M and Wu J (2015). Novel codon-optimized mini-intronic plasmid for efficient, inexpensive, and xeno-free induction of pluripotency. Sci Rep-UK 5: 8081

- Dorsey ER, Constantinescu R, Thompson JP, Biglan KM, Holloway RG, Kieburtz K, Marshall FJ, Ravina BM, Schifitto G, Siderowf A and Tanner CM (2007). Projected number of people with Parkinson disease in the most populous nations, 2005 through 2030. Neurology 68: 384-386

- Doudna J and Charpentier E (2014). The new frontier of genome engineering with CRISPR-Cas9. Science 346: 1077-1087

- Dyson H and Wright P (2005). Intrinsically unstructured proteins and their functions. Nat Rev Mol Cell Biol 6: 197-208

- Ellis P, Fagan B, Magness S, Hutton S, Taranova O, Hayashi S, McMahon A, Rao M and Pevny L (2003). Sox2, a persistent marker for multipotential neural stem cells derived from embryonic stem cells, the embryo or the adult. Dev Neurosci 26: 148-165

- Epstein D, McMahon A and Joyner A (1999). Regionalization of sonic hedgehog transcription factor along the anteroposterior axis of the mouse central nervous system is regulated by Hnf3-dependent and independent mechanisms. Development 126: 281-292

- Fahn S (2006). Levodopa in the treatment of Parkinson's disease. J Intern Transm (2006) 71: 1-15

- Farah M, Olson J, Sucic H, Hume R, Tapscott J and Turner D (2000). Generation of neurons by transient expression of neural bHLH proteins in mammalian cells. Development 127: 693-702

- Fasano C, Chambers S, Lee G, Tomishima M and Studer L (2010). Efficient derivation of functional floor plate tissue from human embryonic stem cells. Cell Stem Cell 6: 336-347

- Fero M, Rivkin M, Tasch M, Porter P, Carow C, Firpo E, Polyak K, Tsai LH, Broudy V, Perlmutter R, Kaushansky K and Roberts J (1996). A syndrome of multiorgan hyperplasia with features of gigantism, tumorigenesis, and female sterility in p27Kip1-deficient mice. Cell 85: 733-744

- Ferri A, Lin W, Mavromatakis Y, Wang J, Sasaki H, Whitsett J and Ang SL (2007). Foxa1 and Foxa2 regulate multiple phases of midbrain dopaminergic neuron development in a dosage-dependent manner. Development 134: 2761-2769

- Fode C, Ma Q, Casarosa S, Ang SL, Anderson D and Guillemot F (2000). A role of neural determination genes in specifying the dorsoventral identity of telencephalic neurons. Gene Dev 14: 67-80

- Forno L (1995). Neuropathology of Parkinson's Disease. J Neuropath Exp Neur 55(3): 259-272

- Fox S, Katzenschlager R, Lim SY, Barton B, de Bie R, Seppi K, Coelho M and Sampaio C (2018). International Parkinson and movement disorder society evidence-based medicine review: update on treatments for the motor symptoms of Parkinson's Disease. Mov Dis doi: 10.1002/mds.27372

- Freed C, Breeze R, Rosenberg N, Schneck S, Kriek E, Qi JX, Lone T, Zhang YB, Snyder J, Wells T, Ramig L, Thompson L, Mazziotta J, Huang SC, Grafton S, Brooks D, Sawle G, Schroter G and Ansari A (1992). Survival of implanted fetal dopamine cells and neurologic improvement 12 to 46 months after transplantation of Parkinson's disease. N Engl J Med 327: 1541-1548

- Freed C, Greene P, Breeze R, Tsai WT, DuMouchel W, Kao R, Dillon S, Winfield H, Culver S, Trojanowksi J, Eidelberg D and Fahn S (2001). Transplantation of embryonic dopamine neurons for severe Parkinson's disease. N Engl J Med 344: 710-719

- Freed C, Zhou W and Breeze R (2011). Dopamine cell transplantation of Parkinson's disease: the importance of controlled clinical trials. Neurotherapeutics 8: 549-561

- Friling S, Andersson E, Thompson L, Jönsson M, Hebsgaard J, Nanou E, Alekseenko Z, Marklund U, Kjellander S, Volakakis N, Hovatta O, El Manira A, Björklund A, Perlmann T and Ericson J (2009). Efficient production of mesenchymal dopamine neurons by Lmx1a expression in embryonic stem cells. Proc Natl Acad Sci USA 106(18): 7613-7618

- Gallastegui E, Biçer A, Orlando S, Besson A, Pujol MJ and Bachs O (2017). p27Kip1 represses the Pitx2-mediated expression of p21Cip1 and regulates DNA replication during cell cycle progression. Oncogene 36: 350-361

- Gallastegui E, Domuro C, Serratosa J, Larrieux A, Sin L, Martinez J, Besosn A, Morante-Redolat JM, Orlando S, Aligue R, Fariñas I, Pujol MJ and Bachs O (2018). p27Kip1 regulates alpha-synuclein expression. Oncotarget 9(23): 16368-16379

- García-Ramos R, López Valdes E, Ballesteros L, Jesús S and Mir P (2016). The social impact of Parkinson's disase in Spain: Report by the Spanish Foundation of the Brain. Neurología 31(6): 401-413

- GBD 2016 Parkinson's Disease Collaborators (2018). Global, regional, and national burden of Parkinson's disease, 1990-2016: a systematic analysis for the Global Burden of Disease Study 2016. Lancet Neurol 17: 939-953

- Geng Y, Yu Q, Sicinska E, Das M, Bronson R and Sicinski P (2001). Development of the p27Kip1 gene restores normal development in cyclin D1-deficient mice. Proc Natl Acad Sci USA 98(1): 194-199

- Glavaski-Joksimovic A and Bohn M (2013). Mesenchymal stem cells and neurodegeneration in Parkinson's disease. Exp Neurol 247: 25-38

- Godin J, Thomas N, Laguesse S, Malinouskaya L, Close P, Malaise O, Purnelle A, Raineteau O, Campbell K, Fero M, Moonen G, Malgrange B, Chariot A, Metin C, Besson A and Nguyen L (2012). p27Kip1 is a microtubule-associated protein that promtes microtubule polymerization during neuron migration. Dev Cell 23: 729-744

- González C, Bonilla S, Flores A, Cano E and Liste I (2015). An update on human stem cell-based therapy in Parkinson's disease. Curr Stem Cell Res T 10: 1-8

- Graham C, Khudyakov J, Ellis P and Pevny L (2003). Sox2 functions to maintain neural progenitor identity. Neuron 39: 749-765

- Grealish S, Diguet E, Kirkeby A, Mattsson B, Heuer A, Bramoulle Y, can Camp N, Perrier A, Hantraye P, Björklund A and Parmar M (2014). Human ESC-derived dopamine neurons show similar preclinical efficacy and potency to fetal neurons when grafted in a rat model of Parkinson's disease. Cell Stem Cell 15: 653-665

- Guillemot F (1999). Vertebrate bHLH genes and the determination of neuronal fates. Exp Cell Res 253: 357-364

- Guillemot F (2007). Spatial and temporal specification of neural fates by transcription factor codes. Development 134: 3771-3780

- Hampl A, Pachernik J and Dvorak P (2000). Levels and interactions of p27, Cyclin D3 and CDK4 during the formation and maintenance of the corpus luteum in mice. Bio Reprod 62: 1393-1401

- Hara T, Kamura T, Nakayama K, Oshikawa K, Hatakeyama S and Nakayama KI (2001). Degradation of p27Kip1 at the G0-G1 transition mediated by a Skp2-independent ubiquination pathway. Biol Chem 276(52): 48937-48943

- He Q, Li J, Bettiol E and Jaconi E (2003). Embryonic stem cells: new possible therapy for degenerative diseases that affect elderly people. J Gerontol 58A(3): 279-287

- Hegarty S, Sullivan A and O'Keeffe (2013). Midbrain dopaminergic neurons: a review of the molecular circuitry that regulates their development. Dev Biol 379: 123-138

- Helms A, Battiste J, Henke R, Nakada Y, Simpicio N, Guillemot F and Johnson J (2005). Sequential roles for Mash1 and Ngn2 in the generation of dorsal spinal cord interneurons. Development 132: 2709-2719

- Hindley C, Ali F, McDowell G, Cheng K, Jones A, Guillemot F and Philpott A (2012). Post-transcriptional modification of Ngn2 differentially affects transcription of distinct targets to regulate the balance between progenitor maintenance and differentiation. Development 139: 1718-1723

- Hnit S, Xie C, Yao M, Holst J, Bensoussan A, de Souza P, Li Z and Dong Q (2015). p27Kip1 signaling: transcriptional and post-translational regulation. Biochem Cell Biol doi: 10.1016/j.biocel.2015.08.005

- Hirsch MR, Tiveron MC, Guillemot F, Brunet JF and Goridis C (1998). Control of noradrenergic differentiation and Phox2a expression by Mash1 in the central and peripheral nervous system. Development 125: 599-608

- Huang Y, Yoon MK, Otieno S, Lelli M and Kriwacki R (2015). The activity and stability of the intrinsically disordered Cip/Kip protein family are regulated by non-receptor tyrosine kinases. J Mol Biol 427: 371-386

- Jacobs F, van Erp S, van der Linden A, von Oerthel L, Burbach P and Smidt M (2009). Pitx3 potentiates Nurr1 in dopamine neuron terminal differentiation through release of SMRT-mediated repression. Development 136: 531-540

- Joseph B, Wallén-Mackenzie Å, Benoit G, Murata T, Joodmardi E, Okret S and Perlmann T (2003). p57Kip2 cooperates with Nurr1 in developing dopamine cells. P Natl Acad Sci USA 100: 15619-15624

- Kadkhodaei B, Ito T, Joomardi E, Mattson B, Rouillard C, Carta M, Muramatsu SI, Sumi-Ichinose C, Nomura T, Metzger D, Chambon P, Lindqvist E, Larsson NG, Olson L, Björklund A, Ichinose H and Perlmann T (2009). Nurr1 is required for maintenance of maturing and adult midbrain dopamine neurons. J Neurosci 29(50): 15923-15932s

- Kaldis P and Richardson H (2012). When cell cycle meets development. Development 139: 225-230

- Kalia L and Lang A (2015). Parkinson's disease. Lancet 386: 896-912

- Kefalopoulou Z, Politis M, Piccini P, Mencacci N, Bhatia K, Jahanshani M, Widner H, Rehncrona S, Brundin P, Björklund A, Lindvall O, Limousin P, Quinn N and Foltynie T (2014). Long-term clinical outcome of fetal transplantation for Parkinson disease: two case reports. JAMA Neurol 71: 83-87

- Kele J, Simplicio N, Ferri, Mira H, Guillemot F, Arenas E and Ang SL (2006). Neurogenin 2 is required for the development of ventral midbrain dopaminergic neurons. Development 133: 495-505

- Kirkeby A, Grealish S, Wolf D, Nelander J, Wood J, Lundblad M, Lindvall O and Parmar M (2012). Generation of regionally specified neural progenitors and functional neurons from human embryonic stem cells under defined conditions. Cell Rep 1: 703-714

- Kittappa R, Chang W, Awatramani R and McKay R (2007). The Foxa2 gene controls the birth and spontaneous degeneration of dopamine neurons in old age. PLoS Biol 5(12): 2875-2884

- Kiyokawa H, Kineman R, Manova-Todorova K, Soares V, Hoffman E, Ono M, Khanam D, Hayday A, Froham L and Koff A (1996). Enhanced growth of mice lacking the cyclin-dependent kinase inhibitor function of p27Kip1. Cell 85(5): 721-732

- Klein C and Westenberger A (2012). Genetics of Parkinson's Disease. Cold Spring Harb Perspect Med doi: 10.1101/cshperspect.a008888

- Kossatz U, Diertrich N, Zender, Buer J, Manns M and Malek N (2001). Skp2-dependent degradation of p27Kip1 is essential for cell cycle progression. Gene Dev 18: 2602-2607

- Kouli A, Torsney K and Kuan W (2018). Parkinson's Disease: Etiology, Neuropathology and Pathogenesis. Codon Publications doi: http://dx.doi.org/10.15586/codonpublications.parkinsonsdisease.2018

- Kriks S, Shim J, Piao J, Ganat Y, Wakeman D, Xie Z, Carrillo-Reid L, Auyeung G, Antonacci C, Buch A, Yang L, Beal M, Surmeier J, Kordower J, Tabar V and Studer L (2011). Dopamine neurons derived from human ES cells efficiently engraft in animal models of Parkinson's disease. Nature 480: 547-553

- La Manno G, Gyllborg D, Codeluppi S, Nishimura K, Salto C, Zeisel A, Borm LE, Stott SR, Toledo EM, Villaescusa JC, Lönneberg P, Ryge J, Barker RA, Arenas E and Linnarsson S

(2016). Molecular diversity of midbrain development in mouse, human and stem cells. Cell 167(2): P566-580

- LaBaer J, Garrett M, Stevenson L, Slingerland J, Sandhu C, Chou H, Fattaey A and Harlow E (1997). New functional activities for the p21 family of CDK inhbitors. Gene Dev 11: 847-862

- Lacy E, Filippov I, Lewis W, Otieno S, Xiao L, Weiss S, Hengst L and Kriwacki R (2004). p27 binds cyclin-CDK complexes through a sequential mechanism involving binding-induced protein folding. Nat Struct Mol Biol 11(4): 358-364

- Lang A (2011). A critical appraisal of the premotor symptoms of Parkinson's disease: Potential usefulness in early diagnosis and design of neuroprotective trials. Mov Disord 26(5): 775–783

- Lange C and Calegari F (2010). Cdks and cyclins link G1 length and differentiation of embryonic, neural and hematopoietic stem cells. Cell Cycle 9(10): 1893-1900

- Lee J and Kim S (2009). The function of p27Kip1 during tumor development. Exp Mol Med 41(11): 765-771

- Lee J, Hollenberg S, Snider L, Turner D, Lipnick N and Weintraub H (1995). Conversion of Xenopus ectoderm into neurons by NeuroD1, a basic helix-loop-helix protein. Science 268: 836-844

- Li H, Collado M, Villasante A, Matheu A, Lynch C, Cañamero M, Rizzoti K, Carneiro C, Martínez G, Vidal A, Lovell-Badge R and Serrano M (2012). p27Kip1 directly represses Sox2 during embryonic stem cell differentiation. Cell Stem Cell 11: 845-852

- Li J, Dani J and Le W (2009). The role of transcription factor Pitx3 in dopamine neuron development and Parkinson's disease. Curr Top Med Chem 9(10): 855-859

- Lim S and Kaldis P (2013). Cdks, cyclins and CKIs: roles beyond cell cycle regulation. Development 140: 3079-3093

- Lindvall O (2015a). Clinical translation of stem cell transplantation in Parkinson's disease. J Intern Med 279: 30-40

- Lindvall O (2015b). Treatment of Parkinson's disease using cell transplantation. Phil Trans R Soc B 370(20140370): 1-7

- Lindvall O and Kokaia Z (2009). Prospects of stem cell therapy for replacing dopamine neurons in Parkinson's disease. Trends Pharmcol Sci 30(5): 260-267

- Lindvall O, Brundin P, Widner H, Rehncrona S, Gustavii B, Frackowiak, Leenders K, Sawle G, Rothwell J, Marsden D and Björklund A (1990). Grafts of fetal dopamine neurons survive and improve motor function in Parkinson's disease. Science 247: 574-577

- Lindvall O, Rehncron S, Brundin P, Gustavii B, Åstedt D, Widner H, Lindholm T, Björklund A, Leenders K, Rothwell J, Frackowiak R, Marsden D, Johnels B, Steg G, Freedman R, Hoffer B, Seiger Å, Bygdemann M, Strömberg I and Olson L (1989). Human fetal dopamine neurons grafted into the striatum in two patients with severe Parkinson's disease. Arch Neurol 46: 615-631

- Ludlow J, Shon J, Pipas J, Livingston D and DeCaprio J (1990). The retinoblastoma susceptibility gene product undergoes cell cycle-dependent dephosphorylation and binding to and release from SV40 Large T. Cell 60: 387-396

- Ma Q, Fode C, Guillemot F and Anderson D (1999). Neurogenin1 and Neurogenin2 control two distinct waves of neurogenesis in developing dorsal root ganglia. Gene Dev 13: 1717-1728

- Marinus J, Zhu K, Marras C, Aarsland D and van Hilten J (2018). Risk factors for non-motor symptoms of Parkinson's Disease. Lancet Neurol 17: 559-568

- Martinez S, Crossley P, Cobos I, Rubenstein J and Martin G (1999). FGF8 induced formation of an ectopic isthmic organizer and isthmocerebellar development via repressive effect on Otx2 expression. Development 126: 1189-1200

- Martínez-Morales P and Liste I (2012). Stem cells as in vitro models of Parkinson's disease. Stem Cells Int doi: 10.115572012/980941

- Martínez-Serrano A and Liste I (2010). Recent progress and challenges for use of stem cell derivatives in neuron replacement therapy for Parkinson's disease. Future Neurol 5(2): 161-165

- Martynoga B, Drechsel D and Guillemot F (2012). Molecular control of neurogenesis: a view from the mammalian cerebral cortex.Cold Spring Harb Perspect Biol 2012: 4:a008359

- Metzakopian E, Lin W, Salmon-Divon M, Dvinge H, Andersson E, Ericson J, Perlmann T, Whitsett J, Bertone P and Ang SL (2012). Genome-wide characterization of Foxa2 targets reveals upregulation of floor plate genes and repression of ventrolateral genes in midbrain dopaminergic neurons. Development 139: 2625-2634

- Miller F and Gauthier A (2007). Timing is everything: making neurons versus glia in the developing cortex. Neuron 54: 357-369

- Millet S, Campbell K, Epstein D, Losos K, Harris E, Joyner A (1999). A role of Gbx2 in repression of Otx2 and positioning the mid/hindbrain organizer. Nature 401: 161-164

- Miyata T, Maeda T and Lee J (1999). NeuroD is required for differentiation of the granule cells in the cerebellum and hippocampus. Gene Dev 13: 1647-1652

- Moldovan G, Pfander B and Jentsch S (2007). PCNA, the maestro of the replication fork. Cell 129: 665-679

- Morales M and Root D (2014). Glutamate neurons within the midbrain dopamine regions. Neuroscience 282: 60-68

- Nakayama K and Nakayama K (2006). Ubiquitin ligases: cell cycle control and cancer. Nat Rev 6: 369-381

- Nguyen L, Besson A, Heng J, Schuurmans C, Teboul L, Parras C, Philpott A, Roberts J and Guillemot F (2006). p27Kip1 independently promotes neuronal differentiation and migration in the cerebral cortex. Gene Dev 20: 1511-1524s

- Ohnuma S and Harris W (2003). Neurogenesis and the cell cycle. Neuron 40: 199-208

- Ohtsuka T, Ishibashi M, Gradwohl G, Nakanishi S, Guillemot F and Kageyama R (1999). Hes1 and Hes5 as Notch effectors in mammalian neuronal differentiation. EMBO 18(8): 2196-2207

- Olanow C and Tatton W (1999). Etiology and pathogenesis of Parkinson's disease. Annu Rev Neurosci 22: 123-144

- Olanow C, Goetz C, Kordower J, Stoessl J, Sossi V, Brin M, Shannon K, Nauert M, Perl D, Godbold J and Freeman T (2003). A double-blind controlled trial of bilateral fetal nigral transplantation in Parkinson's disease. Ann Neurol 54: 403-414

- Ono Y, Nakatani T, Sakamoto Y, Mizuhara E, Minaki Y, Kumai M, Hamaguchi A, Nishimura M, Inoue Y, Hayashi H, Takahashi J Imai T (2007). Differences in neurogenic potential in floor plate cells along an anteroposterior location: midbrain dopaminergic neurons originate from mesencephalic floor plate cells. Development 134: 3213-3225

- Orlando S, Gallastegui E, Besson A, Abril G, Aligué R, Pujol MJ and Bachs O (2015). P27Kip1 and p21Cip1 collaborate in the regulation of transcription by recruiting cyclin-CDK complexes on the promoters of target genes. Nuc Acid Res 43(14): 6860-6873

- Otieno S, Grace C and Kriwacki R (2011). The role of the LH subdomain in the function of the Cip/Kip cyclin dependent kinase regulators. Biophys J 100: 2486-2494

- Palmer C and Liste I (2016). Stem cell-based therapies for Parkinson's disease. Neurological Regeneration, Springer doi: 10.1007/978-3-319-33720-3

- Palmer C, Coronel R and Liste I (2016). Treatment of Parkinson's disease using stem cells. J Stem Cell Res Med 1(3): 71-77

- Palmer C, Coronel R, Bernabeu-Zornoza A and Liste I (2018). Therapeutic application of stem cell and gene therapy in Parkinson's disease. Pathology, prevention and therapeutics of neurodegenerative diseases, Springer doi: 10.1007/978-981-13-0944-1_14

- Parkinson J (1817). An Essay on the Shaking Palsy. London: Whittingham and Rowland Sherwood, Neely and Jones

- Parras C, Schuurmans C, Scardigli R, Kim J, Anderson D and Guillemot F (2002). Divergent functions of the porneural genes Mash1 and Ngn2 in the specification of neural subtype identity. Gene Dev 16: 324-338

- Pattyn A, Simplicio N, Doorninck H, Goridis C, Guillemot F and Brunet JF (2004). Ascl1/Mash1 is required for the development of central serotonergic neurons. Nat Neurosci 7(6): 589-595

- Perearnau A, Ornaldo S, Islam A, Gallastegui E, Martínez J, Jordan A, Bigas A, Aligué, Pujol MJ and Bachs O (2017). p27Kip1, PCAF and PAX5 cooperate in the transcriptional regulation of specific target genes. Nuc Acid Res 45(9): 5086-5099

- Piccini P, Lindvall O, Björklund A, Brundin P, Hagell P, Ceravolo R, Oertel W, Quinn N, Samuel M, Rehncrona S, Widner H and Brooks D (2000). Delayed recovery of movement-related cortical function in Parkinson's disease after striatal dopaminergic grafts. Ann Neurol 48: 689-695

- Pippa R, Espinosa L, Gundem G, García-Escudero R, Dominguez A, Orlando S, Gallastegui E, Saiz C, Besson A, Pujol MJ, López-Bigas N, Paramio JM, Bigas A and Bachs O (2012). p27Kip1 represses transcription by direct interaction with p130/E2F4 at the promoters of target genes. Oncogene 31: 4207-4220

- Poewe W, Seppi K, Tanner C, Halliday G, Brundin P, Volkmann J, Schrag AE, Lang A (2017). Parkinson disease. Nat Rev Dis Primers 3(17013): 1-21

- Pollanen M, Dickson D and Bergeron C (1993). Pathology and biology of Lewy bodies. J Neuropath Exp Neur 52(3): 183-191

- Porter A and Jänicke R (1999). Emerging roles of caspase-3 in apoptosis. Cell Death Differ 6: 99-104

- Prakash N and Wurst W (2006). Development of dopaminergic neurons in the mammalian brain. Cell Mol Life Sci 63: 187-206

- Revilla A, González C, Iriondo A, Fernández B, Prieto C, Marín C and Liste I (2015). Current advances in the generation of human iPS cells: implications in cell-based regenerative medicine. J Tissue Eng Regen Med doi: 10.1002/term.2021

- Rhinn M and Brand M (2001). The midbrain-hindbrain boundary organizer. Curr Opin Neurobiol 11: 34-42

- Richard-Parpaillon L, Cosgrove R, Devine C, Vernon A and Philpott A (2004). G1/S phase cyclin-dependent kinase overexpression perturbs early development and delays tissue-specific differentiation in Xenopus. Development 131: 2577-2586

- Rocca W (2018). The burden of Parkinson's disease: a worldwide perspective. Lancet Neurol 17: 928-929

- Roelink H, Porter J, Chiang C, Tanabe Y, Cheng D, Beachy P and Jessell T (1995). Floor plate and motor neuron induction by different concentrations of the amino-terminal cleavage product of sonic hedgehog autoproteolysis. Cell 81: 445-455

- Roeper J (2013). Dissecting the diversity of midbrain dopamine neurons. Trends Neurosci 36(6): 336-342

- Root D, Wang H, Liu B, Barker D, Mód L, Szocsics P, Silva A, Maglóczky Z and Morales M (2016). Glutamate neurons are intermixed with midbrain dopamine neurons in nonhuman primates and humans. Sci Rep-UK 6: 30615 doi: 10.1038/srep30615

- Russo A, Jeffrey P, Patten A, Massagué J and Pavletich N (1996). Crystal structure of the p27Kip1 cyclin-dependent kinase inhibitor bound to the cyclin A-Cdk2 complex. Nature 382: 325-331

- Sacchetti P, Sousa K, Hall A, Liste I, Steffensen K, Theofilopoulos S, Parish C, Hazenberg C, Richter L, Hovatta O, Gustafsson JÅ and Arenas E (2009). Liver X receptors and oxysterols promote ventral midbrain neurogenesis in vivo and in human embryonic stem cells. Cell Stem Cell 5: 409-419

- Saucedo-Cardenas O, Quintana-Hau J, Le WD, Smidt M, Cox J, de Mayo F, Burbach P and Conneely O (1998). Nurr1 is essential for the induction of the dopaminergic phenotype and the survival of ventral mesencephalic late dopaminergic precursor neurons. Proc Natl Acad Sci USA 95: 4013-4018

- Schafer K (1998). The cell cycle: a review. Vet Pathol 35: 461-478

- Seo S, Lim JW, Yellajoshyula D, Chang LW and Kroll K (2007). Neurogenin and NeuroD direct transcriptional targets and their regulatory enhancers. EMBO 26: 5093-5108

- Sherr C and Roberts J (1999). CDK inhibitors: positive and negative regulators of G1-phase progression. Gene Dev 13: 1501-1512

- Sherr C and Roberts J (2004). Living with and without cyclins and cyclin-dependent kinases. Gene Dev 18: 2699-2711

- Shirane M, Harumiya Y, Ishida N, Hirai A, Miyamoto C, Hatakeyama S, Makayama K and Kitagawa M (1999). Down-regulation of p27Kip1 by two mechanisms, ubiquitin-mediated degradation and proteolytic processing. J Biol Chem 274(29): 13886-13893

- Sikorska M, Sandhu J, Deb-Rinker P, Jezierksi A, LeBlanc J, Charlebois C, Ribecco-Lutkiewicz M, Bani-Yaghoub M and Walker R (2008). Epigenetic modifications of Sox2 enhancers, SRR1 and SRR2, correlate with in vitro neural differentiation. J Neurosci Res 86: 1680-1693

- Smidt M, Asbreuk A, Cox J, Chen H, Johnson R and Burbach P (2000). A second independent pathway for development of mesencephalic dopaminergic neurons requires Lmx1b. Nat Neurosci 3(4): 337-341

- Smidt M, Smits S, Bouwmeeester H, Hamers F, van der Linden A, Hellemons A, Graw J and Burbach P (2004). Early developmental failure of substantia nigra dopamine neurons in mice lacking the homeodomain gene Pitx3. Development 131: 1145-1155

- Smits S, Ponnio T, Conneely O, Burbach P and Smidt M (2003). Involvement of Nurr1 in specifying the neurotransmitter identity of ventral midbrain dopaminergic neurons. Eur J Neurosci 18: 1731-1738

- Sommer L, Ma Q and Anderson D (1996). Neurogenins, a novel family of atonal-related bHLH transcription factors, are putative mammalian neuronal determination genes that reveal progenitor cell heterogeneity in the developing CNS and PNS. Mol Cell Neurosci 8: 221-241

- Spencer D, Robbins R, Naftolin F, Marek K, Vollmer T, Leranth C, Roth R, Price L, Gjedde A, Bunney B, Sass K, Elsworth J, Kier L, Makuch R, Hoffer P and Redmond E (1992). Unilateral transplantation of human fetal mesencephalic tissue into the caudate nucleus of patients with Parkinson's disease. N Engl J Med 327: 1541-1548

- Spillantini M, Crowther R, Jakes R, Hasegawa M and Goedert M (1998). α-synuclein in filamentous inclusions of Lewy bodies from Parkinson's disease and dementia with Lewy bodies. Proc Natl Acad Sci USA 95: 6469-6473

- Sun K and Kaufman P (2018). Ki67: more than a proliferation marker. Chromosoma doi: 10.1007/s00412-018-06559-8

- Susaki E, Nakayama K, Yamasaki L and Nakayama K (2009). Common and specific roles of the related CDK inhibitors p27 and p57 revealed by a knock-in mouse model. Proc Natl Acad Sci USA 106(13): 5192-5197

- Takahashi K and Yamanaka S (2006). Induction of pluripotent stem cells from mouse embryonic and adult fibroblast cultured by defined factors. Cell 126: 663-676

- Takahashi K, Tanabe K, Ohnuki, Narita M, Ichisaka T, Tomoda K and Yamanaka S (2007). Induction of pluripotent stem cells from adult human fibroblasts by defined factors. Cell 131: 861-872

- Teixeira L and Reed S (2013). Ubiquitin ligases and cell cycle control. Annu Rev Biochem 82: 14.1-14.28

- Thompson L, Andersson E, Jensen J, Barraud P, Guillemot F, Parmar M and Björklund A (2006). Neurogenin2 identifies a transplantable dopamine neuron precursor in the developing ventral mesencephalon. Exp Neurol 198: 183-198

- Thomson J, Itskovitz-Eldor J, Shapiro S, Waknitz M, Swiergiel J, Marshall V and Jones J (1998). Embryonic stem cell lines derived from human blastocysts. Science 282: 1145-1147

- Villa A, Liste I, Courtois E, Seiz E, Ramos M, Meyer M, Juliusson B, Kusk P and Martínez-Serrano A (2009). Generation and properties of a new human ventral mesencephalic neural stem cell line. Exp Cell Res 315: 1860-1874

- Waite M, Skidmore J, Bili A, Martin JF and Martin DM (2011). GABAergic and glutamatergic identities of developing midbrain Pitx2 neurons. Dev Dyn 240(2): 333-346

- Wallén Å, Zetterström R, Solomin L, Arvidsson M, Olson L and Perlmann T (1999). Fate of mesencephalic AHD2-expressing dopamine progenitor cells in Nurr1 mutant mice. Exp Cell Res 253: 737-746

- Wasserman K, Lewandoski M, Campbell K, Joyner A, Rubenstein J, Martinez S and Martin G (1997). Specification of the anterior hindbrain and establishment of a normal mid/hindbrain organizer is dependent on Gbx2 gene function. Development 124: 2923-2934

- Wojtowicz J and Kee N (2006). BrdU assay for neurogenesis in rodents. Nat Protoc 1(3): 1399-1405

- Yan C, Levesque M, Claxton S, Johnson R and Ang SL (2011). Lmx1a and Lmx1b function cooperatively to regulate proliferation, specification, and differentiation of midbrain dopaminergic progenitors. J Neruosci 31(35): 12413-12425

- Yang Q and Al-Hendy A (2018). The emerging role of p27 in development of diaseas. Cancer Stud Mol Med 4(1): 1-5

- Yu J, Vodyanik M, Smuga-Otto K, Antosiewicz-Bourget J, Frane J, Tian S, Nie J, Jonsdottir G, Ruotti V, Stewart R, Slukvin I and Thomson J (2007). Induced pluripotent stem cell lines derived from human somatic cells. Sicence 318: 1917-1920.

- Zetterström R, Solomin L, Jansson L, Hoffer B, Olson L and Perlmann T (1997). Dopamine neuron agenesis in Nurr1-deficient mice. Science 276: 248-250

APPENDIX I